

NIST Special Publication 260-194

**Certification of SRM 2497:
Standard Reference Concrete for
Rheological Measurements**

Chiara F. Ferraris
Nicos S. Martys
Max Peltz
William L. George
Edward J. Garboczi
Blaza Toman

This publication is available free of charge from:
<https://doi.org/10.6028/NIST.SP.260-194>

NIST
**National Institute of
Standards and Technology**
U.S. Department of Commerce

NIST Special Publication 260-194

Certification of SRM 2497: Standard Reference Concrete for Rheological Measurements

Chiara F. Ferraris
Nicos S. Martys
Max Peltz

*Materials and Construction Research Division
Engineering Laboratory*

William L. George
*Applied and Computational Mathematics Division
Information Technology Laboratory*

Edward J. Garboczi
*Applied Chemicals and Materials Division
Material Measurement Laboratory*

Blaza Toman
*Statistical Engineering Division
Information Technology Laboratory*

This publication is available free of charge from:
<https://doi.org/10.6028/NIST.SP.260-194>

April 2019



U.S. Department of Commerce
Wilbur L. Ross, Jr., Secretary

National Institute of Standards and Technology
Walter Copan, NIST Director and Under Secretary of Commerce for Standards and Technology

Certain commercial entities, equipment, or materials may be identified in this document in order to describe an experimental procedure or concept adequately. Such identification is not intended to imply recommendation or endorsement by the National Institute of Standards and Technology, nor is it intended to imply that the entities, materials, or equipment are necessarily the best available for the purpose.

The opinions, recommendations, findings, and conclusions in this publication do not necessarily reflect the views or policies of NIST or the United States Government.

National Institute of Standards and Technology Special Publication 260-194
Natl. Inst. Stand. Technol. Spec. Publ. 260-194, 116 pages (April 2019)
CODEN: NSPUE2

This publication is available free of charge from:
<https://doi.org/10.6028/NIST.SP.260-194>

Abstract

Rotational rheometers are commonly used to measure a material's rheological properties such as viscosity and yield stress [1]. Manufacturers of rheometers generally recommend the use of a standard oil of known viscosity to calibrate the instrument in order to ensure it's proper operation. These oils are Newtonian fluids and are not representative of the flow of concrete, mortar or paste which behave as a Bingham, Hershel-Bulkley, or power-law fluid. Also, oils are expensive, and would be cost prohibitive because large volumes of the reference material would be needed to calibrate concrete rheometers. Therefore, a relatively inexpensive, well characterized reference material, with properties similar to concrete, (e.g., non-Newtonian and contains aggregates similar in dimension to that in concrete for testing in concrete rheometers) is needed.

The purpose of this report is to describe the process used to create and certify a new Standard Reference Material, SRM 2497, a "Standard Reference Concrete for Rheological Measurements". The development of this new Standard Reference Material (SRM) is based on a three-step-multi-scale approach. The first step was to develop a paste rheology reference material (SRM2492) [2], the second step involved creating a mortar rheology reference material, SRM2493 [3]. The final step, described in this work, is development of a concrete rheology reference material, SRM 2497.

All measurements used for the development of SRM 2497 are provided along with statistical analyses. A brief description, along with references, of the computational model that was utilized to predict the behavior of the SRM is also provided. The data analyzed in this study serves to certify that the proposed models and values are validated with proper quantification of uncertainty.

Acknowledgements

The authors would also like to thank some key persons at NIST without whom this certification could not have been completed.

John “Rusty” Hettenhouser provided the 3-D printing of the mortar spiral and was instrumental in securing the design of the spiral for the concrete rheometer.

Louis W. Toth, P.E. (L.T. Engineering, Inc.) was instrumental in designing and building the spiral that was used in this study, and the authors are very grateful of his contribution.

Dr. Kenneth Snyder, for his careful reading and helpful suggestions for this report.

We would also like to acknowledge that this research used resources of the Argonne Leadership Computing Facility at Argonne National Laboratory, which is supported by the Office of Science of the U.S. Department of Energy under contract DE-AC02-06CH11357.

Table of Contents

1	Introduction.....	1
2	Materials	2
2.1	Limestone and corn syrup.....	2
2.2	Glass beads.....	2
2.2.1	X-ray computed tomography and spherical harmonic analysis of 10 mm beads 3	
2.2.2	10 mm bead analysis results	4
2.3	Mixing and composition	5
2.4	Packaging.....	7
3	Definitions.....	9
4	Modeling approach	10
4.1	Mortar simulation.....	11
4.2	Concrete simulation	15
5	Rheological measurements set-up.....	19
5.1	Coaxial geometries.....	19
5.1.1	Mortar and paste geometries.....	19
5.1.2	Concrete geometries.....	19
5.1.3	Spirals design	20
5.2	Experimental design.....	21
5.3	Concrete rheometer calibration.....	22
5.3.1	Calibration based on the Bingham parameters	22
5.3.2	Calibration using the Viscosity vs. Shear rate curve	24
6	Results and analysis	29
6.1	Introduction.....	29
6.2	Paste on parallel plate	29
6.2.1	Statistical analysis.....	29
6.2.2	OpenBUGS code.....	31
6.3	Paste with the coaxial.....	32
6.3.1	Statistical Analysis.....	32
6.3.2	Calibration factors and data in fundamental units for paste coaxial.....	35
6.4	Mortar data with the coaxial paste/mortar rheometer	38
6.4.1	Statistical analysis.....	38
6.4.2	Yield stress and plastic viscosity	38
6.4.3	Calibration factors and data in fundamental units for paste coaxial.....	41
6.5	Data with the concrete rheometer	43
6.5.1	Statistical analysis.....	43
6.5.2	Calibration factors and data in fundamental units in concrete rheometer	49
7	Comparison between concrete model and experimental data.....	54
8	Summary	58

9 References..... 59
Appendix A: Original paste data measured using the Parallel plate rheometer A-1
Appendix B: Original data measured from Coaxial Rheometer.....B-1
Appendix C: Original data measured from Concrete Rheometer..... C-1

List of Figures

Figure 1: Particle size distribution of the limestone as measured by laser diffraction. The standard deviation is smaller than the symbols.....	2
Figure 2: Picture of the two sizes of beads, A) 1 mm beads (see SRM 2493 report for full analysis of 1 mm beads; B) 10 mm beads.....	3
Figure 3: Skyscan 1172 (left) and Re-construction monitors (right).....	3
Figure 4: Picture of the impeller of hand-held mixer used for mixing the materials.....	7
Figure 5: SRM 2497 buckets shown with the full labels.....	8
Figure 6: Numerical model simulation for mortar from scaling parameters is shown here. The yellow curve is the fit of the data measured with the paste (black dots) (see Table 6 for values). The uncertainty is about 5 % (see text)	12
Figure 7: Numerical model simulation for concrete from scaling parameters in Table 8 is shown here. The concrete model curve is representing two overlapping curves, generated either from the paste (green curve) or the mortar model (red curve). The uncertainty is about 10 % (see text).....	16
Figure 8: Geometries used for paste and mortar testing	19
Figure 9: Container for the concrete measurements	20
Figure 10: Two geometries types used for testing concrete.	20
Figure 11: Schematic for using Bingham parameters to calibrate a concrete rheometer from raw torque and rotational speed and converting results to fundamental rheological variables, viscosity and shear rate.....	24
Figure 12: Schematic for the calibration of rheometer data from raw torque and rotational speed to fundamental rheological variables, viscosity and shear rate.	28
Figure 13: Paste data after calibration. See uncertainty in Table 22 to Table 24.	36
Figure 14: Data calibrated for mortar in the paste/mortar rheometer. Uncertainty is shown in Table 31 to Table 33	41
Figure 15: Rheometer data for paste using both geometries. See uncertainty in.....	50
Figure 16: All data using the concrete rheometer based on the K factors from Table 44. Uncertainty in Table 47 to Table 52	50
Figure 17: Comparison of concrete rheometer data for mortar with the mortar simulation obtained from the paste based on K factors from Table 44.	54
Figure 18: Comparison of concrete data calibrated using the paste fit and the factors K from Table 46 with the simulation curves	55
Figure 19: Comparison of concrete data calibrated using the concrete model and the factors K from Table 51 with the simulation curves.	56
Figure 20: Comparison of concrete data calibrated using the concrete model and the factors L from Table 52 with the simulation curves.....	57

List of Tables

Table 1: Showing what number fraction of the 103 glass beads had VESD values within \pm y standard deviations of the mean.....	4
Table 2: Showing the average and standard deviations, based on number, of L, W, T, L/W, and W/T.	5
Table 3: Simulation data portrayed in Figure 6 for mortar.....	12
Table 4: Scaling parameters to factor the SRM2497-paste component curve to a mortar curve. The uncertainty shown is based on a least square fit.	12
Table 5: Bingham parameters from the mortar simulation curve (see Table 6), for values of shear rate greater than 1 s^{-1}	13
Table 6: Values for paste and mortar model with uncertainties provided in fundamental units (data were rounded to nearest hundredth). The uncertainty is 10 % on the shear stress and viscosity.....	14
Table 7: Simulation results for concrete.	15
Table 8: Scaling parameters to factor the SRM2497- paste or mortar component curve to a concrete curve.	16
Table 9: Bingham parameters from the concrete simulation curve (data in Table 10).....	16
Table 10: Values for concrete model (40 % of 10 mm beads) with uncertainties provided in fundamental units (data were rounded to nearest hundredth) calculated from the paste model. The uncertainty is 10 %	17
Table 11: Values for concrete model (40 % of 10 mm beads) with uncertainties provided in fundamental units (data were rounded to nearest hundredth) calculated from the mortar model. The uncertainty is 10 %	18
Table 12: Measurement type at the various stages of mixing.....	21
Table 13: Paste on parallel plate average curve with uncertainty.....	30
Table 14: Bingham parameters for each run and the average, parallel plate measurements with paste	31
Table 15: Flow curve and uncertainty for Spiral for paste. SR is the rotational speed and SS is the torque, U is the uncertainty of the torque	33
Table 16: Flow curve and uncertainty for 4-vane for paste. SR is the rotational speed and SS is the torque, U is the uncertainty of the torque	33
Table 17: Flow curve and uncertainty for 6-vane for paste. SR is the rotational speed and SS is the torque, U is the uncertainty of the torque	33
Table 18 Yield stress and plastic viscosity values for each sample and for consensus for paste– spiral spindle.....	34
Table 19 Yield stress and plastic viscosity values for each sample and for consensus for paste – 4-vane spindle.....	35
Table 20: Yield stress and plastic viscosity values for each sample and for consensus for paste – 6-vane spindle.....	35
Table 21: Calibration factors for the three geometries used for paste	36
Table 22: Calibrated data for Spiral for paste.....	37
Table 23: Calibrated data for 4-vane for paste.....	37
Table 24: Calibrated data for 6-Vane for paste.....	37
Table 25: Flow curve and uncertainty for Spiral for mortar. SR is the rotational speed and SS is the torque, U is the uncertainty of the torque	39

Table 26: Flow curve and uncertainty for 4-vane for mortar. SR is the rotational speed and SS is the torque, U is the uncertainty of the torque	39
Table 27: Flow curve and uncertainty for 6-vane for mortar. SR is the rotational speed and SS is the torque, U is the uncertainty of the torque	39
Table 28: Yield stress and viscosity for each sample and for consensus for mortar– spiral	40
Table 29: Yield stress and viscosity for each sample and for consensus for mortar– 4-vane	40
Table 30 Yield stress and viscosity for each sample and for consensus for mortar– 6-vane	41
Table 31: Calibrated data for Spiral for mortar. U is the uncertainty of the shear stress .	42
Table 32: Calibrated for 4-Vane for mortar. U is the uncertainty of the shear stress	42
Table 33: Calibrated for 6-Vane for mortar. U is the uncertainty of the shear stress	42
Table 34: Flow curve and uncertainty for Helical for paste. SR is the rotational speed and SS is the torque, U is the uncertainty of the torque	44
Table 35: Flow curve and uncertainty for 4-vane for paste. SR is the rotational speed and SS is the torque, U is the uncertainty of the torque	44
Table 36: Flow curve and uncertainty for helical for mortar. SR is the rotational speed and SS is the torque, U is the uncertainty of the torque	45
Table 37: Flow curve and uncertainty for vane for mortar. SR is the rotational speed and SS is the torque, U is the uncertainty of the torque	45
Table 38: Flow curve and uncertainty for concrete helical. SR is the rotational speed and SS is the torque, U is the uncertainty of the torque	46
Table 39: Flow curve and uncertainty for concrete vane. SR is the rotational speed and SS is the torque, U is the uncertainty of the torque	46
Table 40: Yield stress and plastic viscosity for each sample and for consensus – paste Helical in concrete rheometer	47
Table 41: Yield stress and plastic viscosity for each sample and for consensus – paste vane in concrete rheometer.....	47
Table 42: Yield stress and plastic viscosity for each sample and for consensus – mortar Helical in concrete rheometer	48
Table 43: Yield stress and plastic viscosity for each sample and for consensus – mortar vane in concrete rheometer	48
Table 44: Yield stress and plastic viscosity for each sample and for consensus – concrete Helical in concrete rheometer	49
Table 45: Yield stress and viscosity for each sample and for consensus – concrete vane in concrete rheometer.....	49
Table 46: Calibration factors for the two geometries of spindles used in concrete rheometer based on the paste data.....	49
Table 47: Data calibrated for paste on a spiral in the concrete rheometer. U is the uncertainty of the shear stress	51
Table 48: Data calibrated for paste on a Vane in the concrete rheometer. U is the uncertainty of the shear stress	51
Table 49: Data calibrated for mortar on a Spiral in the concrete rheometer. U is the uncertainty of the shear stress	52

Table 50: Data calibrated for mortar on a Vane in the concrete rheometer. U is the uncertainty of the shear stress 52

Table 51: Data calibrated for concrete on a spiral in the concrete rheometer. U is the uncertainty of the shear stress 53

Table 52: Data calibrated for concrete on a Vane in the concrete rheometer. U is the uncertainty of the shear stress 53

Table 53: Calibration factors, K, for the two geometries used in concrete rheometer, based on the concrete simulation 56

Table 54: Calibration factors, L, for the two geometries used in concrete rheometer based on the concrete simulation 56

Notations:

SD: Standard Deviation

SRM: Standard Reference Material

$\dot{\gamma}$: Shear rate [s^{-1}]

τ : Shear stress [Pa]

τ_0 : Yield stress [Pa]

N: Rotational speed [rad/s] or [rpm]

Γ : Measured torque [$N\cdot m$]

μ : Viscosity [$Pa\cdot s$]

μ_B : plastic viscosity (Bingham model) [$Pa\cdot s$]

μ_R : Relative viscosity [-]

μ_{sc-m} : Viscosity scaling factor for mortar [-]

$\dot{\gamma}_{sc-m}$: Shear rate scaling factor for mortar [-]

μ_{sc-c} : Viscosity scaling factor for concrete [-]

$\dot{\gamma}_{sc-c}$: Shear rate scaling factor for concrete [-]

K_τ : Shear stress calibration factor [$Pa/N\cdot m$]

K_μ : Viscosity calibration factor [$Pa\cdot s/N\cdot m\cdot s$]

K_γ : Shear rate calibration factor [-]

L_τ : Shear stress calibration factor based on viscosity curves [$Pa/(N\cdot m)$]

L_μ : Viscosity calibration factor based on viscosity curves [$Pa\cdot s/(N\cdot m\cdot s)$]

L_γ : Shear rate calibration factor based on viscosity curves [-]

1 Introduction

A National Institute of Standards and Technology (NIST) Standard Reference Material[®] (SRM) meets specific certification criteria and is issued with a certificate of analysis that reports the results of its characterization and provides information regarding the appropriate use(s) of the material. An SRM is prepared and used for three main purposes: 1) to help develop accurate methods of analysis; 2) to calibrate measurement systems used to facilitate exchange of goods, institute quality control, determine performance characteristics, or measure a property at the state-of-art limit; and 3) to ensure the long-term adequacy and integrity of measurement quality assurance programs. NIST provides over 1300 different SRMs to industry and academia. Every NIST SRM is provided with a certificate of analysis that gives the official characterization of the material's properties. In addition, supplementary documentation, such as this report, describing the development, analysis, and use of SRMs, is also often provided to ensure effective use and reproducibility of measurements made with these materials.

There are several related SRMs utilized by the cement industry, however, none are designed for the purpose of determining the rheological properties of cement paste, mortar or concrete. After completing two inter-laboratory studies related to testing of the rheological properties of concrete, it was determined that the use of expensive oils, typically used for calibration of conventional rotational rheometers, was not suitable for calibration of concrete rheometers [4] [5]. Thus, as requested by industry, a need exists for a granular reference material with rheological properties representative of concrete. Designing such a representative reference material presents a significant challenge as the contents of concrete are varied in properties and span many decades in length scale. For the sake of simplicity, assume that the solids part of concrete is composed of cement, sand, and coarse aggregates - that can be characterized by three typical length scales. The largest cement particles are of order 100 μm , the sand is 1mm, and the coarse aggregates are about 10 mm in size. To reflect this characteristic in a concrete SRM, a three-step-multi-scale approach was developed. In the first step a paste reference material, SRM2492, that is composed of a mixture of corn syrup and limestone particles of similar size to cement particles was developed. The second step was the development of the mortar reference material, SRM2493, which is SRM2492 with the addition of 1 mm glass beads to represent sand. The third and last step is the concrete reference material, SRM 2497 [3], which is SRM2493 with the addition of 10 mm glass beads. In this multi-scale approach, the mixture associated with the smallest particles serves as a matrix fluid that larger solids are added to in hierarchal order. That is, one starts with SRM paste 2492, adds 1mm beads to make a mortar SRM2493, and finally, 10 mm beads are added to the mortar SRM 2493 to create the concrete SRM2497.

The individual raw components for SRM2497 are separately packaged and sold together as a unit. The operator has to mix the paste, add 1 mm beads and then add 10 mm beads. Once mixed the material shelf life of the mixture is 7 d [6]. The certified values were obtained through a combination of measurements using parallel plate rheometers, coaxial rheometers (double spiral, and a vane rheometer geometry) and computer simulation of the SRM's properties.

This report contains a description of the methodology and all measurements made, computer simulations methods, along with the statistical analysis in the making of SRM2497.

2 Materials

2.1 Limestone and corn syrup

The paste, which serves as a matrix for the SRM concrete, consists of a limestone, corn syrup and water mixture and is identical in composition to SRM 2492 with the exception that the limestone and corn syrup used are from a different batch. The limestone is referred to as a micro-limestone flour with an average particle size of 45 μm and a density of $2620 \text{ kg/m}^3 \pm 30 \text{ kg/m}^3$ (one standard deviation) as measured at NIST using a helium pycnometer. The corn syrup used was specified as a 100 % glucose corn syrup with no additives by the manufacturer and verified via NIST testing. The limestone particle size distribution, as measured by laser diffraction, is shown in Figure 1.

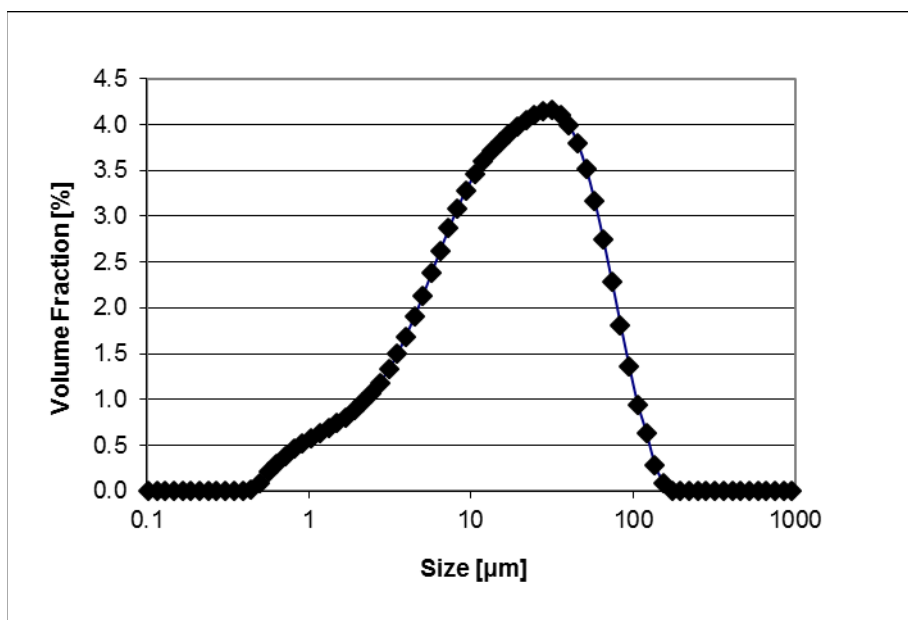


Figure 1: Particle size distribution of the limestone as measured by laser diffraction. The standard deviation is smaller than the symbols

2.2 Glass beads

The component of SRM 2497 that was added to the paste to transform it into a concrete were 1 mm glass beads, as used for the SRM 2493 mortar, and 10 mm beads (Figure 2).

The 1 mm glass beads were the same as used for SRM 2493, with a density of $2465 \text{ kg/m}^3 \pm 3 \text{ kg/m}^3$ (one standard deviation), as measured at NIST by using ASTM C188-09. The beads were checked for sphericity and other shape properties and is fully described in the SRM 2493 report [3].

The 10 mm glass beads were obtained from one source. The density was $2465 \text{ kg/m}^3 \pm 3 \text{ kg/m}^3$ (one standard deviation) as measured at NIST. The beads were also tested for shape and sphericity (section 2.2.1).

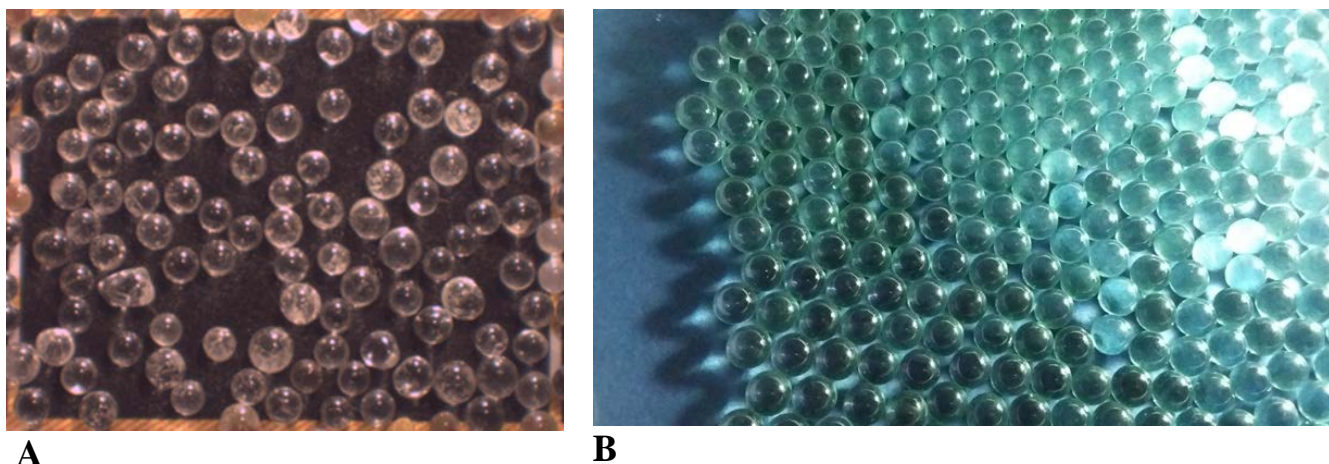


Figure 2: Picture of the two sizes of beads, A) 1 mm beads (see SRM 2493 report for full analysis of 1 mm beads; B) 10 mm beads

2.2.1 X-ray computed tomography and spherical harmonic analysis of 10 mm beads

The bead shape analysis process consisted of an X-ray computed tomography (CT) analysis, which uses X-ray technology and reconstruction algorithm [7] to acquire the 3-D particle shapes, that are then analyzed by a spherical harmonic process. The CT scans were performed using a Skyscan 1172 instrument, shown in Figure 3. The glass beads were loaded into holes drilled into wooden dowels, so that many beads could be scanned in one sample. Pieces of light polymer foam were placed between beads so that no beads were touching each other. A total of 103 beads were scanned.



Figure 3: Skyscan 1172 (left) and Re-construction monitors (right).

The X-ray CT instrument makes X-ray absorption images as the sample is rotated. The reconstruction algorithm takes this image data and constructs accurate 2D slices orthogonal to the cylindrical axis of the specimen [7]. These slices are thresholded so that

the particles are white and the background is black, and by stacking the slices on top of each other the result is a 3D model of the specimen. A computer program utilized to scan each 3D structure, identifies each of the sphere-like particles and fits them with a 3D spherical harmonic series. Then, it automatically computes various geometrical parameters of each bead, such as volume, surface area, and dimensions of a box that merely surrounds the beads (length L, width W, and thickness T). The volume equivalent spherical diameter (VESD), which is the diameter of a perfect sphere having the same volume as the particle in questions, the mean curvature integrated over the surface and normalized by the surface area, and other geometric factors are also included in these automatic calculations [8].

The usefulness of the L, W, and T parameters are that they can be quickly used to separate out grossly distorted or double particles in the following way. A sphere has $L = W = T$. A double sphere (or two identical spheres glued lightly together) has $L = 2$, $W = 1$, $T = 1$. Any particle that has values of L, W, and T outside what is considered to be the spherical range (see below for details) can be considered to be distorted. None of the 103 beads studied herein were double particles or significantly distorted from spherical shape.

2.2.2 10 mm bead analysis results

2.2.2.1 Size analysis for 10 mm beads

There were 103 glass beads analyzed. VRML images of these particles, constructed from their spherical harmonic series, were, to the eye, quite spherical. Some of the particles were very slightly tear-drop shaped, and this was real and not an artifact of the X-ray CT imaging and image analysis (e.g. segmentation) processes. The maximum particle volume was 564.8 mm^3 and the minimum volume was 389.1 mm^3 . The VESD values corresponding to these limits were 10.26 mm and 9.058 mm. The average volume was 468.7 mm^3 and the standard deviation was 54.3 mm^3 . The average VESD was 9.623 mm and the standard deviation was 0.375 mm. Table 1 below shows what fraction (by number) of the total fell within $\pm y$ standard deviations of the mean for the VESD.

Table 1: Showing what number fraction of the 103 glass beads had VESD values within $\pm y$ standard deviations of the mean.

y	Number fraction
1.0	0.534
1.1	0.689
1.2	0.786
1.3	0.874
1.4	0.932
1.5	0.981
1.6	0.990
1.7	1.000

2.2.2.2 Shape analysis

For each glass bead, the parameters L, W, and T were computed using the spherical harmonic series. L is the longest surface-to-surface distance on the particle, W is the same except it is constrained to be perpendicular to L, and T is the same except that it must be perpendicular to both W and L. For the 103 glass beads, the average values and standard deviations of L, W, and T, and the average and standard deviations of the L/W and W/T aspect ratios, are listed in Table 2 below. Note that for a perfect sphere, $L/W = W/T = 1$ exactly.

Table 2: Showing the average and standard deviations, based on number, of L, W, T, L/W, and W/T.

Dimension	Average (mm)	Std (mm)
L	9.818	0.422
W	9.685	0.382
T	9.591	0.375
L/W	1.014	0.010
W/T	1.010	0.005

By the measures of Table 2, the particles on average were within 1 % to 2 % of being perfectly round, and the one standard deviation ranges for L, W, and T strongly overlap each other.

Another measure of the sphericity of the particles is to compare the VESD to a dimension constructed from the mean curvature of each particle integrated over the surface area and inverted and normalized such that a perfect sphere of diameter D would give a value equal to D . The average VESD value for the spheres was $9.623 \text{ mm} \pm 0.375 \text{ mm}$ and the average of this curvature-related dimension is $9.598 \text{ mm} \pm 0.399 \text{ mm}$. The fact that these two values are so close to each other also implies that the particles are very spherical.

2.3 Mixing and composition

The composition of SRM 2497 is a paste where 1 mm beads (20 % by volume) and 10- mm beads (40 % by volume) are added. The total volume, using most of the materials provided, would produce 20 L of the SRM 2497. To achieve that goal, the constituents need to be added in stages during mixing:

- Corn syrup and water
- Addition of limestone
- Addition of 1 mm beads
- Addition of 10 mm beads

The 5-gallons buckets used for shipment of the materials can be used as the mixing vessel. The mixer that was used is a handheld grout mixer with a single helical blade (Figure 4).

The steps to prepare the mixture and the amounts with some tips are provided here.

- Store and use the corn syrup, glass beads, limestone and the water needed at $23 \text{ }^\circ\text{C} \pm 2 \text{ }^\circ\text{C}$ at least a day prior of the mixing. The corn syrup container provided should be placed upside down to facilitate emptying it.
- Weigh the bucket to be used for mixing, $M_b [g]$
- Determine the mass of the paste ingredients:
 - Weigh the corn Syrup directly in the mixing bucket: $5257.8 \text{ g} \pm 0.5 \text{ g}$
 - Weigh the distilled water (set aside) $1660.4 \text{ g} \pm 0.5 \text{ g}$
 - Weigh the limestone (set aside): $12043.0 \text{ g} \pm 0.5 \text{ g}$
- **Mix procedure for the corn syrup solution**
 - Add water to corn syrup
 - Mix 2 min at slow speed
 - Mix 2 min a high speed

- Scrape side for 30 s
- Mix at high speed for 4 min (scrape again after 2 min)
- **Mix procedure for the paste**
 - Add some limestone into the bucket containing the corn syrup solution
 - While mixing at slow speed for 2 min, slowly add the rest of the limestone
 - Mix for 1 min at medium speed
 - Scrape the sides
 - Mix for 4 min a high speed
- Calculation of the amount of 1-mm beads needed for 20 % by volume
 - Weigh the bucket with the paste, M_{bp} [g]
 - Densities:
 - paste, ρ_p , is: $1930 \text{ kg/m}^3 \pm 30 \text{ kg/m}^3$ (or measure it)
 - beads: 2465 kg/m^3
 - Volume of paste: $V_p [\text{m}^3] = (M_{bp} - M_b) / (\rho_p / 1000)$
 - Mass of beads [g] = $V_p * 0.25 * 2.465$.
- **Mix procedure of the mortar (20% beads by volume)**
 - Add the beads into the paste while mixing for 2 min on medium
 - Mix for 2 min on high
- Calculation of the amount of 10-mm beads needed for 40% by volume:
 - Weigh the bucket, M_{bm} [g]
 - Densities:
 - mortar, ρ_m is $2020 \text{ kg/m}^3 \pm 5 \text{ kg/m}^3$ (or measure it)
 - Beads: 2465 kg/m^3
 - Volume of mortar, $V_m [\text{m}^3] = (M_{bm} - M_b) / (\rho_m / 1000)$
 - Mass of beads [g] = $V_m * 0.67 * 2.465$
- **Mix procedure of the concrete (40% beads by volume)**
 - Add the beads to mortar while mixing for 2 min on medium
 - Mix for 2 min on high (2 persons are needed, one to hold the bucket or it will rotate with the mixer)

The SRM can be stored in the bucket with the provided lid at 23 °C. The shelf life of the concrete is 7 d (limited by the shelf life of the paste [6]).

Important tip: If some material was removed for intermediate measurements (paste or mortar), it is advisable that the density be measured, in case some water or beads were not removed uniformly.



Figure 4: Picture of the impeller of hand-held mixer used for mixing the materials.

2.4 Packaging

The corn syrup and the limestone used is similar to that used in SRM 2492 [1] and SRM 2493 [3] but from another batch. The beads were from the same manufacturer as used for SRM 2493. The 1 mm and the 10 mm beads were packaged in two separate bags: 6 kg and 20 kg, respectively. All the components were placed in two (2) 5-gal buckets. Twenty-six units were packaged.

The final packaging would include in one unit (Figure 5):

- Bucket 1 (labelled P): Limestone (12 kg) and 4 L of corn syrup
- Bucket 2 (labelled A): 1 mm beads (6 kg) and 10 mm beads (20 kg).

The material provided is enough to make 20 L of SRM 2497.



Figure 5: SRM 2497 buckets shown with the full labels

3 Definitions

Definitions of terminology used throughout this report are provided. For a more detailed discussion of the rheological properties, see the fluid review ref [3].

Viscosity of a fluid, μ , is the ratio of shear stress, τ , to the shear rate, $\dot{\gamma}$: $\mu = \tau / \dot{\gamma}$

Bingham equation is an idealized model of fluid behavior that is described by a linear relationship between shear stress and shear rate:

$$\tau = \mu_B \dot{\gamma} + \tau_0$$

where τ is the shear stress, μ_B , is the plastic viscosity and, τ_0 is the yield stress.

Pseudo-viscosity, Γ/N , is defined as the ratio of the measured torque and the applied rotational speed. This value is proportional to the viscosity.

4 Modeling approach

The conceptual framework for developing the concrete SRM is based on a multiscale approach. This framework follows the following paradigm. Once given a homogeneous matrix fluid representing a paste, a composite fluid (mortar) is made by adding solid inclusions (spherical beads), whose size is approximately an order of magnitude or so larger than the largest of the solid inclusions in the matrix fluid. This composite fluid now serves as a new matrix fluid into which larger inclusions are added to create yet another new composite fluid. In this case, to create the concrete SRM, a SRM paste is the starting point. Its largest particles are approximately 100 μm . A new composite fluid is made by adding 1mm beads such that there is 20 % volume fractions of beads. This composite fluid has rheological properties similar to that of a mortar. Finally, the concrete SRM is created by adding 10 mm beads to the mortar matrix fluid. A sufficient quantity of 10 mm beads are used to fill 40 % by volume of the entire mixture.

To predict the viscosity of the concrete SRM, a multistep modeling procedure is used. First, the paste viscosity vs. shear-rate relationship is determined experimentally. Then a direct numerical simulation that incorporates the paste SRM rheological properties into a computational model of a hard sphere suspension, having 20 % volume fraction is carried out to determine the rheological properties of the mortar for a finite set of shear rates. Two scaling parameters are determined that map the viscosity vs. shear rate data of the suspension to the viscosity vs. shear rate data of the matrix fluid (SRM paste). By performing the inverse of this transformation to the matrix viscosity vs. shear rate curve, the full viscosity vs shear rate curve is obtained for the suspension. It has been shown [9] that the general shape for the viscosity vs. shear rate curve is $\mu_\varphi(\dot{\gamma}) = a_\varphi \mu_{(\varphi=0)}(b_\varphi \dot{\gamma})$, where a_φ and b_φ depend on the solid volume fraction φ . Having this form implies that the viscosity vs shear rate of a suspension, for different volume fractions, can be estimated by rescaling the viscosity and shear rate of the constitutive relation of the matrix fluid. The same process is repeated for this Concrete SRM where the viscosity vs shear rate of the mortar fluid is now used as input for the matrix fluid for a simulation of a hard sphere suspension with 40 % volume fraction.

The computational approach used in this work, for modeling suspensions, is based on Smooth Particle Hydrodynamics (SPH) [10]. SPH is a Lagrangian formulation of the Navier-Stokes equations that has been adapted to model non-Newtonian fluids containing solid inclusions. While a full description of this approach is beyond the scope of this work, it is worth mentioning a few features of this simulation. A Lees-Edwards boundary condition is used to model Couette flow in the simulation cell [11]. This approach allows for the establishment of a Couette-like velocity profile in an infinite periodic system. As a result, wall effects, which might produce an inhomogeneous density variation or slip effects, are avoided. For an applied rate of strain, the volume average stress is calculated. The viscosity is then determined by dividing the volume averaged stress by the shear rate. An additional feature in this simulation is that lubrication forces are included to properly model the interactions between solid inclusions when they are in close proximity as the numerical resolution needed to model such effects is too demanding to accomplish using SPH alone. The approach utilized for this work has been validated for a variety of flow scenarios where excellent agreement with analytic solutions of flow fields for non-Newtonian continuum fluids in channel, tube geometries and in experimental measurements of suspensions composed of micrometer sized spheres with different power law matrix fluids in a Couette geometry. [9, 12]

Measurements in this work utilize a paste with the same composition as SRM 2492 (the materials are from a different batch), to serve as the matrix fluid of a mortar suspension composed of mono-sized glass bead inclusions. The matrix fluid is described by the following viscosity vs. shear rate curve:

$$\mu = [(\tanh(-a(\dot{\gamma} - 1)) + 1)f_1(\dot{\gamma}) + (\tanh(a(\dot{\gamma} - 1)) + 1)f_2(\dot{\gamma})]/2 \quad [1]$$

where [2]

$$f_1(\dot{\gamma}) = \frac{A_1}{\dot{\gamma}^{B_1}} + C_1$$

$$f_2(\dot{\gamma}) = \frac{A_2}{\dot{\gamma}^{B_2}} + C_2 \quad [3]$$

where

$\dot{\gamma}$ = Shear rate

μ = Viscosity

$A_i, B_i,$ and C_i ($i= 1,2$) = coefficients to fit the curve

a = fitting parameter to smoothly combine curves f_1 and f_2 .

The coefficients were determined by a least square fit to the paste SRM 2497 data obtained with the parallel plate geometry with an additional constraint that $f_1 = f_2$ at $\dot{\gamma}=2$ s^{-1} . Equation (1) is within 3 % of the experimental values shown. The viscosity (μ) can be calculated at any given shear rate using equation (1) with the following parameters for shear rates in units of s^{-1} and viscosity in units of Pa-s:

$$A_1=8.62 (1.18); B_1=0.94 (0.05); C_1=7.49 (0.35)$$

$$A_2=8.89 (0.18); B_2=0.53 (0.04); C_2=5.94 (0.24)$$

$$a = 4$$

Uncertainty in the parameter estimates, shown in parentheses, was calculated as in ref [3].

4.1 Mortar simulation

The paste viscosity from equation (1) was input into the simulation code to serve as the matrix fluid. The 1 mm glass beads were modeled as spherical inclusions with 472 spheres used to model the 20 % suspensions. The uncertainty of the simulated suspension viscosity was derived from calculating the standard deviation of the stress values, which is proportional to viscosity, over a range of strain values of approximately 5 to 10. Four different shear rates were used in the mortar simulation and the viscosity at each shear rate was determined (Table 3). It has been shown [9] that, by suitable rescaling, the mortar simulation data should fall on top of the viscosity vs. shear rate curve of the matrix fluid. Conversely, one can define scaling parameters, μ_{sc-m} and γ_{sc-m} , to multiply the viscosity and shear rate, respectively, in Equation 1, such that the rescaled curve will fall on top of the simulations data. These scaling parameters, determined by a least squares fit and shown in Table 4, are used to generate predictive curves of the suspension's viscosity vs. shear-rate,

as illustrated in Figure 6, for the 20 % volume fraction suspension.. In other words, to produce the scaled predictive curves, the μ_{sc-m} scaling parameter was factored into the viscosity variable, μ , in equation (1). Similarly, the γ_{sc-m} scaling parameter was factored into the shear rate variable, $\dot{\gamma}$, in equation (1).

In Figure 6 and Table 6, the SRM 2497 (paste component) certified data baseline is shown as a solid yellow line, along with the simulation data for 20 % volume fraction (O's) or mortar curve. From the data obtained, it is possible to calculate the plastic viscosity and yield stress, i.e., the Bingham parameters (Table 5).

Table 3: Simulation data portrayed in Figure 6 for mortar.

Shear Rate [1/s]	Mortar Simulated Viscosity [Pa-s]
0.1	110 ± 6
1	25 ± 1
10	14.4 ± 0.6
100	12.5 ± 0.6

Table 4: Scaling parameters to factor the SRM2497-paste component curve to a mortar curve. The uncertainty shown is based on a least square fit.

Concentration	μ_{sc-m} factor	γ_{sc-m} factor
20 % 1 mm beads mortar	1.8 ± 0.1	0.77 ± 0.01

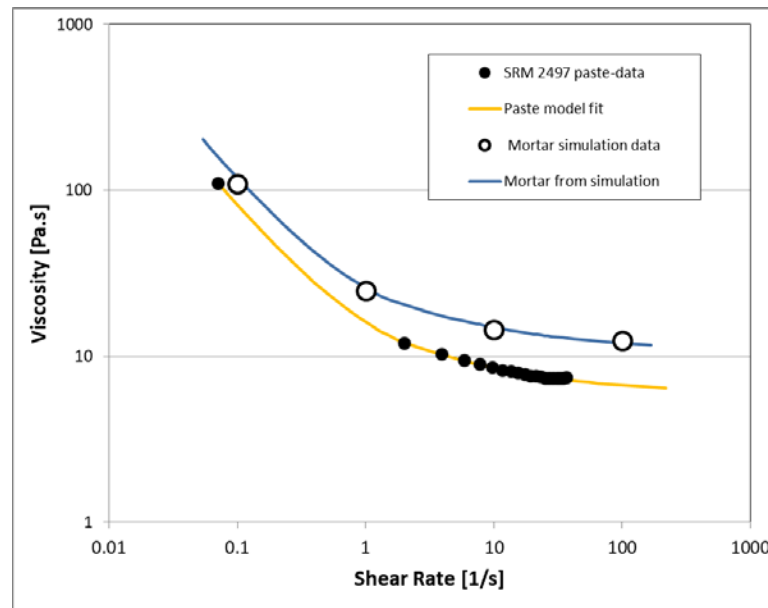


Figure 6: Numerical model simulation for mortar from scaling parameters is shown here. The yellow curve is the fit of the data measured with the paste (black dots) (see Table 6 for values). The uncertainty is about 5 % (see text)

Table 5: Bingham parameters from the mortar simulation curve (see Table 6), for values of shear rate greater than 1 s^{-1}

Concentration	Yield stress	Plastic Viscosity
0% Neat	22 ± 4	6.40 ± 0.06
20 % 1 mm beads mortar	34 ± 5	11.6 ± 0.1

Table 6: Values for paste and mortar model with uncertainties provided in fundamental units (data were rounded to nearest hundredth). The uncertainty is 10 % on the shear stress and viscosity.

0% Model (paste)			20% Model (mortar)		
Shear Rate [1/s]	Shear Stress [Pa]	Viscosity [Pa·s]	Shear Rate [1/s]	Shear Stress [Pa]	Viscosity [Pa·s]
220.0	1416.6	6.4	169.4	1985.2	11.7
150.0	982.8	6.6	115.5	1377.3	11.9
100.0	670.0	6.7	77.0	939.0	12.2
65.0	448.3	6.9	50.1	628.2	12.6
55.0	384.2	7.0	42.4	538.5	12.7
45.0	319.7	7.1	34.7	448.0	12.9
36.6	264.9	7.2	28.2	371.3	13.2
34.7	252.5	7.3	26.7	353.8	13.2
32.7	239.7	7.3	25.2	335.9	13.3
30.8	226.9	7.4	23.7	318.0	13.4
28.9	214.4	7.4	22.3	300.4	13.5
27.0	201.7	7.5	20.8	282.6	13.6
25.0	188.5	7.5	19.3	264.2	13.7
23.1	175.8	7.6	17.8	246.4	13.8
21.2	163.0	7.7	16.3	228.4	14.0
19.3	150.1	7.8	14.9	210.3	14.1
17.3	136.6	7.9	13.4	191.4	14.3
15.4	123.5	8.0	11.9	173.1	14.6
13.5	110.4	8.2	10.4	154.7	14.8
11.6	97.0	8.3	9.0	135.9	15.2
10.0	85.4	8.5	7.7	119.7	15.5
9.7	83.0	8.6	7.4	116.3	15.6
7.8	69.2	8.9	6.0	97.0	16.2
5.8	54.9	9.4	4.5	77.0	17.1
3.9	40.0	10.2	3.0	56.1	18.6
2.0	24.0	12.0	1.5	33.6	21.8
1.7	21.6	12.7	1.3	30.3	23.2
1.5	20.1	13.4	1.16	28.1	24.4
1.3	18.5	14.2	1.00	25.9	25.9
1.1	16.9	15.4	0.85	23.7	28.0
1.0	16.1	16.1	0.77	22.6	29.3
0.9	15.3	17.0	0.69	21.4	30.9
0.7	13.7	19.5	0.54	19.1	35.5
0.5	12.0	24.0	0.39	16.8	43.6
0.4	11.1	27.8	0.31	15.6	50.6
0.20	9.3	46.3	0.23	14.3	62.0
0.15	8.7	58.3	0.15	13.0	84.3
0.10	8.2	81.7	0.12	12.3	106.1
0.08	7.9	99.0	0.08	11.5	148.8
0.07	7.8	111.1	0.06	11.1	180.1

4.2 Concrete simulation

The mortar viscosity from Section 4.1 was input into the simulation code to serve as the matrix fluid for the simulated concrete. The 10 mm glass beads were modeled as spherical inclusions with 944 spheres used to represent the 40 % volume fraction suspension. The uncertainty of the simulated suspension viscosity was derived from calculating the standard deviation of the stress values, which is proportional to viscosity, over a range of strain (usually strain values of approximately 5 to 10). Four different shear rates were used in the concrete simulation and the viscosity at each shear rate are given in Table 7. When suitably rescaled [9], the model concrete simulation data falls on top of the viscosity vs. shear rate curve of the matrix fluid (or indeed, the matrix fluid of the concrete which is a mortar). The scaling parameters, with uncertainty calculated as in Section 5.3.2, shown in Table 8, are then used to generate predictive curves of the suspension's viscosity vs shear-rate, as shown in Figure 7 for the 40 % volume fraction suspensions. In other words, to produce the scaled predictive curves, the μ_{sc-c} scaling parameter was factored into the viscosity variable, μ , in equation (1). Similarly, the γ_{sc-c} scaling parameter was factored into the shear rate variable, $\dot{\gamma}$, in equation (1).

In Figure 7, the SRM 2497 (concrete) is shown as the simulation data for 40 % volume fraction (\square symbol). Two lines are calculated (green and red). The green line (Table 10) is calculated using the scaling factors in Table 8 and the paste baseline, while the red line (Table 11) is calculated using the scaling factors and the mortar baseline. Clearly the red and green curves overlap as the same functional form, as expressed in equation (1), is being rescaled.

From the data obtained (Tables 10-11), it is possible to calculate the plastic viscosity and yield stress, i.e., the Bingham parameters (Table 9).

The curve for concrete can be also described using the function in equation 1. The new coefficients would be: (uncertainty in parenthesis)

$$\begin{aligned} A1 &= 35 \text{ (6.6)}; B1 = 0.94; C1 = 107.1 \text{ (9.7)} \\ A2 &= 62.3 \text{ (8.1)}; B2 = 0.53; C2 = 84.9 \text{ (7.4)} \\ a &= 4 \end{aligned}$$

Again, the viscosity is in units Pa-s and shear rate is in units s^{-1} . The uncertainty is evaluated using the NIST Uncertainty Machine (<https://uncertainty.nist.gov/>) with the assumption that the errors in the Eq. 1 parameters are Gaussian.

Table 7: Simulation results for concrete.

Shear Rate [1/s]	Concrete Simulated Viscosity [Pa-s]
0.124	339 \pm 10
1.24	138 \pm 4
12.38	101 \pm 3
123.85	87 \pm 3

Table 8: Scaling parameters to factor the SRM2497- paste or mortar component curve to a concrete curve.

Concentration- 10 mm beads (40 %)	μ_{sc-m} factor	$\dot{\gamma}_{sc-m}$ factor
From the paste	14 ± 1	0.25 ± 0.03
From the mortar	7.9 ± 0.7	0.33 ± 0.06

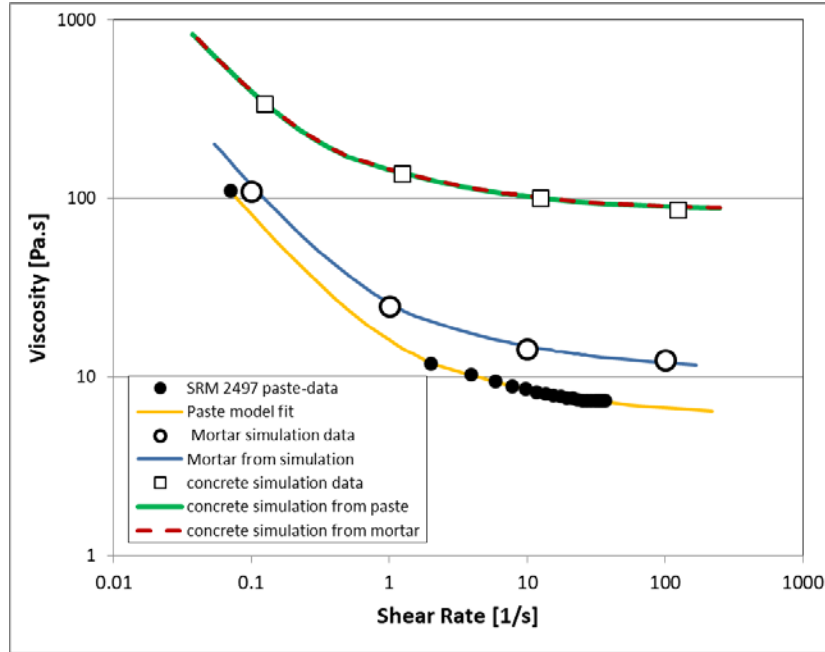


Figure 7: Numerical model simulation for concrete from scaling parameters in Table 8 is shown here. The concrete model curve is representing two overlapping curves, generated either from the paste (green curve) or the mortar model (red curve). The uncertainty is about 10 % (see text).

Table 9: Bingham parameters from the concrete simulation curve (data in Table 10)

Concentration	Yield stress	Plastic Viscosity
40 % 10 mm beads mortar	129 ± 22	88.5 ± 0.4

Table 10: Values for concrete model (40 % of 10 mm beads) with uncertainties provided in fundamental units (data were rounded to nearest hundredth) calculated from the paste model. The uncertainty is 10 %.

Shear Rate [1/s]	Shear Stress [Pa]	Viscosity [Pa·s]
250.0	22030.0	88.1
125.0	11193.0	89.5
100.0	9012.6	90.1
55.0	5064.2	92.1
37.5	3513.6	93.7
25.0	2395.3	95.8
16.3	1602.6	98.6
13.8	1373.6	99.9
11.3	1142.9	101.6
9.1	947.1	103.5
8.7	902.6	104.1
8.2	856.8	104.7
7.7	811.3	105.3
7.2	766.3	106.0
6.8	721.0	106.8
6.3	674.0	107.7
5.8	628.6	108.7
5.3	582.6	109.8
4.8	536.6	111.1
4.3	488.3	112.7
3.9	441.7	114.4
3.4	394.6	116.6
2.9	346.7	119.2
2.5	305.3	122.1
2.4	296.6	122.8
1.9	247.4	127.5
1.5	196.4	134.5
1.0	143.0	146.3
0.50	85.8	171.5
0.43	77.4	182.1
0.38	71.8	191.4
0.33	66.1	203.5
0.28	60.5	219.8
0.25	57.6	230.3
0.23	54.7	243.1
0.18	48.9	279.1
0.13	42.8	342.8
0.10	39.7	397.5

Table 11: Values for concrete model (40 % of 10 mm beads) with uncertainties provided in fundamental units (data were rounded to nearest hundredth) calculated from the mortar model. The uncertainty is 10 %.

Shear Rate [1/s]	Shear Stress [Pa]	Viscosity [Pa·s]
250.25	22172.3	88.6
125.13	11265.3	90.0
100.10	9070.8	90.6
55.06	5096.9	92.6
37.54	3536.3	94.2
25.03	2410.8	96.3
16.27	1613.0	99.2
13.76	1382.5	100.4
11.26	1150.3	102.1
9.16	953.2	104.1
8.68	908.4	104.6
8.19	862.3	105.2
7.71	816.5	105.9
7.23	771.3	106.6
6.76	725.7	107.4
6.26	678.4	108.3
5.79	632.6	109.3
5.31	586.3	110.4
4.83	540.1	111.7
4.34	491.5	113.3
3.86	444.5	115.0
3.39	397.1	117.2
2.91	348.9	119.9
2.50	307.3	122.8
2.42	298.5	123.5
1.94	249.0	128.2
1.46	197.6	135.2
0.98	144.0	147.1
0.50	86.3	172.5
0.43	77.9	183.1
0.38	72.3	192.5
0.33	66.6	204.6
0.28	60.8	221.0
0.25	58.0	231.6
0.23	55.1	244.4
0.18	49.2	280.7
0.13	43.1	344.7
0.10	40.0	399.7

5 Rheological measurements set-up

In this study, the configuration of the rheometer refers to the shape of the spindle for shearing the material inside a holding cup or container. The spindle is typically engaged into the rheometer, which is connected to a computer. The operator then uses a program to control the rotational speed of the spindle while the container is stationary. This approach was used for paste, mortar and concrete.

The paste was also measured using a parallel plate geometry as described in SRM 2492 reports [2]. In brief, it consists of two serrated plates of 35 mm in diameter. The top plate rotates and is connected to a load cell to record the torque generated by the material. The bottom plate is fixed. The gap is $0.600 \text{ mm} \pm 0.001 \text{ mm}$. All tests were conducted after 1 d of mixing and at $23 \text{ }^\circ\text{C} \pm 0.5 \text{ }^\circ\text{C}$.

The next two sections will describe the spindles used as coaxial configuration for paste, mortar and concrete.

5.1 Coaxial geometries

5.1.1 Mortar and paste geometries

The container into which the spindle is lowered is a cylindrical steel cup of 80 mm height and 43 mm diameter with serrated walls. The rheometer used for NIST testing allows a variety of spindles, so long as an adaptor is placed atop the spindle's rod. Three types of spindles were used for this certification study as shown in Figure 8: four-blade vane (vane-type), 6 blades vane and the double helical spiral. A discussion on the various possible geometries for the spindles could be found in the ref [3] and [13].

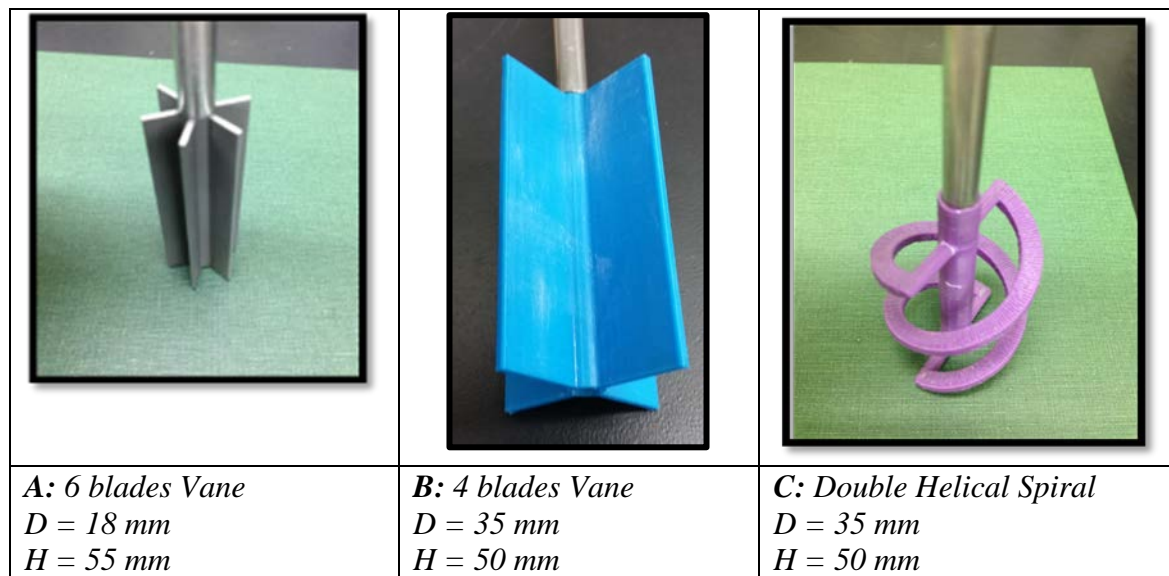


Figure 8: Geometries used for paste and mortar testing

5.1.2 Concrete geometries

The rheometer used for concrete operates on the same principle as the rheometer used for mortar. The concrete container dimensions were 210 mm in diameter and 350 mm height (Figure 9). The surface of the container had vertical ribs to control slippage. Two different spindles were used: a vane and a spiral. The vane has the following dimension: Diameter of 101.6 mm (4 in) and a length of 177.8 mm (7 in) and it is shown in Figure 10.

The spiral has the same diameter and length as the vane (Figure 10). The Section 5.1.3 describes how the spiral was constructed.



Figure 9: Container for the concrete measurements

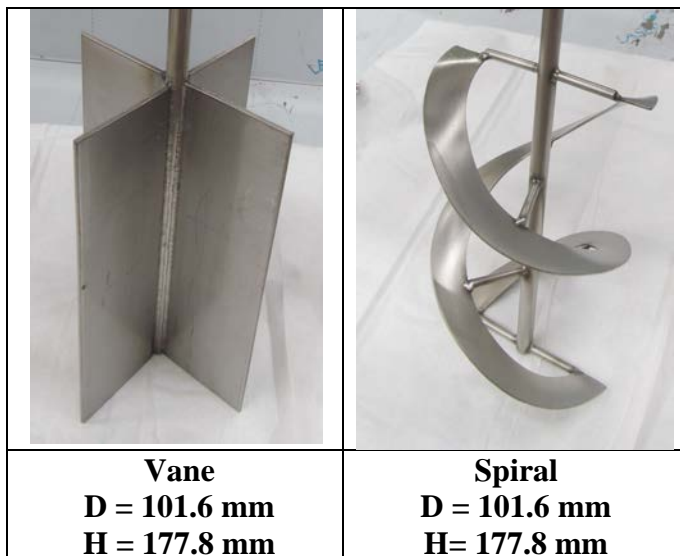


Figure 10: Two geometries types used for testing concrete.

5.1.3 Spirals design

The spiral used for the paste and mortar testing was 3D printed in polymer and a metal axis was placed in the center. The design can be found in the SRM 2493 website and more details are in ref. [13].

The concrete spiral consists of a center 9.52 mm (3/8 in) diameter stainless steel shaft surrounded by two spiral wound stainless auger blades attached to the center shaft with eight 4.76 mm (3/16 in) diameter stainless mounting pins. Manufacturing of the center shaft and support pins is very straightforward. However, translating the spiral blades into a flat panel was a little challenging. From the model spiral available, it was possible to determine the inside and outside arc lengths of the finished spirals. It was also known that both ends of the spiral were square; therefore, the arc length of the inside and outside of the flat pattern would be equal. Also, the width of the spiral was 18.99 mm (0.748 in). Therefore, the outside diameter (OD) of the pattern would equal an internal diameter (ID) of 37.99 mm (1.496 in). Now enough information was available to mathematically determine the shape and dimensions of the flat patterns. Setting the arc lengths equal and knowing that $OD = ID +$

37.99 mm (1.496 in), lead to two equations and two unknowns through which can be solved for the OD and ID of the flat pattern ring. Once, the OD and ID are known, the equation could be solved for the arc length to determine the flat patterns. These dimensions were used to cut the flat patterns using a water jet process. The flat pattern was twisted along the axis of the spindle to form the finished spirals. The spirals fit with the mounting pins perfectly. The spirals were attached to the mounting pins and the pins to the center shaft by Tungsten Inert Gas (TIG) Welding. The spindle was then metal finished and polished to create the final product.

5.2 Experimental design

To determine the certified values, two units of the SRM prepared were selected randomly. For each unit, the mixing procedure described in Section 2.3 was followed and measurements were taken according Table 12.

Table 12: Measurement type at the various stages of mixing

Material type	Parallel plate	Mortar rheometer Section 5.1.1	Concrete rheometer Section 5.1.2
Paste	✓	✓	✓
Mortar (1 mm beads)		✓	✓
Concrete (10 mm beads)			✓

At each stage, the density of paste and mortar were measured using small container of known volume. The temperature was also monitored to ensure that it stays at $23\text{ }^{\circ}\text{C} \pm 2\text{ }^{\circ}\text{C}$. To allow all the test work to be performed, the following schedule was followed:

Day 1: Prepare the paste

Day 2:

- Measure the paste on all rheometer geometries (Table 12)
- The material used in the concrete rheometer is poured back into the mixing bucket after the measurements.
- Measure the density of the paste
- Add the 1 mm beads after calculation of the mass needed (Section 2.3)

Day 3:

- Measure the mortar on all rheometer geometries (Table 12 – not the parallel plate)
- The material used in the concrete rheometer is poured into the mixing bucket after the measurements.
- Measure the density of the mortar
- Add the 10 mm beads after calculation of the mass needed (Section 2.3)

Day 4:

- Measure the concrete in the concrete rheometer only

At each stage of addition of the beads, the concentration of the beads was verified by washing the paste out over sieves to extract the beads.

This schedule was considered acceptable as it is known [2] [6] that the paste rheological properties do not change significantly for up to 7 d.

5.3 Concrete rheometer calibration

To calibrate a rheometer using the data developed in this report, two methods are suggested: 1) using the approximation of the Bingham equation, Section 5.3.1 and 2) using a method based on the viscosity vs. shear rate curve and the model described in Section 5.3.2. Here, step by step instruction will be provided on how to proceed using these two suggested methods.

The first step with either method is to prepare the SRM 2497 mixture (paste, mortar or concrete) and to load it in the rheometer to be calibrated. Run at least three tests and use the average to extract the raw data, which consists of the measured torque (T) [N·m] and rotational speed (N) [rad/s] for at least 10 points in the decreasing rotations speed curve (down-curve). The next goal is to convert these values in fundamental units of Pa and s^{-1} , respectively, by using one of the two suggested methods.

The certified values for SRM 2497 paste tested in a parallel plate rheometer are used here as reference points. Ideally, the results of any other spindle that is used to test the SRM 2497 should reproduce the certified values. Using such criteria, the raw data simply needs to be calibrated to the SRM 2497 certified values. Thus, the next step would be to convert the data obtained with the different tools (Section 5.1) into fundamental units by using SRM 2497. The next two Sections 5.3.1 and 5.3.2 will describe how this is done.

The same process described in Sections 5.3.1 and 5.3.2 could be used to calibrate any rheometer by using SRM 2497, by selecting either method as described in the certificate¹. A web based software and a spreadsheet are posted on the NIST website that should help the user to calculate the necessary calibration factors.

5.3.1 Calibration based on the Bingham parameters

To transform the data generated in this report using the Bingham approach, the SRM 2497 paste certified values were used as the base line. The Bingham parameters of the SRM 2497 paste were extracted from the certificate and compared to the parameters calculated from the experimental or model data, using only the linear part of the curve (torque vs. rotational speed). The schematic shown in Figure 1 explains the calibration process in a sequential form. A spreadsheet was developed for this procedure and is posted on the SRM 2497 website. This file can be used by following a “how to” fact sheet, which will be available on the same spreadsheet.

The calibration process begins by running at least three tests with a geometry of choice on a sample of SRM 2497 and finding the average values from the produced torque and respective rotational speed. Since the raw data ideally matches the SRM 2497 certified values either for the paste, or the model data, then the torque and rotational speed can be scaled to match the known certified viscosity and shear rate. This implies that the shear stress (τ), shear rate ($\dot{\gamma}$), and viscosity (μ) are fundamentally proportional to the torque (T),

¹ www.nist.gov under “Standard Reference Materials”

rotational speed (N), and angular momentum (Γ/N), respectively. In other words, the (Γ vs. N) results from the new geometry are scaled to match the (τ vs. $\dot{\gamma}$) certified SRM 2497 values by calculating scaling factors K_τ and K_μ . Figure 11 provides a schematic of the procedure. The calibration factors convert the two raw variables into fundamental rheology units by using the proportionality relationships. Also, if preferable, the two calibration factors listed would produce a direct shear rate scaling factor, K_γ , by means of *equation (5)* which is derived from the known relationship for Bingham materials shown in *equation (4)*.

$$\mu = \tau / \dot{\gamma} \quad [\text{Pa}\cdot\text{s}] \quad [4]$$

Thus, the shear rate calibration factor would be:

$$K_\gamma = K_\tau / K_\mu \quad [5]$$

The best results using this method are obtained when the shear rate is larger than 1 s^{-1} or when using the linear portion of the curve. The flow curve of shear stress vs. shear rate is not linear for shear rates lower than 1 s^{-1} , while the Bingham model implies that the relationship remains linear. The factors K represent the influence of the rheometer geometry on the results.

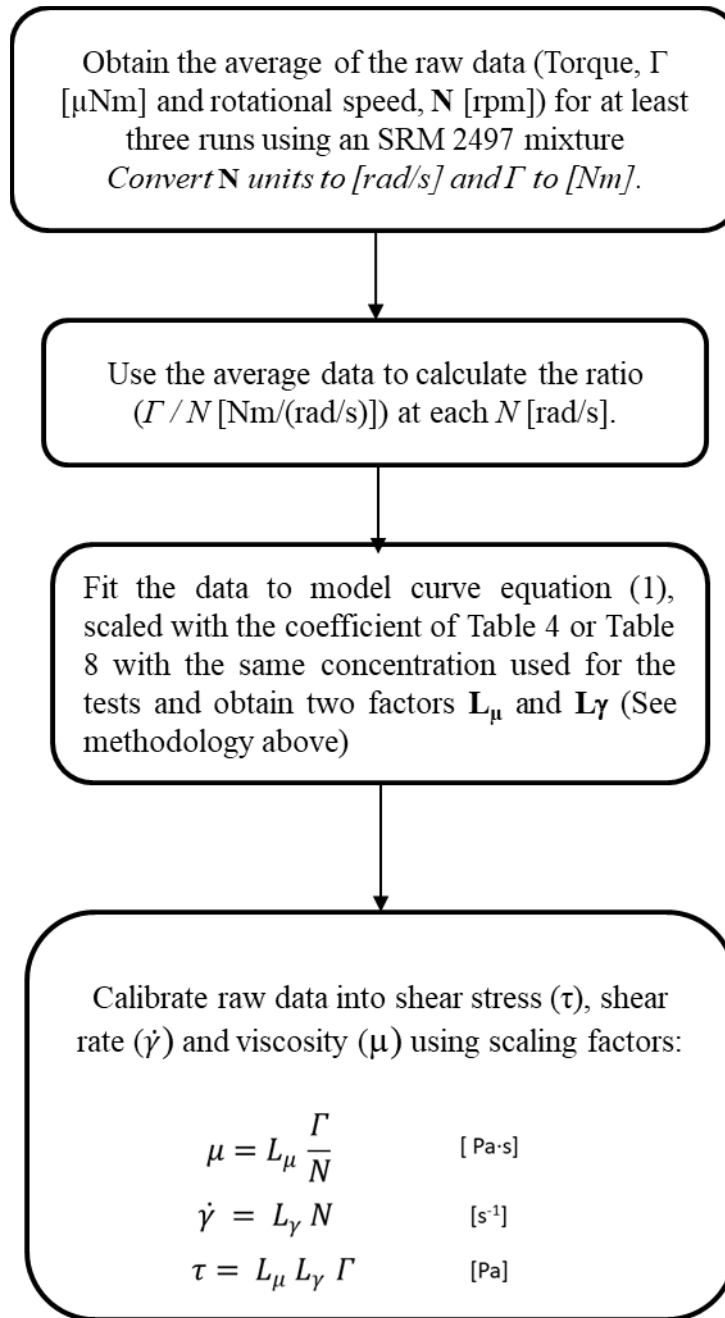


Figure 11: Schematic for using Bingham parameters to calibrate a concrete rheometer from raw torque and rotational speed and converting results to fundamental rheological variables, viscosity and shear rate.

Note: a) This process is applied for calibration of any spindle used in coaxial rheometer.

b) The conversion from rpm to rad/s requires multiplication by $2\pi/60$.

5.3.2 Calibration using the Viscosity vs. Shear rate curve

The second method proposed is to use the viscosity vs. shear rate curve, as represented by equation (1) and comparing with the data measured using the same material (i.e., same concentration of beads). This comparison can be achieved by calculating two scaling factors, L_μ and L_γ , that will be used for all future calculation to convert torque to shear rate when measuring unknown materials. See Figure 12 for a scheme of the calibration process.

$$\mu = L_{\mu} \frac{\Gamma}{N} \quad [Pa \cdot s] \quad [6]$$

$$\dot{\gamma} = L_{\gamma} N \quad [s^{-1}] \quad [7]$$

$$\tau = L_{\mu} L_{\gamma} \Gamma \quad [Pa] \quad [8]$$

To calculate the factors L , the measured curve needs to be shifted along both the Y and X axes until it matches the reference curve (SRM 2497 paste or the concrete model curve). An algorithm was developed to fit the data by least square regression to equation (1). This equation can be simplified by algebra, using the same parameters as equation (1), arriving at the following equivalent:

$$\mu = \frac{\left(C_2 + \frac{A_2}{\dot{\gamma}^{B_2}}\right) + \left(C_1 + \frac{A_1}{\dot{\gamma}^{B_1}}\right) e^{a(\dot{\gamma}-1)}}{1 + e^{a(\dot{\gamma}-1)}} \quad [9]$$

The computation of the L factors can be accomplished as follows:

1. Define a statistical model for the n measurement pairs $\left(N_i, \frac{\Gamma_i}{N_i}\right)$ based on the SRM 2497 paste as:

$$\dot{\gamma}_i = L_{\gamma} \cdot N_i, \quad i = 1, \dots, n$$

$$\frac{\Gamma_i}{N_i} \sim N(\mu_i, \sigma^2), \quad i = 1, \dots, n$$

where

$$\mu_i = L_{\mu} \cdot \frac{\left(C_2 + \frac{A_2}{\dot{\gamma}_i^{B_2}}\right) + \left(C_1 + \frac{A_1}{\dot{\gamma}_i^{B_1}}\right) e^{2a(\dot{\gamma}_i-1)}}{1 + e^{2a(\dot{\gamma}_i-1)}}, \quad i = 1, \dots, n,$$

$$A_1=8.62; B_1=0.94; C_1=7.49$$

$$A_2=8.89; B_2=0.53; C_2=5.94$$

$$a = 4$$

Prior distributions:

$$\sigma \sim \text{Gamma}(1.0E - 5, 1.0E - 5)$$

$$L_{\gamma} \sim \text{Uniform}(0.5, 10)$$

$$L_{\mu} \sim \text{Uniform}(0, 4)$$

2. Compute the values of L_{γ} and L_{μ} using a Markov Chain Monte Carlo method implemented in OpenBUGS [14], executed using the following R code [15].

The code requires that both R and OpenBUGS be installed, both are free to download. R can be obtained at <http://www.R-project.org/>, OpenBUGS at <http://www.openbugs.net/w/Downloads>.

The only input to the program that is needed are the values N and $\frac{r}{N}$, and the sample size n . Pasting the entire program below into an R window will produce the estimates of the L factors as well as a plot which shows the fit to the SRM 2497 function.

The following is an example using the measurement data for SRM 2497 with six-blade vane configuration (Figure 10). In the program $X = N$ in rad/s, and $Y = \frac{r}{N}$ in $Pa \cdot s$

```
#####  
library(R2OpenBUGS)  
  
##### type data X, Y, n here:  
  
linedata<-  
list(y=c(0.489,0.509,0.542,0.599,0.662,0.767,0.9,1.04,1.208,1.402,1.691,2.032,2.426,3.02  
4,3.822,4.512,6.063,7.747,9.554,13.074,17.743,22.93),  
x=c(10.477,7.538,5.426,3.905,2.81,2.022,1.455,1.048,0.754,0.542,0.39,0.281,0.202,0.145,  
0.105,0.075,0.054,0.039,0.028,0.02,0.015,0.01), n=22)  
  
#####  
  
####SRM 2497 curve for comparison to see the fit  
visc97<-  
c(7.45,7.39,7.39,7.38,7.4,7.4,7.4,7.53,7.66,7.68,7.82,7.96,8.12,8.28,8.59,8.95,9.48,10.4,12,  
111.14)  
  
sr97<-  
c(36.59,34.69,32.74,30.81,28.91,27,25.03,23.13,21.22,19.32,17.34,15.44,13.54,11.63,9.66,  
7.76,5.84,3.91,2,0.07)  
#####  
##### OpenBUGS code and inits  
  
lineinits<-function(){list(sig=1)}  
linemodel <- function() {sig~dgamma(1.0E-5,1.0E-5)  
Lg~dunif(0.5,10)  
  
Lm~dunif(0,4)  
Lmu<-1/Lm  
Ltau<-Lg/Lm  
a<--4  
a2n<-8.89  
a2sig<-1/(0.18*0.18)  
b2n<-0.53  
b2sig<-1/(0.06*0.06)  
c2n<-5.94  
c2sig<-1/(0.24*0.24)  
a1n<-8.62
```

```

a1sig<-1/(1.18*1.18)
b1n<-0.94
b1sig<-1/(0.05*0.05)
c1n<-7.49
c1sig<-1/(0.35*0.35)

```

```

a2~dnorm(a2n,a2sig)
b2 ~dnorm(b2n,b2sig)
c2 ~dnorm(c2n,c2sig)
a1 ~dnorm(a1n,a1sig)
b1 ~dnorm(b1n,b1sig)
c1 ~dnorm(c1n,c1sig)

```

```

for (i in 1:n){ srd[i]<-x[i]*Lg
                num[i]<-a*srd[i]
                top[i]<-a*(srd[i]-1)
mu[i]<-Lm*(c2*exp(a)+c1*exp(num[i])+a1*exp(num[i])/pow(srd[i],b1)+a2*exp(a)/
pow(srd[i],b2))/(exp(a)+exp(num[i]))
y[i]~dnorm(mu[i],sig)
                }
}

```

```
#####
```

```
##### run the OpenBUGS
```

```

lineout<-bugs(data=linedata,inits=lineinits,parameters=c("Lg","Lmu","Ltau"),
model.file=linemodel,n.chains=1,n.iter=100000,n.burnin=15000,n.thin=10)

```

```
#####print the values of the L factors
```

```
print(lineout, digits=7)
```

```
#####
```

```
##### compute the calibrated curve
```

```
Lg<-lineout$mean["Lg"]
```

```
Lmu<-lineout$mean["Lmu"]
```

```
viscnew<-linedata$y*Lmu$Lmu
```

```
srnew<-linedata$x*Lg$Lg
```

```
### plot the SRM 2497 curve and the calibrated curve
```

```
plot(visc97~sr97,type="p",col="blue", lwd=3, xlab="shear rate (1/s)", ylab =" viscosity
(Pa s)", log="x")
```

```
title("Viscosity vs. Shear rate ", sub="blue points are SRM 2497, cyan line new material")
```

```
lines(viscnew~srnew, type="l",col="Cyan",log="x")
```

```
#####
```

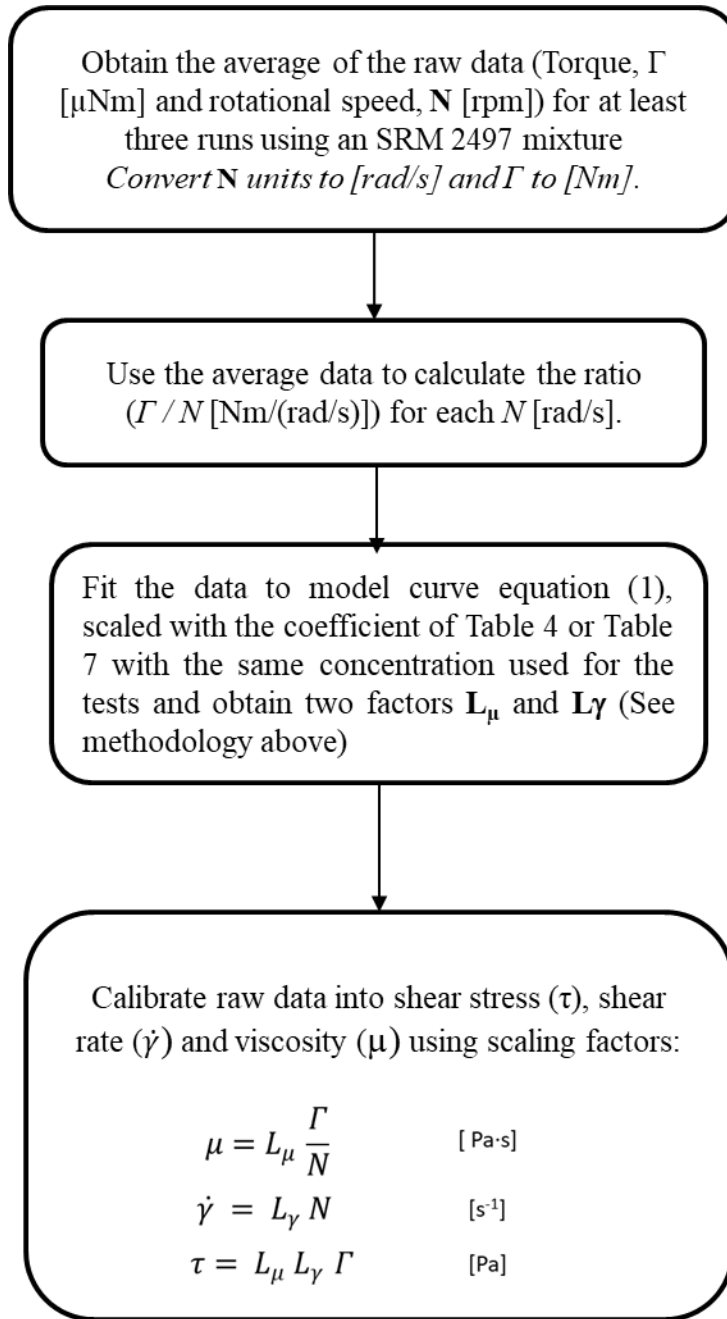



Figure 12: Schematic for the calibration of rheometer data from raw torque and rotational speed to fundamental rheological variables, viscosity and shear rate.

*Note: a) This process is applied for calibration of any spindle used in coaxial rheometer.
b) The conversion from rpm to rad/s requires multiplication by $2\pi/60$.*

6 Results and analysis

6.1 Introduction

This section and the appendices provide all the data collected with the statistical analysis. Also, the data were calibrated as described in Section 5.3. The parallel plate data are presented first as they are considered the fundamental basis for all the paste results in all the rheometers' configurations.

6.2 Paste on parallel plate

The paste, a mixture of corn syrup solution and limestone, was prepared as described in Section 2.3. It was then tested using a parallel plate rheometer. Two mixtures were prepared, and each was run 3 times. All the data obtained are provided in Appendix A:

Mix A: NIST code CR-46 B, C, D

Mix B: NIST code CR-58 A, B, C

6.2.1 Statistical analysis

The 6 runs were treated as independent replicates of the flow curves. Only the “down curve” data was used, that is, the shear stress for the 20 shear rates starting at 36.59 s^{-1} and decreasing to 0.07 s^{-1} .

For each of the shear rates, a consensus shear stress was computed together with an uncertainty using the model

$$SS_{ij} = \theta_i + \varepsilon_{ij}, i = 1, \dots, 20, j = 1, \dots, 6$$

where θ_i were the consensus torque values for the 6 replicates.

Estimation was performed via Markov Chain Monte Carlo methods [14] (which require prior distributions on the parameters of the model) with

$$\theta_i \sim N(0, 1.0E5), \varepsilon_{ij} \sim N(0, \sigma_i^2), \sigma_i^2 \sim \text{Gamma}(1.0E5, 1.0E5), i = 1, \dots, 20.$$

The computations were done using the software OpenBUGS [15] using the code given in Section 6.2.2. The posterior mean, standard deviation, and 95% highest posterior density interval at each shear rate were used for the estimate (SS), standard (u(SS)) and expanded uncertainty (Table 13). These estimates were very stable with respect to the Gaussian and Gamma distributions of the parameters. The following table contains the results.

Table 13: Paste on parallel plate average curve with uncertainty.

Shear rate (1/s)	Shear Stress (Pa)	Uncertainty Shear Stress (Pa)
36.59	272.5	6.1
34.69	256.5	5.5
32.74	241.9	4.5
30.81	227.4	4.1
28.91	214.0	4.2
27.00	199.7	4.2
25.03	185.3	3.2
23.13	174.1	3.3
21.22	162.5	3.2
19.32	148.5	2.9
17.34	135.5	2.6
15.44	122.9	2.5
13.54	110.0	2.3
11.63	96.3	1.9
9.659	83.0	1.7
7.76	69.4	1.4
5.84	55.4	1.1
3.91	40.65	0.85
2.00	23.99	0.50
0.07	7.78	0.38

Yield stress and viscosity are respectively the intercept and slope of a straight line fitted to shear stress vs. shear rate. Only the “down curve” data (decreasing shear rates) was used to fit the regression. A linear model fits the flow curve data reasonably well and provides an approximation to the flow curves given in the previous section. The results for each run are shown in Table 14.

Yield stress and viscosity were estimated using a random effects regression model

$$SS_{ij} = a_i + b_i \Omega_j + \varepsilon_{ij}$$

where

$$a_i \sim N(\alpha, \sigma_\alpha^2), b_i \sim N(\beta, \sigma_\beta^2), \varepsilon_{ij} \sim N(0, \sigma_i^2), i = 1, \dots, 6, j = 1, \dots, 20.$$

In this model, a_i are the yield stress values for the 6 individual replicates, and α is the consensus yield stress value. Similarly, b_i are the viscosity values for the 6 individual mixes and β is the consensus viscosity. This model accounts for measurement uncertainty

and lack of fit of each replicate using σ_i , and also for between replicate variability using σ_α and σ_β .

Fitting was done using Markov Chain Monte Carlo methods which require prior distributions on the parameters of the model. These were

$$\alpha \sim N(0,1.0E2), \beta \sim N(0,1.0E2), \sigma_\alpha^2 \sim \text{Gamma}(1.0E5,1.0E5), \sigma_\beta^2 \sim \text{Gamma}(1.0E5,1.0E5)$$

$$\sigma_i^2 \sim \text{Gamma}(1.0E5,1.0E5), i = 1, \dots, 6.$$

Table 14: Bingham parameters for each run and the average, parallel plate measurements with paste

Sample NIST code	Yield stress a_i, α [Pa]	Yield stress standard uncertainty	Plastic Viscosity b_i, β [Pa.s]	Plastic Viscosity standard uncertainty
CR-46 A	12.58	0.52	7.45	0.03
CR-46 B	12.47	0.54	6.64	0.03
CR-46 C	12.53	0.51	7.03	0.03
CR-58 A	12.47	0.53	6.96	0.03
CR-58 B	12.60	0.54	7.22	0.03
CR-58 C	12.60	0.53	6.89	0.03
Consensus (α, β)	12.53	0.47	7.03	0.15

6.2.2 OpenBUGS code

This program computes the yield stress in 1000*Nm (alpha) and viscosity in 1000*Nm*s (betad) for the cases where there are 5 replicates of 20 points each. The data is first reduced so that only the down-curve is included, that is, the first 25 points are eliminated. It also obtains the average curves in $\mu\text{Nm}/1000$ (theta).

Use with pre20zerods.txt, pre40zerods.txt, 20ds.txt, 40ds.txt and the same for the other two geometries (bv and scc)

OpenBUGS code:

```
{ alpha~dnorm(0,1.0E-2)
beta~dnorm(0,1.0E-2)
siga~dgamma(1.0E-5,1.0E-5)
sigb~dgamma(1.0E-5,1.0E-5)
sigd~dgamma(1.0E-5,1.0E-5)
for(i in 1:6){ a[i]~dnorm(alpha,siga)
               b[i]~dnorm(beta,sigb)
}
for(i in 1:120){ mean[i]<-a[mix[i]]+b[mix[i]]*sr[i]
```

```

ss[i]~dnorm(mean[i],sigd)}

for(j in 1:20){theta[j]~dnorm(0,1.0E-5)
  sigthe[j]~dgamma(1.0E-5,1.0E-5)

}

for(i in 1:120){ss2[i]~dnorm(theta[posit[i]],sigthe[posit[i]])}

}

list(sigd=1,siga=1,sigb=1, sigthe=c(1,1,1,1,1,1,1,1,1,1,1,1,1,1,1,1,1,1,1,1))

```

6.3 Paste with the coaxial

This section presents the paste data collected (corn solution and limestone) in a coaxial rheometer using the three different spindles shown in Section 5.1.1. Appendix B shows the raw data as collected, while this section will provide the average curve as well as the statistical analysis. The data will also be calibrated using the parallel plate rheometer data (Section 6.2) following the method described in Section 5.3.

There were two mixes, and each was tested three consecutive times, thus, 6 runs were analyzed for each geometry. Also, only the down curves were used in the analysis.

6.3.1 Statistical Analysis

Using the data from Appendix B, for each of the shear rates, a consensus sheer stress was computed together with an uncertainty using the model

$$SS_{ij} = \theta_i + \varepsilon_{ij}, i = 1, \dots, 20, j = 1, \dots, 6$$

where θ_i were the consensus torque values for the 6 replicates.

Estimation was performed via Markov Chain Monte Carlo methods [14] (which require prior distributions on the parameters of the model) with

$$\theta_i \sim N(0, 1.0E5), \varepsilon_{ij} \sim N(0, \sigma_i^2), \sigma_i^2 \sim \text{Gamma}(1.0E5, 1.0E5), i = 1, \dots, 20.$$

The computations were done using the software OpenBUGS [15]. The posterior mean, standard deviation, and 95% highest posterior density interval at each shear rate were used for the estimate (SS), standard (u(SS)) and expanded uncertainty. These estimates were very stable with respect to the Gaussian and Gamma distributions of the parameters. The tables Table 15 to Table 17 contains the results.

A straight-line model fits the flow curve data reasonably well and provides an approximation to the flow curves given in the previous section. Yield stress and viscosity were estimated using a random effects regression model

$$SS_{ij} = a_i + b_i \Omega_j + \varepsilon_{ij}$$

where

$$a_i \sim N(\alpha, \sigma_\alpha^2), b_i \sim N(\beta, \sigma_\beta^2), \varepsilon_{ij} \sim N(0, \sigma_i^2), i = 1, \dots, 6, j = 1, \dots, 20.$$

Table 15: Flow curve and uncertainty for Spiral for paste. SR is the rotational speed and SS is the torque, U is the uncertainty of the torque

SR (1/min)	SS (μNm)	U(SS)
21.2	6799.51	60.13
14.7	5115.09	34.81
10.2	3923.34	18.66
7.12	3071.76	16.64
4.95	2446.58	19.77
3.44	1993.26	23.99
2.39	1671.67	28.46
1.66	1428.04	32.51
1.16	1251.68	36.04
0.803	1121.77	36.26
0.558	1021.05	35.85
0.388	944.63	36.22
0.27	886.45	37.98
0.187	841.51	35.92
0.13	806.05	36.4
0.0905	778.22	36.27
0.0628	756.81	36.27
0.0436	739.99	35.86
0.0302	726.47	36.02
0.0209	716.86	36.94

Table 16: Flow curve and uncertainty for 4-vane for paste. SR is the rotational speed and SS is the torque, U is the uncertainty of the torque

SR (1/min)	SS (μNm)	U(SS)
69.2	25381.60	149.12
48.1	18516.70	113.84
33.5	13599.90	92.34
23.3	10080.30	72.32
16.2	7579.68	65.03
11.2	5771.45	60.18
7.82	4471.66	58.81
5.43	3526.12	59.96
3.78	2843.34	60.17
2.63	2346.82	59.29
1.83	1980.58	55.67
1.27	1713.79	55.95
0.88	1514.93	59.22
0.61	1365.01	57.67
0.43	1253.41	57.43
0.30	1169.57	55.73
0.21	1104.62	56.15
0.14	1052.08	53.29
0.10	1013.03	52.56
0.07	982.86	52.93

Table 17: Flow curve and uncertainty for 6-vane for paste. SR is the rotational speed and SS is the torque, U is the uncertainty of the torque

SR (1/min)	SS (μNm)	U(SS)
69.2	5364.66	41.97
48.1	3986.76	35.45
33.5	3000.01	30.10
23.3	2291.81	27.10
16.2	1776.55	27.02
11.2	1409.92	24.07
7.82	1131.67	22.88
5.43	929.80	22.37
3.78	776.34	21.19
2.63	659.72	20.27
1.83	571.03	18.86
1.27	502.48	18.66
0.88	449.31	18.58
0.61	407.84	16.99
0.43	375.52	16.68
0.30	349.04	16.28
0.21	328.66	15.69
0.14	312.40	15.26
0.10	298.56	14.72
0.07	287.68	14.53

In this model, a_i are the yield stress values for the 6 individual replicates, and α is the consensus yield stress value. Similarly, b_i are the viscosity values for the 6 individual mixes and β is the consensus viscosity. This model accounts for measurement uncertainty and lack of fit of each replicate using σ_i , and also for between replicate variability using σ_α and σ_β .

Fitting was done using Markov Chain Monte Carlo methods which require prior distributions on the parameters of the model. These were

$$\alpha \sim N(0,1.0E2), \quad \beta \sim N(0,1.0E2), \quad \sigma_\alpha^2 \sim \text{Gamma}(1.0E5,1.0E5), \quad \sigma_\beta^2 \sim \text{Gamma}(1.0E5,1.0E5)$$

$$\sigma_i^2 \sim \text{Gamma}(1.0E5,1.0E5), i = 1, \dots, 6.$$

Table 18 to Table 13 show the results obtained for each run as well as the average data and the uncertainty. These values are not in fundamental units, as they need to be transformed using the data from the calibration method and the parallel plate values. (see

Table 18 Yield stress and plastic viscosity values for each sample and for consensus for paste– spiral spindle

Sample NIST Code	Yield Stress		Plastic Viscosity	
	Value a_i, α [μNm]	standard uncertainty [μNm]	Value b_i, β [$\mu\text{Nm}\cdot\text{min}$]	Standard uncertainty [$\mu\text{Nm}\cdot\text{min}$]
CR-46 E	809.85	29.87	291.03	3.25
CR-46 F	814.94	28.44	292.04	3.51
CR-46 G	823.25	27.22	293.48	4.19
CR-58 D	867.87	28.23	287.56	4.03
CR-58 E	870.44	28.13	288.36	3.66
CR-58 F	877.85	29.94	289.93	3.24
Consensus (α, β)	844	25	290.4	2.9

Table 19 Yield stress and plastic viscosity values for each sample and for consensus for paste – 4-vane spindle

Sample NIST Code	Yield Stress		Plastic Viscosity	
	Value a_i, α [μNm]	standard uncertainty [μNm]	Value b_i, β [$\mu\text{Nm}\cdot\text{min}$]	Standard uncertainty [$\mu\text{Nm}\cdot\text{min}$]
CR-46 H	1279.27	66.19	354.85	2.91
CR-46 I	1295.49	54.58	356.21	2.46
CR-46 J	1309.37	49.93	357.47	2.55
CR-58 G	1322.99	50.00	355.91	2.46
CR-58 H	1333.42	53.09	356.63	2.42
CR-58 I	1354.05	68.09	358.44	2.98
Consensus (α, β)	1316	45	356.6	2.2

Table 20: Yield stress and plastic viscosity values for each sample and for consensus for paste – 6-vane spindle

Sample NIST Code	Yield Stress		Plastic Viscosity	
	standard uncertainty [μNm]	Value b_i, β [$\mu\text{Nm}\cdot\text{min}$]	standard uncertainty [μNm]	Viscosity standard uncertainty [$\mu\text{Nm}\cdot\text{min}$]
CR-46 H	406.64	21.72	73.47	1.00
CR-46 I	409.41	19.77	73.81	0.92
CR-46 J	413.35	18.02	74.24	0.88
CR-58 G	424.66	18.56	74.17	0.87
CR-58 H	427.08	19.57	74.48	0.90
CR-58 I	429.92	21.58	74.84	0.99
Consensus (α, β)	419	16	74.17	0.77

6.3.2 Calibration factors and data in fundamental units for paste coaxial

Using the method described in Section 5.3, the data from **Table 15** to **Table 17** were used to calculate the calibration factors. The data are shown in **Table 22** to **Table 24** (Figure 13) are generated using these factors to convert them in fundamental units. This information is provided as an example on how the data from Section 6.3.1 can be used for other geometries.

Table 21: Calibration factors for the three geometries used for paste

	Spiral	4-Vane	6-Vane
$K\tau$ [Pa/N·m]	10.1	9.5	20.3
$K\gamma$ [-]	3.8	4.6	1.9
$K\mu$ [Pa·s/N·m·s]	2.7	2.1	10.5

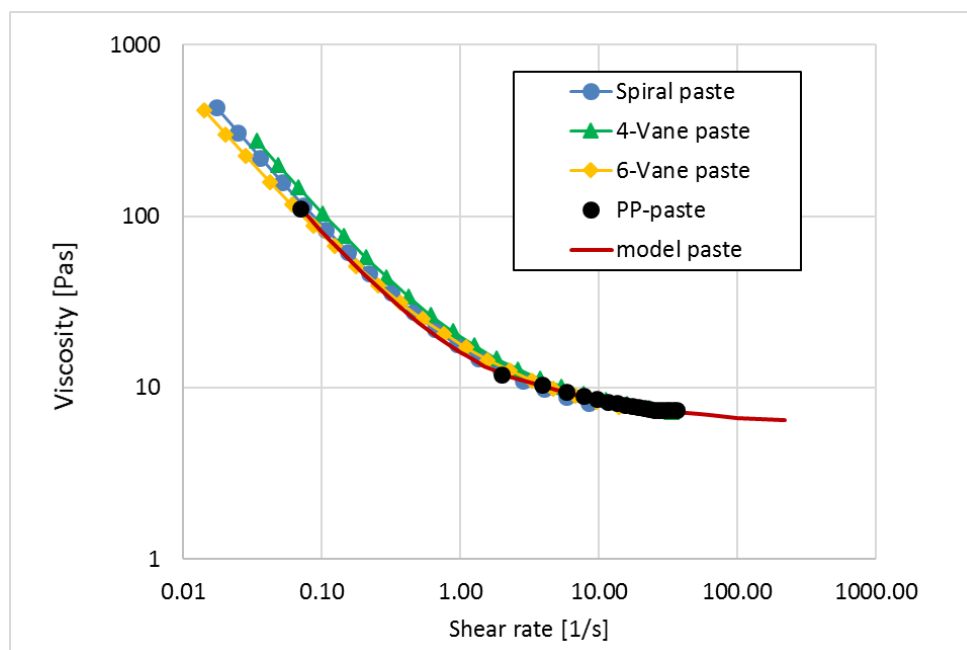


Figure 13: Paste data after calibration. See uncertainty in Table 22 to Table 24.

Table 22: Calibrated data for Spiral for paste

Shear Rate, $\dot{\gamma}$ [1/s]	Shear Stress, τ [Pa]	Uncertainty [Pa]	Viscosity, μ [Pa-s]
8.59	70.7	0.6	8.2
5.96	53.2	0.4	8.9
4.13	40.8	0.2	9.9
2.89	31.9	0.2	11.1
2.01	25.4	0.2	12.7
1.39	20.7	0.3	14.9
0.97	17.4	0.3	17.9
0.67	14.9	0.3	22.1
0.47	13.0	0.4	27.7
0.33	11.7	0.4	35.8
0.23	10.6	0.4	47.0
0.16	9.8	0.4	62.5
0.11	9.2	0.4	84.2
0.08	8.8	0.4	115.5
0.05	8.4	0.4	159.1
0.04	8.1	0.4	220.7
0.03	7.9	0.4	309.2
0.02	7.7	0.4	435.5
0.01	7.6	0.4	617.3
0.008	7.5	0.4	880.1

Table 23: Calibrated data for 4-vane for paste

Shear Rate, $\dot{\gamma}$ [1/s]	Shear Stress, τ [Pa]	Uncertainty [Pa]	Viscosity, μ [Pa-s]
33.41	241.6	1.4	7.2
23.22	176.2	1.1	7.6
16.17	129.45	0.88	8.0
11.25	95.95	0.69	8.5
7.82	72.14	0.62	9.2
5.41	54.93	0.57	10.2
3.78	42.56	0.56	11.3
2.62	33.56	0.57	12.8
1.82	27.06	0.57	14.8
1.27	22.34	0.56	17.6
0.88	18.85	0.53	21.3
0.61	16.31	0.53	26.6
0.42	14.42	0.56	33.9
0.29	12.99	0.55	44.1
0.21	11.93	0.55	57.5
0.14	11.13	0.53	76.9
0.10	10.51	0.53	103.7
0.07	10.01	0.34	148.2
0.05	9.64	0.34	199.7
0.03	9.35	0.35	276.8

Table 24: Calibrated data for 6-Vane for paste

Shear Rate, $\dot{\gamma}$ [1/s]	Shear Stress, τ [Pa]	Uncertainty [Pa]	Viscosity, μ [Pa-s]
13.99	108.9	1.3	7.8
9.72	80.9	1.1	8.3
6.77	60.9	0.9	9.0
4.71	46.5	0.8	9.9
3.28	36.1	0.8	11.0
2.26	28.6	0.7	12.6
1.58	23.0	0.7	14.5
1.10	18.9	0.7	17.2
0.76	15.8	0.6	20.6
0.53	13.4	0.6	25.2
0.37	11.6	0.6	31.3
0.26	10.2	0.6	39.7
0.18	9.1	0.6	51.3
0.12	8.3	0.5	67.1
0.09	7.6	0.5	87.7
0.06	7.1	0.5	116.8
0.04	6.7	0.5	157.1
0.03	6.3	0.5	224.1
0.02	6.1	0.4	299.8
0.01	5.8	0.4	412.6

6.4 Mortar data with the coaxial paste/mortar rheometer

This section presents the mortar data collected (corn solution and limestone and 20 % by volume of 1 mm beads) in a coaxial rheometer using the three different spindles shown in Section 5.1.1. Appendix C shows the raw data collected, while this section provides the average curve as well as the statistical analysis (Table 25 to Table 27). The data will also be calibrated using the parameters calculated in Section 6.3.2.

There were two mixes, and each was tested three consecutive times, thus, 6 runs were analyzed for each geometry. Also, only the down curves were used in the analysis.

6.4.1 Statistical analysis

For each of the shear rates, a consensus sheer stress was computed together with an uncertainty using the model

$$SS_{ij} = \theta_i + \varepsilon_{ij}, i = 1, \dots, 20, j = 1, \dots, 6$$

where θ_i were the consensus torque values for the 6 replicates.

Estimation was performed via Markov Chain Monte Carlo methods [16] (which require prior distributions on the parameters of the model) with

$$\theta_i \sim N(0, 1.0E5), \varepsilon_{ij} \sim N(0, \sigma_i^2), \sigma_i^2 \sim Gamma(1.0E5, 1.0E5), i = 1, \dots, 20.$$

The computations were done using the software OpenBUGS [15]. The posterior mean, standard deviation, and 95% highest posterior density interval at each shear rate were used for the estimate (SS), standard (u(SS)) and expanded uncertainty. These estimates were very stable with respect to the Gaussian and Gamma distributions of the parameters. The following tables contains the results

6.4.2 Yield stress and plastic viscosity

Yield stress and viscosity are respectively the intercept and slope of a straight line fitted to shear stress in terms of shear rate. Only the “down curve” data was used to fit the regression. A straight-line model fits the flow curve data reasonably well and provides an approximation to the flow curves given in the previous section. (Table 28 to Table 30)

Yield stress and viscosity were estimated using a random effects regression model

$$SS_{ij} = a_i + b_i \Omega_j + \varepsilon_{ij}$$

where

$$a_i \sim N(\alpha, \sigma_\alpha^2), b_i \sim N(\beta, \sigma_\beta^2), \varepsilon_{ij} \sim N(0, \sigma_i^2), i = 1, \dots, 6, j = 1, \dots, 20.$$

In this model, a_i are the yield stress values for the 6 individual replicates, and α is the consensus yield stress value. Similarly, b_i are the viscosity values for the 6 individual mixes and β is the consensus viscosity. This model accounts for measurement uncertainty and lack of fit of each replicate using σ_i , and also for between replicate variability using σ_α and σ_β .

Table 25: Flow curve and uncertainty for Spiral for mortar. SR is the rotational speed and SS is the torque, U is the uncertainty of the torque

SR (1/min)	SS (μNm)	U(SS)
21.2	11313.8	262.79
14.7	8433.53	186.03
10.2	6408.28	113.82
7.11	4935.37	73.05
4.95	3866.49	38.69
3.44	3096.61	18.01
2.39	2541.67	6.14
1.66	2124.90	11.53
1.15	1820.00	19.56
0.80	1606.74	25.41
0.56	1435.29	27.69
0.39	1310.26	31.03
0.27	1209.96	34.50
0.19	1133.34	32.59
0.13	1076.72	35.12
0.099	1029.73	35.17
0.069	992.64	35.25
0.049	968.50	37.15
0.039	946.64	36.28
0.029	930.19	38.47

Table 26: Flow curve and uncertainty for 4-vane for mortar. SR is the rotational speed and SS is the torque, U is the uncertainty of the torque

SR (1/min)	SS (μNm)	U(SS)
69.2	49214.20	771.83
48.1	35725.30	512.75
33.5	26180.30	344.56
23.3	19250.10	255.11
16.2	14332.10	177.23
11.2	10816.10	121.08
7.82	8233.28	90.17
5.43	6384.27	78.30
3.77	5043.33	72.70
2.62	4075.17	68.98
1.82	3372.35	66.03
1.27	2840.59	72.77
0.88	2463.23	73.99
0.61	2178.34	65.49
0.43	1961.76	68.83
0.30	1802.79	70.44
0.21	1681.61	70.37
0.14	1590.30	66.22
0.10	1520.26	69.02
0.07	1465.03	65.52

Table 27: Flow curve and uncertainty for 6-vane for mortar. SR is the rotational speed and SS is the torque, U is the uncertainty of the torque

SR (1/min)	SS (μNm)	U(SS)
69.2	10478.90	266.61
48.1	7775.53	139.34
33.5	5798.21	99.08
23.3	4368.81	67.40
16.2	3343.67	54.89
11.2	2598.55	40.53
7.81	2047.15	31.77
5.43	1649.73	28.57
3.78	1341.80	25.59
2.63	1116.73	21.11
1.83	946.57	22.90
1.27	819.31	22.93
0.88	719.53	21.82
0.61	644.14	20.16
0.43	586.01	19.65
0.30	540.71	20.81
0.21	505.58	20.83
0.14	475.92	19.44
0.10	455.32	18.61
0.07	437.32	20.81

Fitting was done using Markov Chain Monte Carlo methods which require prior distributions on the parameters of the model. These were

$$\alpha \sim N(0,1.0E2), \quad \beta \sim N(0,1.0E2), \quad \sigma_\alpha^2 \sim \text{Gamma}(1.0E5,1.0E5), \sigma_\beta^2 \sim \text{Gamma}(1.0E5,1.0E5)$$

$$\sigma_i^2 \sim \text{Gamma}(1.0E5,1.0E5), i=1,\dots,6.$$

Table 28: Yield stress and viscosity for each sample and for consensus for mortar–spiral

Sample NIST Code	Yield Stress		Plastic Viscosity	
	Value a_i, α [μNm]	standard uncertainty [μNm]	Value $a_i,$ α [μNm]	standard uncertainty [μNm]
CR-49 A	1131.81	28.27	511.99	6.93
CR-49 B	1131.53	27.99	512.49	6.91
CR-49 C	1131.74	28.23	519.63	7.11
CR-63 A	1144.32	28.71	474.14	6.97
CR-63 B	1143.81	27.88	475.64	6.93
CR-63 C	1143.28	28.09	482.95	6.83
Consensus (α, β)	1138	24	496	12

Table 29: Yield stress and viscosity for each sample and for consensus for mortar– 4-vane

Sample NIST Code	Yield Stress		Plastic Viscosity	
	Value a_i, α [μNm]	standard uncertainty [μNm]	Value a_i, α [μNm]	standard uncertainty [μNm]
CR-49 F	2074.59	80.53	691.44	6.69
CR-49 G	2079.15	77.29	709.64	6.68
CR-49 H	2081.97	77.49	722.73	6.99
CR-63 E	2081.98	78.02	669.14	7.01
CR-63 F	2088.51	77.98	692.04	6.62
CR-63 G	2092.45	80.85	705.21	6.64
Consensus (α, β)	2083	73	698	11

Table 30 Yield stress and viscosity for each sample and for consensus for mortar– 6-vane

Sample NIST Code	Yield Stress		Plastic Viscosity	
	Value a_i, α [μNm]	standard uncertainty [μNm]	Value $a_i,$ α [μNm]	standard uncertainty [μNm]
CR-49 I	651.08	25.12	142.25	2.12
CR-49 J	651.78	24.60	147.47	2.06
CR-49 K	652.46	24.36	152.50	2.11
CR-63 H	655.53	24.62	141.29	2.13
CR-63 I	657.53	25.36	152.79	2.11
CR-63 J	654.60	24.81	155.22	3.02
Consensus (α, β)	654	22	148.6	3.5

6.4.3 Calibration factors and data in fundamental units for paste coaxial

Using the method described in Section 5.3, the data from Table 25 to Table 27 and the factors shown in Table 21 were used to calculate the data are shown in Figure 14 and in Table 31 to Table 33 in fundamental units.

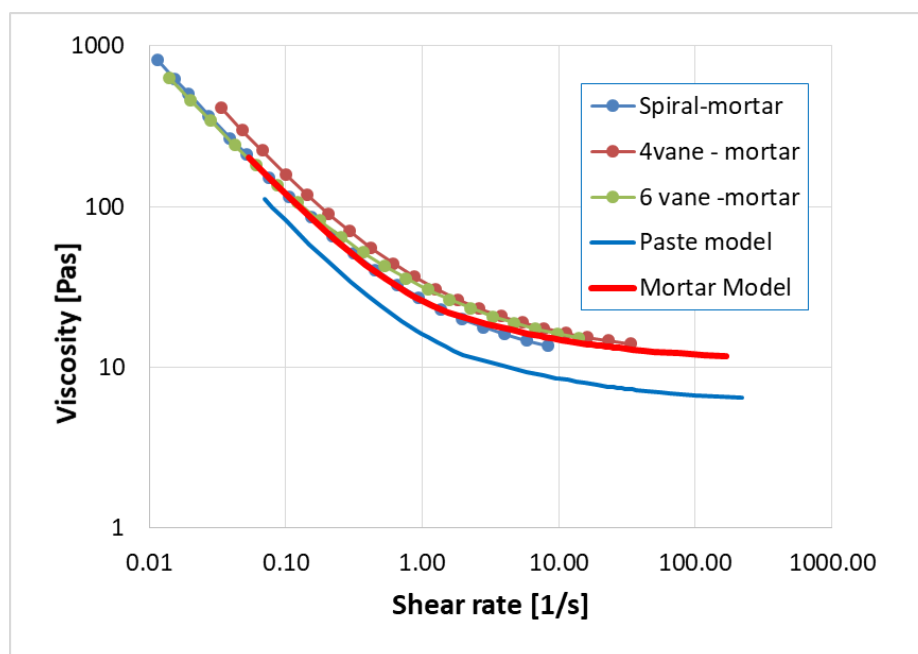


Figure 14: Data calibrated for mortar in the paste/mortar rheometer. Uncertainty is shown in Table 31 to Table 33

Table 31: Calibrated data for Spiral for mortar. U is the uncertainty of the shear stress

Shear Rate, γ [1/s]	Shear Stress, τ [Pa]	U [Pa]	Viscosity, μ [Pa-s]
8.38	114.3	2.7	13.6
5.81	85.2	1.9	14.7
4.03	64.7	1.1	16.0
2.81	49.8	0.7	17.7
1.96	39.1	0.4	19.9
1.36	31.3	0.2	23.0
0.95	25.7	0.1	27.2
0.66	21.5	0.1	32.7
0.45	18.4	0.2	40.4
0.32	16.2	0.3	51.3
0.22	14.5	0.3	65.5
0.15	13.2	0.3	85.8
0.11	12.2	0.3	114.5
0.08	11.4	0.3	152.3
0.05	10.9	0.4	211.5
0.04	10.4	0.4	265.7
0.03	10.0	0.4	367.4
0.02	9.8	0.4	504.8
0.02	9.6	0.4	619.9
0.01	9.4	0.4	819.2

Table 32: Calibrated for 4-Vane for mortar. U is the uncertainty of the shear stress

Shear Rate, γ [1/s]	Shear Stress, τ [Pa]	U [Pa]	Viscosity, μ [Pa-s]
33.33	467.5	7.3	14.0
23.17	339.4	4.9	14.7
16.13	248.7	3.3	15.4
11.22	182.9	2.4	16.3
7.80	136.2	1.7	17.5
5.39	102.8	1.2	19.0
3.77	78.2	0.9	20.8
2.62	60.7	0.7	23.2
1.82	47.9	0.7	26.4
1.26	38.7	0.7	30.7
0.88	32.0	0.6	36.5
0.61	27.0	0.7	44.1
0.42	23.4	0.7	55.2
0.29	20.7	0.6	70.4
0.21	18.6	0.7	90.0
0.14	17.1	0.7	118.5
0.10	16.0	0.7	158.0
0.07	15.1	0.6	224.1
0.05	14.4	0.7	299.9
0.03	13.9	0.6	412.8

Table 33: Calibrated for 6-Vane for mortar. U is the uncertainty of the shear stress

Shear Rate, γ [1/s]	Shear Stress, τ [Pa]	U [Pa]	Viscosity, μ [Pa-s]
13.99	212.7	5.4	15.2
9.72	157.8	2.8	16.2
6.77	117.7	2.0	17.4
4.71	88.7	1.4	18.8
3.28	67.9	1.1	20.7
2.26	52.8	0.8	23.3
1.58	41.6	0.6	26.3
1.10	33.5	0.6	30.5
0.76	27.2	0.5	35.6
0.53	22.7	0.4	42.6
0.37	19.2	0.5	51.9
0.26	16.6	0.5	64.8
0.18	14.6	0.4	82.1
0.12	13.1	0.4	106.0
0.09	11.9	0.4	136.8
0.06	11.0	0.4	181.0
0.04	10.3	0.4	241.7
0.03	9.7	0.4	341.3
0.02	9.2	0.4	457.2
0.01	8.9	0.4	627.3

6.5 Data with the concrete rheometer

The concrete rheometer was used to obtain torque versus rotational speed using the two spindles described in Section 5.1.2. For each mixture, paste, mortar and concrete were measured. For each geometry and type of material three measurements were conducted. All the data collected are in Appendix C, while the summary average curves and the statistical analysis are presented here.

6.5.1 Statistical analysis

For each geometry there were 6 runs treated as independent replicates of the flow curves. Only the “down curve” data was used. For each of the shear rates, a consensus shear stress was computed together with an uncertainty using the model

$$SS_{ij} = \theta_i + \varepsilon_{ij}, i=1,\dots,22, j=1,\dots,6$$

where θ_i were the consensus torque values for the 6 replicates.

Estimation was performed via Markov Chain Monte Carlo methods [1] (which require prior distributions on the parameters of the model) with

$$\theta_i \sim N(0, 1.0E5), \varepsilon_{ij} \sim N(0, \sigma_i^2), \sigma_i^2 \sim \text{Gamma}(1.0E5, 1.0E5), i=1, \dots, 22.$$

The computations were done using the software OpenBUGS [2]. The posterior mean, standard deviation, and 95% highest posterior density interval at each shear rate were used for the estimate (SS), standard (u(SS)) and expanded uncertainty. These estimates were very stable with respect to the Gaussian and Gamma distributions of the parameters. The following tables contains the results (Table 38 to Table 39).

Yield stress and viscosity are, respectively, the intercept and slope of a straight line fitted to shear stress in terms of shear rate. Only the “down curve” data was used to fit the regression. A straight-line model fits the flow curve data reasonably well and provides an approximation to the flow curves given in the previous section.

Yield stress and viscosity were estimated using a random effects regression model

$$SS_{ij} = a_i + b_i \Omega_j + \varepsilon_{ij}$$

where

$$a_i \sim N(\alpha, \sigma_\alpha^2), b_i \sim N(\beta, \sigma_\beta^2), \varepsilon_{ij} \sim N(0, \sigma_i^2), i=1,\dots,6, j=1,\dots,22.$$

In this model, a_i are the yield stress values for the 6 individual replicates, and α is the consensus yield stress value. Similarly, b_i are the viscosity values for the 6 individual mixes and β is the consensus viscosity. This model accounts for measurement uncertainty and lack of fit of each replicate using σ_i , and for between replicate variability using σ_α and σ_β .

Fitting was done using Markov Chain Monte Carlo methods which require prior distributions on the parameters of the model. These were

$$\alpha \sim N(0,1.0E2), \quad \beta \sim N(0,1.0E2), \quad \sigma_\alpha^2 \sim \text{Gamma}(1.0E5,1.0E5), \sigma_\beta^2 \sim \text{Gamma}(1.0E5,1.0E5)$$

$$\sigma_i^2 \sim \text{Gamma}(1.0E5,1.0E5), i = 1, \dots, 6.$$

The results are in Table 34 to Table 39.

The Bingham parameters were also calculated and are shown in Table 40 to Table 45.

Table 34: Flow curve and uncertainty for Helical for paste. SR is the rotational speed and SS is the torque, U is the uncertainty of the torque

SR (rpm)	SS (Nm)	U(SS)
100.07	0.5465	0.0036
72.04	0.4094	0.0034
51.83	0.3119	0.0029
37.30	0.2403	0.0029
26.84	0.1873	0.0027
19.17	0.1475	0.0023
13.85	0.1185	0.0024
10.01	0.0968	0.0026
7.20	0.0801	0.0024
5.18	0.0676	0.0025
3.73	0.0578	0.0024
2.68	0.0505	0.0023
1.93	0.0449	0.0022
1.39	0.0401	0.0023
1.00	0.0367	0.0024
0.72	0.0337	0.0023
0.52	0.0316	0.0022
0.37	0.0302	0.0021
0.27	0.0284	0.0021
0.19	0.0275	0.0023
0.14	0.0259	0.0022
0.10	0.0252	0.0023

Table 35: Flow curve and uncertainty for 4-vane for paste. SR is the rotational speed and SS is the torque, U is the uncertainty of the torque

SR ((rpm)	SS (Nm)	U(SS)
100.07	0.8098	0.0053
72.02	0.6020	0.0046
51.83	0.4549	0.0040
37.30	0.3483	0.0037
26.84	0.2695	0.0034
18.88	0.2082	0.0049
13.91	0.1682	0.0031
10.01	0.1358	0.0029
7.20	0.1120	0.0028
5.18	0.0939	0.0028
3.73	0.0802	0.0027
2.68	0.0690	0.0026
1.93	0.0609	0.0026
1.39	0.0545	0.0025
1.00	0.0493	0.0023
0.72	0.0451	0.0024
0.52	0.0419	0.0022
0.37	0.0398	0.0022
0.27	0.0371	0.0024
0.19	0.0358	0.0024
0.14	0.0333	0.0024
0.10	0.0327	0.0026

Table 36: Flow curve and uncertainty for helical for mortar. SR is the rotational speed and SS is the torque, U is the uncertainty of the torque

SR ((rpm))	SS (Nm)	U(SS)
100.07	0.9229	0.0032
72.01	0.6958	0.0023
51.83	0.5305	0.0016
37.31	0.4076	0.0012
26.84	0.3159	0.0011
19.25	0.2474	0.0013
13.90	0.1962	0.0017
10.01	0.1578	0.0019
7.20	0.1288	0.0023
5.18	0.1072	0.0021
3.73	0.0906	0.0024
2.68	0.0781	0.0024
1.93	0.0679	0.0024
1.39	0.0605	0.0024
1.00	0.0547	0.0023
0.72	0.0498	0.0023
0.52	0.0471	0.0022
0.37	0.0431	0.0023
0.27	0.0405	0.0024
0.19	0.0391	0.0024
0.14	0.0364	0.0023
0.10	0.0353	0.0025

Table 37: Flow curve and uncertainty for vane for mortar. SR is the rotational speed and SS is the torque, U is the uncertainty of the torque

SR ((rpm))	SS (Nm)	U(SS)
100.09	1.3710	0.0050
72.02	1.0311	0.0039
51.82	0.7824	0.0027
37.30	0.5982	0.0023
26.85	0.4613	0.0017
18.94	0.3542	0.0016
13.90	0.2831	0.0016
10.00	0.2268	0.0016
7.20	0.1832	0.0023
5.18	0.1511	0.0026
3.73	0.1271	0.0025
2.68	0.1086	0.0030
1.93	0.0946	0.0029
1.39	0.0827	0.0030
1.00	0.0745	0.0029
0.72	0.0677	0.0026
0.53	0.0628	0.0029
0.37	0.0580	0.0026
0.27	0.0546	0.0027
0.19	0.0508	0.0032
0.14	0.0486	0.0029
0.10	0.0479	0.0028

Table 38: Flow curve and uncertainty for concrete helical. SR is the rotational speed and SS is the torque, U is the uncertainty of the torque

SR ((rpm))	SS (Nm)	U(SS)
100.05	4.49	0.24
72.04	3.40	0.16
51.83	2.62	0.14
37.30	2.07	0.12
26.85	1.63	0.09
19.32	1.29	0.06
13.90	1.05	0.05
10.01	0.84	0.05
7.20	0.71	0.04
5.18	0.59	0.03
3.73	0.50	0.02
2.68	0.43	0.03
1.93	0.36	0.01
1.39	0.32	0.01
1.00	0.29	0.02
0.72	0.27	0.01
0.52	0.24	0.02
0.37	0.22	0.01
0.27	0.21	0.01
0.19	0.20	0.01
0.14	0.20	0.01
0.10	0.18	0.01

Table 39: Flow curve and uncertainty for concrete vane. SR is the rotational speed and SS is the torque, U is the uncertainty of the torque

SR ((rpm))	SS (Nm)	U(SS)
100.07	5.12	0.20
72.03	3.84	0.15
51.83	2.94	0.10
37.31	2.34	0.08
26.85	1.86	0.06
19.32	1.55	0.08
13.91	1.31	0.05
10.01	1.09	0.04
7.20	0.91	0.02
5.18	0.76	0.02
3.73	0.66	0.02
2.68	0.57	0.01
1.93	0.49	0.02
1.39	0.44	0.02
1.00	0.40	0.01
0.72	0.34	0.01
0.53	0.33	0.02
0.37	0.30	0.01
0.27	0.27	0.01
0.19	0.26	0.02
0.14	0.26	0.02
0.10	0.24	0.01

Table 40: Yield stress and plastic viscosity for each sample and for consensus – paste Helical in concrete rheometer

Sample NIST Code	Yield Stress		Plastic Viscosity	
	Value a_i, α [Nm]	standard uncertainty [Nm]	Value a_i, α [Nm·min]	standard uncertainty [Nm·min]
CR-47 B	0.0322	0.00194	0.0052	0.000066
CR-47 C	0.0321	0.00196	0.0052	0.000063
CR-47 D	0.0326	0.00193	0.0052	0.000068
CR-59 A	0.0385	0.00196	0.0053	0.000067
CR-59 B	0.0371	0.00191	0.0053	0.000067
CR-59 C	0.0375	0.00191	0.0053	0.000066
Consensus (α, β)	0.0350	0.0024	0.0052	0.0011
Plastic viscosity in Nm·s			0.050	0.010

Table 41: Yield stress and plastic viscosity for each sample and for consensus – paste vane in concrete rheometer

Sample NIST Code	Yield Stress		Plastic Viscosity	
	Value a_i, α [Nm]	standard uncertainty [Nm]	Value a_i, α [Nm·min]	Viscosity standard uncertainty [Nm·min]
CR-47 E	0.0426	0.00244	0.0077	0.000085
CR-47 F	0.0440	0.00241	0.0077	0.000086
CR-47 G	0.0428	0.00244	0.0077	0.000087
CR-59 E	0.0483	0.00241	0.0078	0.000085
CR-59 F	0.0488	0.00242	0.0079	0.000086
CR-59 G	0.0486	0.00239	0.0079	0.000085
Consensus (α, β)	0.0459	0.0026	0.0078	0.0011
Plastic viscosity in Nm·s			0.075	0.010

Table 42: Yield stress and plastic viscosity for each sample and for consensus – mortar Helical in concrete rheometer

Sample NIST Code	Yield Stress		Plastic Viscosity	
	Value a_i, α [Nm]	standard uncertainty [Nm]	Value a_i, α [Nm·min]	standard uncertainty [Nm·min]
CR-50 D	0.0509	0.00307	0.0090	0.00012
CR-50 E	0.05059	0.00311	0.0090	0.00012
CR-50 F	0.05019	0.00312	0.0091	0.00012
CR-63 D	0.0552	0.00317	0.0089	0.00012
CR-63 E	0.054	0.00306	0.0089	0.00012
CR-63 F	0.0533	0.00301	0.0089	0.00012
Consensus (α, β)	0.0524	0.0027	0.0090	0.0011
Plastic viscosity in Nm·s			0.086	0.010

Table 43: Yield stress and plastic viscosity for each sample and for consensus – mortar vane in concrete rheometer

Sample NIST Code	Yield Stress		Plastic Viscosity	
	Value a_i, α [Nm]	standard uncertainty [Nm]	Value a_i, α [Nm·min]	standard uncertainty [Nm·min]
CR-50 A	0.0677	0.00411	0.0134	0.00016
CR-50 B	0.0690	0.00399	0.0135	0.00016
CR-50 C	0.0691	0.00397	0.0135	0.00016
CR-63 A	0.0716	0.00394	0.0133	0.00016
CR-63 B	0.0723	0.00399	0.0133	0.00016
CR-63 C	0.0730	0.00404	0.0133	0.00016
Consensus (α, β)	0.0705	0.0034	0.0134	0.0011
Plastic viscosity in Nm·s			0.128	0.010

Table 44: Yield stress and plastic viscosity for each sample and for consensus – concrete Helical in concrete rheometer

Sample NIST Code	Yield Stress		Plastic Viscosity	
	Value a_i, α [Nm]	standard uncertainty [Nm]	Value a_i, α [Nm·min]	standard uncertainty [Nm·min]
CR-52 A	0.3014	0.01683	0.0478	0.00081
CR-52 D	0.3045	0.0177	0.0483	0.00081
CR-52 E	0.3026	0.01711	0.0473	0.00081
CR-65 A	0.2917	0.01712	0.0389	0.00081
CR-65 B	0.2885	0.01828	0.0399	0.00082
CR-65 C	0.294	0.01655	0.0396	0.00080
Consensus (α, β)	0.297	0.014	0.0436	0.0028
Plastic viscosity in Nm·s			0.416	0.026

Table 45: Yield stress and viscosity for each sample and for consensus – concrete vane in concrete rheometer

Sample NIST Code	Yield Stress		Plastic Viscosity	
	Value a_i, α [Nm]	standard uncertainty [Nm]	Value a_i, α [Nm·min]	standard uncertainty [Nm·min]
CR-52 F	0.4099	0.01920	0.0543	0.00104
CR-52 G	0.4026	0.01904	0.0493	0.00102
CR-52 H	0.4052	0.01878	0.0502	0.00103
CR-65 D	0.4067	0.01871	0.0441	0.00103
CR-65 E	0.4072	0.01878	0.0449	0.00103
CR-65 F	0.4061	0.01863	0.0489	0.00101
Consensus (α, β)	0.406	0.016	0.0486	0.0024
Plastic viscosity in Nm·s			0.4642	0.0228

6.5.2 Calibration factors and data in fundamental units in concrete rheometer

Using the method described in Section 5.3, the data from

Table 34 and Table 35 were used to calculate the calibration factors (Table 46). The data are shown in

Table 47 to Table 52 (Figure 15 and Figure 16) are generated using these factors to convert them in fundamental units.

Table 46: Calibration factors for the two geometries of spindles used in concrete rheometer based on the paste data

	Spiral	4-Vane
Kτ [Pa/N·m]	243.7	189.1
Kγ [-]	1.73	1.91

$K\mu$ [Pa·s/N·m·s]	151.4	101.6
---------------------	-------	-------

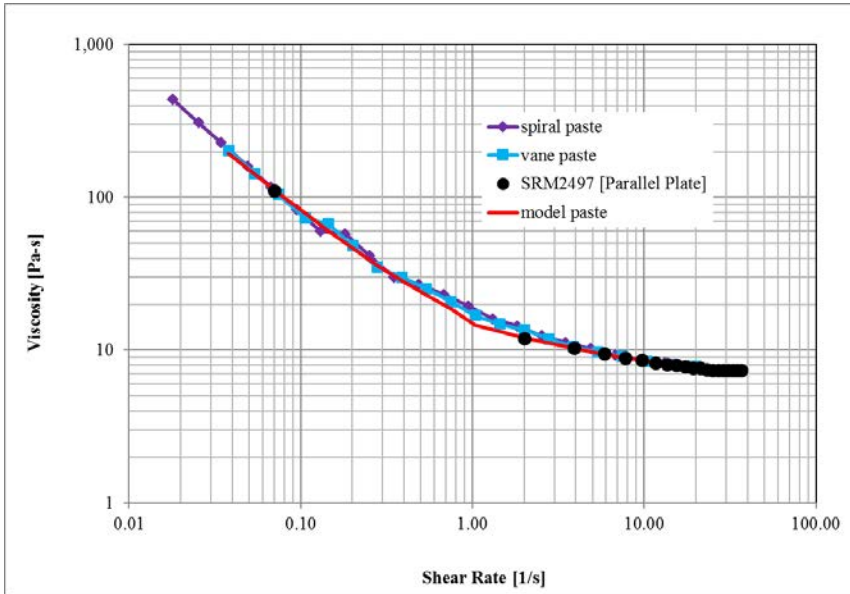


Figure 15: Rheometer data for paste using both geometries. See uncertainty in Table 47 to Table 52

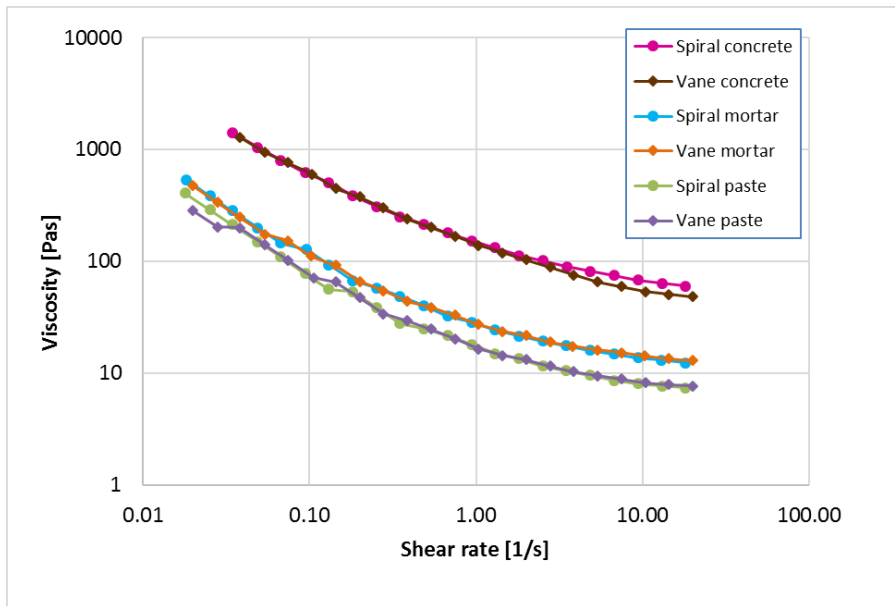


Figure 16: All data using the concrete rheometer based on the K factors from Table 44. Uncertainty in Table 47 to Table 52

Table 47: Data calibrated for paste on a spiral in the concrete rheometer. U is the uncertainty of the shear stress

Shear Rate, $\dot{\gamma}$ [1/s]	Shear Stress, τ [Pa]	U [Pa]	Viscosity, μ [Pa-s]
18.16	134	13	7.7
13.07	100	10	7.9
9.40	75.6	7.6	8.3
6.76	58.5	5.8	9.0
4.87	46.3	4.6	9.9
3.49	36.6	3.7	10.9
2.52	29.3	2.9	12.0
1.82	24.4	2.4	13.9
1.31	19.5	1.9	15.5
0.94	17.1	1.7	18.8
0.68	14.6	1.5	22.4
0.49	12.2	1.2	26.0
0.35	9.8	1.0	28.9
0.25	9.8	1.0	40.1
0.18	9.8	1.0	55.7
0.13	7.3	0.7	58.1
0.09	7.3	0.7	80.4
0.07	7.3	0.7	113.0
0.05	7.3	0.7	154.8
0.03	7.3	0.7	220.0

Table 48: Data calibrated for paste on a Vane in the concrete rheometer. U is the uncertainty of the shear stress

Shear Rate, $\dot{\gamma}$ [1/s]	Shear Stress, τ [Pa]	U [Pa]	Viscosity, μ [Pa-s]
20.07	153	15	7.6
14.44	113	11	7.8
10.39	85.1	8.5	8.1
7.48	66.2	6.6	8.8
5.38	51.1	5.1	9.4
3.86	39.7	4.0	10.2
2.79	32.2	3.2	11.5
2.01	26.5	2.6	13.1
1.44	20.81	2.1	14.3
1.04	17.0	1.7	16.3
0.75	15.1	1.5	20.1
0.54	13.2	1.3	24.5
0.39	11.4	1.1	29.2
0.28	9.5	0.9	33.7
0.20	9.5	0.9	46.9
0.14	9.5	0.9	65.1
0.11	7.6	0.8	70.8
0.07	7.6	0.8	101.4
0.05	7.6	0.8	139.0
0.04	7.6	0.8	197.5

Table 49: Data calibrated for mortar on a Spiral in the concrete rheometer. U is the uncertainty of the shear stress

Shear Rate, $\dot{\gamma}$ [1/s]	Shear Stress, τ [Pa]	U [Pa]	Viscosity, μ [Pa-s]
18.13	224.2	0.8	12.4
13.04	170.6	0.6	13.1
9.39	129.2	0.4	13.8
6.76	99.9	0.3	14.8
4.86	78.0	0.3	16.0
3.48	60.9	0.3	17.5
2.52	48.7	0.4	19.3
1.81	39.0	0.5	21.5
1.30	31.7	0.6	24.3
0.94	26.8	0.5	28.6
0.68	21.9	0.6	32.5
0.49	19.5	0.6	40.2
0.35	17.1	0.6	48.8
0.25	14.6	0.6	58.1
0.18	12.2	0.6	67.3
0.13	12.2	0.6	93.4
0.10	12.2	0.5	126.9
0.07	9.7	0.6	145.5
0.05	9.7	0.6	199.3
0.03	9.7	0.6	283.2
0.03	9.7	0.6	384.4
0.02	9.7	0.6	538.2

Table 50: Data calibrated for mortar on a Vane in the concrete rheometer. U is the uncertainty of the shear stress

Shear Rate, $\dot{\gamma}$ [1/s]	Shear Stress, τ [Pa]	U [Pa]	Viscosity, μ [Pa-s]
20.02	259.1	0.9	12.9
14.40	194.8	0.7	13.5
10.36	147.5	0.5	14.2
7.46	113.5	0.4	15.2
5.37	87.0	0.3	16.2
3.79	66.2	0.3	17.5
2.78	52.9	0.3	19.0
2.00	43.5	0.3	21.7
1.44	34.0	0.4	23.6
1.04	28.4	0.5	27.4
0.75	24.6	0.5	33.0
0.54	20.8	0.6	38.8
0.39	17.0	0.5	44.1
0.28	15.1	0.6	54.4
0.20	13.2	0.5	66.2
0.14	13.2	0.5	91.9
0.10	11.3	0.5	111.2
0.07	11.3	0.5	153.3
0.05	9.5	0.5	175.1
0.04	9.5	0.6	248.8
0.03	9.5	0.5	337.7
0.02	9.5	0.5	472.8

Table 51: Data calibrated for concrete on a spiral in the concrete rheometer. U is the uncertainty of the shear stress

Shear Rate, $\dot{\gamma}$ [1/s]	Shear Stress, τ [Pa]	U [Pa]	Viscosity, μ [Pa-s]
18.12	1094	59	60.4
13.05	828	39	63.5
9.39	639	34	68.0
6.76	505	29	74.7
4.86	397	22	81.7
3.50	314	15	89.8
2.52	256	12	101.6
1.81	205	12	112.9
1.30	173.0	9.7	132.7
0.94	143.8	7.3	153.2
0.68	121.9	4.9	180.4
0.49	104.8	7.3	215.9
0.35	87.7	2.4	251.0
0.25	78.0	2.4	309.7
0.18	70.7	4.9	390.2
0.13	65.8	2.4	504.5
0.09	58.5	4.9	621.0
0.07	53.6	2.4	800.0
0.05	51.2	2.4	1046.4
0.03	48.7	2.4	1416.2
0.03	48.7	2.4	1922.1
0.02	43.9	2.4	2421.8

Table 52: Data calibrated for concrete on a Vane in the concrete rheometer. U is the uncertainty of the shear stress

Shear Rate, $\dot{\gamma}$ [1/s]	Shear Stress, τ [Pa]	U [Pa]	Viscosity, μ [Pa-s]
20.02	968	38	48.4
14.40	726	28	50.4
10.37	556	19	53.6
7.46	443	15	59.3
5.37	352	11	65.5
3.86	293	15	75.9
2.78	247.7	9.5	89.1
2.00	206.1	7.6	103.0
1.44	172.1	3.8	119.5
1.04	143.7	3.8	138.7
0.75	124.8	3.8	167.3
0.54	107.8	1.9	201.1
0.39	92.7	3.8	240.1
0.28	83.2	3.8	299.3
0.20	75.6	1.9	378.2
0.14	64.3	1.9	446.5
0.10	62.4	3.8	600.1
0.07	56.7	1.9	766.7
0.05	51.1	1.9	945.6
0.04	49.2	3.8	1294.0
0.03	49.2	3.8	1756.1
0.02	45.4	1.9	2269.5

7 Comparison between concrete model and experimental data

The goal of this section is to determine the best procedure to calibrate a concrete rheometer using the SRM 2497. There are several possible approaches to obtain the correct factors to transform measured data into fundamental units: 1) calculate the K factors using the paste or mortar data. 2) calculate the L factors using the concrete model curve. It was found, and will be illustrated in this section, that the best method is to use the L factors with the concrete model curve. The main reason is that neither the paste or mortar have inclusions that are comparable in size to the large glass beads found in the concrete SRM. As a result, flow artifacts associated with the larger inclusion are not accounted for by using the paste or mortar based scaling parameters and hence are not representative of typical concrete.

Let's examine the data obtained in this report step-by-step. The data calculated for the concrete rheometer in Section 6.5.2 are compared with the simulation curves shown in Section 4.2. The paste data as shown in Figure 15 are overlapping the model. This is not surprising as the K factors are calculated using the same data. Figure 17 shows the predicted viscosity vs. shear rate of the mortar and experimental values determined from rheometers that have been calibrated using the paste material for SRM 2497 to calibrate the rheometer and the mortar material to verify the calibration. Note the agreement is quite good despite the different impellor designs.

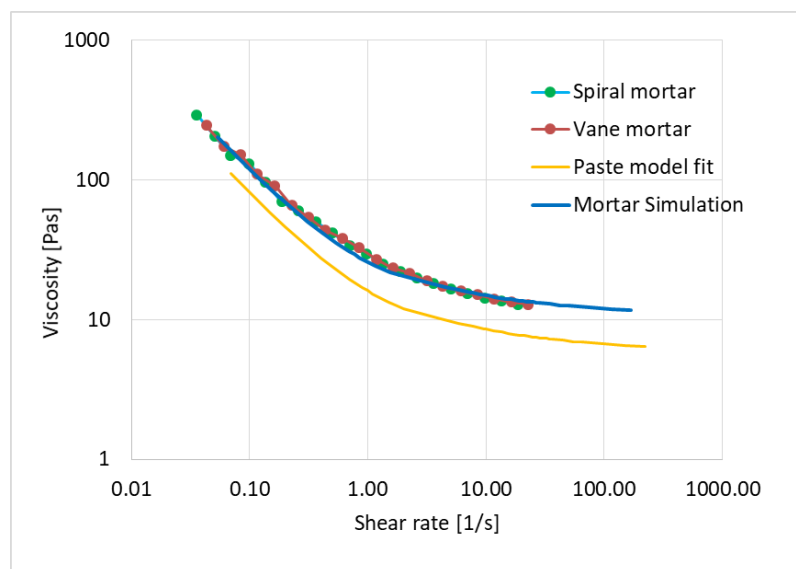


Figure 17: Comparison of concrete rheometer data for mortar with the mortar simulation obtained from the paste based on K factors from Table 44.

Figure 18 shows the prediction of the concrete viscosity vs. shear rate based on computer simulation compared to measurements from rheometer calibrated with the SRM paste. Note that while the experimental and simulation results follow similar trends, there are discrepancies by a factor for two for certain shear rate regimes. There are several possible explanations for this behavior. Given the size of the mortar beads relative to the impellor,

the mortar material likely behaves as a continuum and is not as sensitive to artifacts related to shear induced migration and sedimentation over the time scales of typical measurements.

Figure 19 shows the results of calibration of the concrete rheometer using the concrete SRM, instead of the paste using the K factors from Table 53. Direct calibration with SRM 2497 helps correct for artifacts that result from using the larger beads that are representative of the coarse aggregate. As it can be seen, the data begin to overlap the simulation curves for the shear rates greater than 1 s^{-1} . This is to be expected as the calibration factors, K (Table 53) are based on the Bingham slope and intercept that are only valid in the linear portion of the curve, i.e., over 1 s^{-1} . Thus, if the L factors are used instead (Table 54) the results are better fitted on the simulation curves as all the points of the simulation are considered, as shown in Figure 20. The calculation of the factors L can be obtained following the scheme illustrated in Figure 12. The NIST website would also provide a routine to calculate the factors L based on the concrete simulated curve.

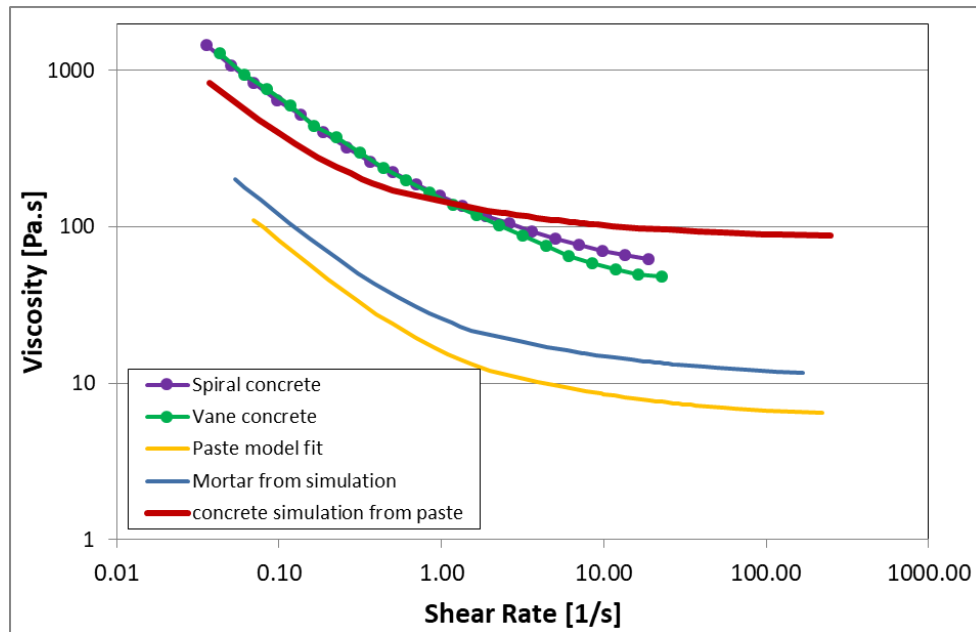


Figure 18: Comparison of concrete data calibrated using the paste fit and the factors K from Table 46 with the simulation curves

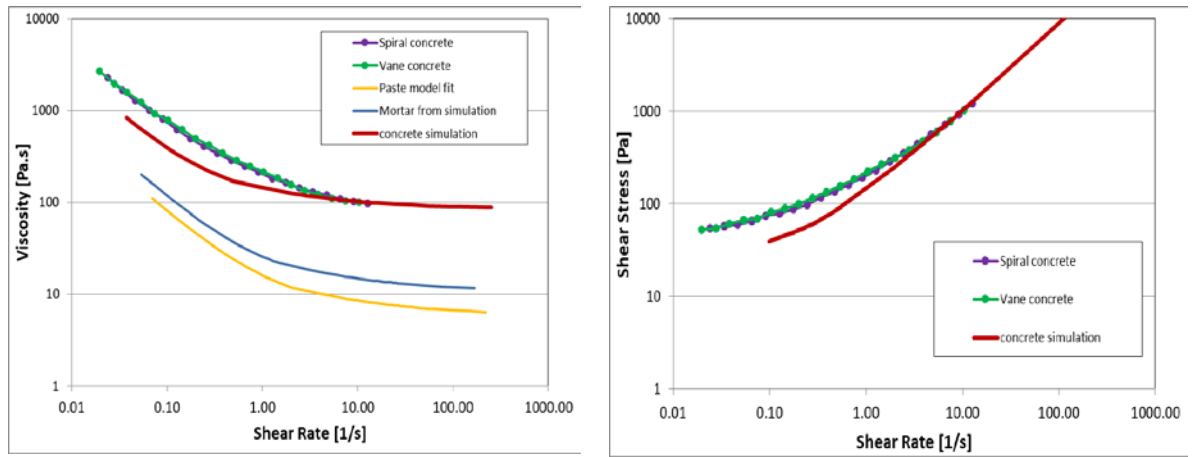


Figure 19: Comparison of concrete data calibrated using the concrete model and the factors K from Table 51 with the simulation curves.

Table 53: Calibration factors, K, for the two geometries used in concrete rheometer, based on the concrete simulation

	Spiral	4-Vane
$K\tau$ [Pa/N·m]	273.8	203.4
$K\gamma$ [-]	1.21	0.99
$K\mu$ [Pa·s/N·m·s]	227.0	206.2

Table 54: Calibration factors, L, for the two geometries used in concrete rheometer based on the concrete simulation

	Spiral	4-Vane
$L\tau$ [Pa/N·m]	114 ± 52	83 ± 34
$L\gamma$ [-]	0.52 ± 0.2	0.46 ± 0.2
$L\mu$ [Pa·s/N·m·s]	221 ± 54	180 ± 33

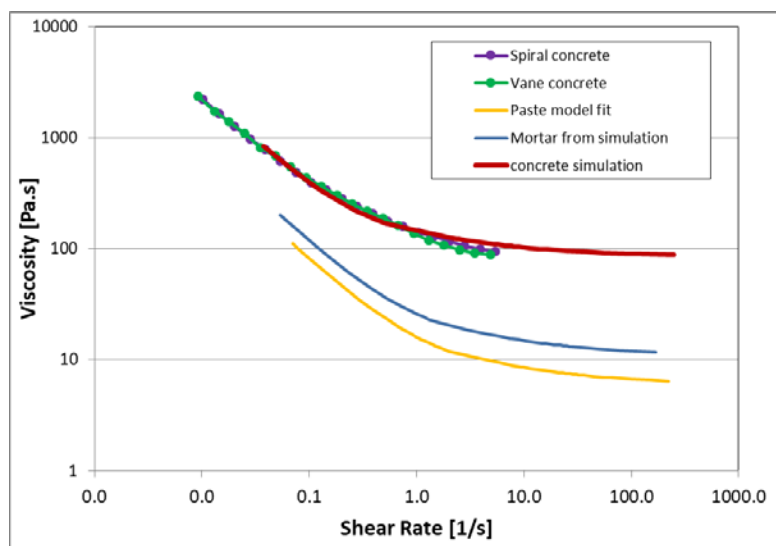


Figure 20: Comparison of concrete data calibrated using the concrete model and the factors L from Table 52 with the simulation curves.

Therefore, it is essential that to calibrate a concrete rheometer, the reference curve should be a concrete simulation curve. The main reasons for the model and experimental relative viscosity discrepancy when the calibration is based on the paste model are possibly due to several phenomena, which can be present in experiments but are not present in the model:

- The simulation model corresponds to an ideal Couette flow with no walls and no changes in the material composition, while the experimental measurement could have particle migration away from the spindle and vertically on the open surface.
- Slippage of the material on the spindle or the container. It is possible that the spiral might lower slippage but while it was visible in the SRM 2493 with 40% beads, it was not apparent in the data presented here.
- The open free surface at the top of the rheometer allows material to move up or down. This additional degree of freedom can result in reduction the measured viscosity, especially for the case of the spiral impellor. This open free surface is not present in the simulation
- It was observed that the 10 mm beads migrated away from the vane blade. This has the consequence of making a weaker coupling between the vane and the concrete fluid. Because of this weaker coupling, for a given applied torque, one will measure higher than anticipated rotational speed and falsely conclude that the viscosity was lower than expected.

8 Summary

A new concrete rheology reference material (SRM 2497) was developed that consists of a non-colloidal suspension made up of corn syrup and fine limestone, with the addition of glass beads 1 mm and 10 mm in diameter. The uniqueness of this reference material is that it is a suspension, which has a Bingham-like behavior having rheological properties similar to concrete. Thus it is more suitable for calibration of rheometers utilized for cement-based materials than typical Newtonian oils because the use of such oils for calibration do not necessarily account for a variety of effects, including non-Newtonian behavior of the fluid matrix and the presence of solid inclusions, which can influence interpretation of measurements.

This report represents the final step of the development of a suite of SRMs for rheological measurements of cement-based materials. SRM 2492, a Paste Reference Material was the first step in the development of a reference material for cement-based materials, the second step being the mortar SRM 2493, which now serves as the matrix fluid for the concrete reference material developed in this report, SRM 2497. The certified values of these SRMs (2492, 2493 and 2497), were determined using extensive experimental design, computer modeling and statistical analysis. This combination of experiment and computer modeling make SRMs 2493 and 2497 unique as the computer modeling played a crucial role in the determination of their certified values

9 References

- [1] C. F. Ferraris, P. Stutzman, J. Winpighler and W. Guthrie, "Certification of SRM 2492: Bingham Paste Mixture for Rheological Measurements," SP-260-174 Rev. 2012, June 2012.
- [2] A. Olivas, C. F. Ferraris, W. F. Guthrie and B. Toman, "Re-certification of SRM 2492: Bingham Paste Mixture for Rheological Measurements," National Institute of Standards and Technology. (NIST Special Publication 260-182). U.S. Department of Commerce, Gaithersburg, MD, August 2015.
- [3] A. Olivas, C. F. Ferraris, N. S. Martys, W. L. George, E. J. Garboczi, B. Toman, "Certification of SRM 2493: Standard Reference Mortar for Rheological Measurements", NIST-SP-260-187 <https://doi.org/10.6028/NIST.SP.260-187>, 2017
- [4] C. F. Ferraris and L. E. Brower, "Comparison of concrete rheometers: International tests at LCPC (Nantes, France) in October 2000 (NISTIR 6819)," National Institute of Standards and Technology, Gaithersburg, MD.
- [5] C. F. Ferraris and L. E. Brower, "Comparison of concrete rheometers: International tests at MB (Cleveland OH, USA) in May 2003 (NISTIR 7154)," National Institute of Standards and Technology, Gaithersburg, MD.
- [6] A. Olivas, C. F. Ferraris, B. Lang, J. Richter, R. P. Ferron, "Cement Paste Reference Material (SRM 2492) Shelf-Life Extension", NIST-TN 1934, Sept. 2016 - [dx.doi.org/10.6028/NIST.TN.1934](https://doi.org/10.6028/NIST.TN.1934).
- [7] E. J. Garboczi, "Three-dimensional mathematical analysis of particle shape using x-ray tomography and spherical harmonics: applications to aggregates used in concrete.," *Cement Concrete Research* 32, 2002.
- [8] M. A. Taylor, E. J. Garboczi, S. T. Erdogan and D. W. Fowler, "Some properties of irregular particles in 3-D," *Powder Technology* 162, pp. 1-15, 2006.
- [9] L. Maxime, N. S. Martys, W. L. George, D. Lootens and P. Hebraud, "Scaling laws for the flow of generalized Newtonian suspensions," *Journal of Rheology*, vol. 58, 2014.
- [10] H. Zhu, N.S. Martys, C.F. Ferraris, D. De Kee, "A numerical study for the flow of Bingham-like Fluids in two Dimensional Vane and Coaxial cylinders using Smoothed Particle Hydrodynamic (SPH) based Method", *J. of Non-Newtonian Fluid Mechanics*, vol. 165, pp. 363-375, 2010.
- [11] M. Allen and D. Tildesley, *Computer simulations of liquids*, Clarendon, Oxford, 1987.
- [12] N. S. Martys, W. L. George, B.-W. Chun and D. Lootens, "A smoothed particle hydrodynamics-based fluid model with a spatially dependent viscosity: application to flow of a suspension with a non-Newtonian fluid matrix.," *Rheologica acta*, vol. 49, no. 10, pp. 1059-1069, 2010.
- [13] A. Olivas, M. A. Helsel, N.S. Martys, C. F. Ferraris, R. P. Ferron, "Rheological Measurement of Suspensions Without Slippage: Experimental and Model" NIST-TN 1946, Dec. 2016 - [dx.doi.org/10.6028/NIST.TN.1946](https://doi.org/10.6028/NIST.TN.1946)

- [14] A. Gelman, J. Carlin , H. Stern , D. Dunson, A. Vehatri and D. Rubin, *Bayesian Data Analysis*, Boca Raton: Chapman & Hall 3rd Edition, 2013.
- [15] D. J. Lunn, D. Spiegelhalter, A. Thomas and N. Best, "The BUGS project: evolution, critique and future directions (with discussion)," *Statistics in Medicine* , pp. 3049-3082, 2009.
- [16] V. A. Hackley and C. F. Ferraris, "The Use of Nomenclature in Dispersion Science and Technology," NIST Recommended Practice Guide, SP 960-3, 2001.

Appendices

Appendix A: Original paste data measured using the Parallel plate rheometer

This Appendix provides all the data obtained for paste using a parallel plate rheometer from each test that was performed and used for the calculations. The results calculated with these data were generated using a Non-Newtonian approach. The viscosity was also calculated as a ratio rather than only a Bingham approximation, as described in Section 6. Also included are the graphs needed for interpretation of the results.

Appendix B: Original data measured from Coaxial Rheometer

This appendix provides all the original data obtained from each test that was recorded directly from the rheometer described in Section 5.1.1. Also included are graphs needed for interpretation of the results, which portray the repeatability of the measured data.

Appendix C: Original data measured from Concrete Rheometer

This appendix provides all the original data obtained from each test that was recorded directly from the rheometer described in Section 5.1.2. Also included are graphs needed for interpretation of the results, which portray the repeatability of the measured data.

Appendix A: Original paste data measured using the Parallel plate rheometer

This Appendix provides all the data obtained for paste using a parallel plate rheometer from each test that was performed and used for the calculations. The results calculated with these data were generated using a Non-Newtonian approach. The viscosity was also calculated as a ratio rather than only a Bingham approximation, as described in Section 6. Also included are the graphs needed for interpretation of the results

Legend of the tables

SR = $\dot{\gamma}$ = Shear Rate

SS = τ = Shear Stress

μ = Viscosity

R2 = r^2 calculated using a Pearson function to determine the linearity of the data

Table A-1: Values for Mix A

Mix A - 7/21/15								
NIST Code: CR-46								
Run #B		Run #C		Run #D		Average		
SR (Υ)	SS (τ)	SR (Υ)	SS (τ)	SR (Υ)	SS (τ)	SR (Υ)	SS (τ)	Viscosity (μ) [Pa·s]
0.07	8.74	0.07	8.66	0.07	8.49	0.07	8.63	118.06
2.68	34.99	2.68	33.14	2.68	33.32	2.68	33.82	12.63
5.29	60.94	5.29	56.98	5.29	57.95	5.29	58.62	11.08
7.90	83.20	7.90	76.49	7.90	79.38	7.90	79.69	10.08
10.54	104.66	10.54	94.73	10.54	99.93	10.54	99.77	9.47
13.10	125.08	13.10	113.08	13.10	119.40	13.10	119.19	9.10
15.73	144.41	15.73	129.83	15.73	136.95	15.73	137.06	8.71
18.29	163.81	18.37	147.13	18.37	155.46	18.34	155.47	8.48
20.93	180.05	20.93	161.59	20.93	172.19	20.93	171.28	8.18
23.56	198.25	23.56	175.64	23.56	188.73	23.56	187.54	7.96
26.12	216.13	26.12	189.80	26.12	202.59	26.12	202.84	7.76
28.76	228.85	28.76	201.88	28.76	215.81	28.76	215.51	7.49
31.39	242.80	31.39	216.67	31.39	231.84	31.39	230.44	7.34
33.95	255.09	33.95	231.01	33.95	243.72	33.95	243.27	7.17
36.59	271.36	36.59	244.15	36.59	251.47	36.59	255.66	6.99
36.59	290.79	36.59	256.98	36.59	273.44	36.59	273.74	7.48
34.68	272.41	34.68	242.76	34.68	255.03	34.68	256.73	7.40
32.78	254.36	32.71	229.78	32.71	242.23	32.73	242.12	7.40
30.80	237.69	30.80	215.13	30.80	228.85	30.80	227.22	7.38
28.90	225.75	28.90	201.00	28.90	213.54	28.90	213.43	7.38
27.00	212.55	27.00	190.49	27.00	197.28	27.00	200.11	7.41
25.02	194.27	25.02	177.34	25.02	185.63	25.02	185.75	7.42
23.12	183.40	23.12	164.36	23.12	175.10	23.12	174.28	7.54
21.22	172.47	21.22	154.29	21.22	162.02	21.22	162.93	7.68
19.32	155.80	19.32	140.38	19.32	148.25	19.32	148.14	7.67
17.34	142.96	17.34	128.73	17.34	135.26	17.34	135.65	7.82
15.44	130.44	15.44	116.80	15.44	122.95	15.44	123.40	7.99
13.54	116.29	13.54	104.14	13.54	110.21	13.54	110.21	8.14
11.63	101.49	11.63	90.99	11.63	96.64	11.63	96.37	8.28
9.66	87.63	9.66	78.37	9.66	82.92	9.66	82.97	8.59
7.76	73.35	7.76	65.70	7.76	69.28	7.76	69.44	8.95
5.84	58.31	5.84	52.20	5.84	55.25	5.84	55.25	9.46
3.91	42.66	3.91	38.11	3.91	40.48	3.91	40.42	10.32
2.00	24.96	2.00	22.46	2.00	23.63	2.00	23.68	11.86
0.07	7.66	0.07	6.76	0.07	7.35	0.07	7.26	100.67

	Run #B	Run #C	Run #D		Avg.	Std. Dev.
Yield Stress [Pa]	12.9	11.8	12.4		12.4	0.5
Viscosity (μ) [Pa·s]	7.4	6.7	7.0		7.0	0.3
R2	1.0	1.0	1.0		1.0	0.0
Hysteresis	233	206	231		223	12

Table A-2: Values for mix B

Mix B - 7/28/15								
NIST Code: CR-58								
Run #A		Run #B		Run #C		Average		
SR (Υ)	SS (τ)	SR (Υ)	SS (τ)	SR (Υ)	SS (τ)	SR (Υ)	SS (τ)	Viscosity (μ) [Pa·s]
0.07	10.21	0.07	10.60	0.07	10.38	0.07	10.40	142.24
2.68	34.95	2.68	36.04	2.68	34.15	2.68	35.05	13.09
5.29	59.45	5.29	61.69	5.29	58.23	5.29	59.79	11.30
7.90	80.11	7.90	82.67	7.90	78.18	7.90	80.32	10.16
10.54	99.81	10.54	102.49	10.54	96.92	10.54	99.74	9.47
13.10	118.68	13.10	121.61	13.10	115.39	13.10	118.56	9.05
15.73	137.27	15.73	139.93	15.73	133.85	15.73	137.02	8.71
18.29	155.48	18.29	159.06	18.29	150.73	18.29	155.09	8.48
20.93	171.61	20.93	175.45	20.93	167.01	20.93	171.36	8.19
23.56	187.52	23.56	191.11	23.56	181.58	23.56	186.73	7.93
26.12	201.44	26.12	207.78	26.12	196.99	26.12	202.07	7.74
28.76	217.57	28.76	220.86	28.76	213.12	28.76	217.18	7.55
31.39	230.18	31.39	238.23	31.39	227.39	31.39	231.93	7.39
33.95	240.75	33.95	249.99	33.95	241.09	33.95	243.95	7.19
36.59	250.59	36.59	260.97	36.59	252.12	36.59	254.56	6.96
36.59	271.68	36.59	278.74	36.59	264.05	36.59	271.49	7.42
34.68	256.09	34.68	263.21	34.68	249.88	34.68	256.39	7.39
32.71	239.26	32.71	249.05	32.71	236.90	32.71	241.73	7.39
30.80	224.83	30.80	233.30	30.80	224.83	30.80	227.65	7.39
28.90	214.19	28.90	217.99	28.90	211.76	28.90	214.64	7.43
27.00	196.50	27.00	206.21	27.00	195.50	27.00	199.40	7.39
25.02	180.90	25.02	189.81	25.02	183.85	25.02	184.86	7.39
23.12	171.66	23.12	176.99	23.12	173.32	23.12	173.99	7.52
21.22	160.25	21.22	165.58	21.22	160.25	21.22	162.02	7.64
19.32	146.47	19.32	153.45	19.32	146.47	19.32	148.79	7.70
17.34	133.48	17.34	139.12	17.34	133.48	17.34	135.36	7.81
15.44	120.90	15.44	126.02	15.44	120.22	15.44	122.38	7.93
13.54	108.06	13.54	113.13	13.54	108.05	13.54	109.75	8.11
11.63	94.77	11.63	99.11	11.63	94.90	11.63	96.26	8.27
9.66	81.49	9.66	85.37	9.66	82.01	9.66	82.96	8.59
7.76	67.99	7.76	71.42	7.76	68.85	7.76	69.42	8.95
5.84	54.41	5.84	57.05	5.84	54.94	5.84	55.47	9.50
3.91	39.98	3.91	42.15	3.91	40.52	3.91	40.88	10.44
2.00	23.64	2.00	25.01	2.00	24.25	2.00	24.30	12.16
0.07	7.68	0.07	8.62	0.07	8.61	0.07	8.30	113.82

	Run #A	Run #B	Run #C		Avg.	Std. Dev.
Yield Stress [Pa]	11.6	13.4	13.5		12.8	0.9
Viscosity (μ) [Pa·s]	7.0	7.2	6.9		7.0	0.1
R2	1.0	1.0	1.0		1.0	0.0
Hysteresis	285	237	199		240	36

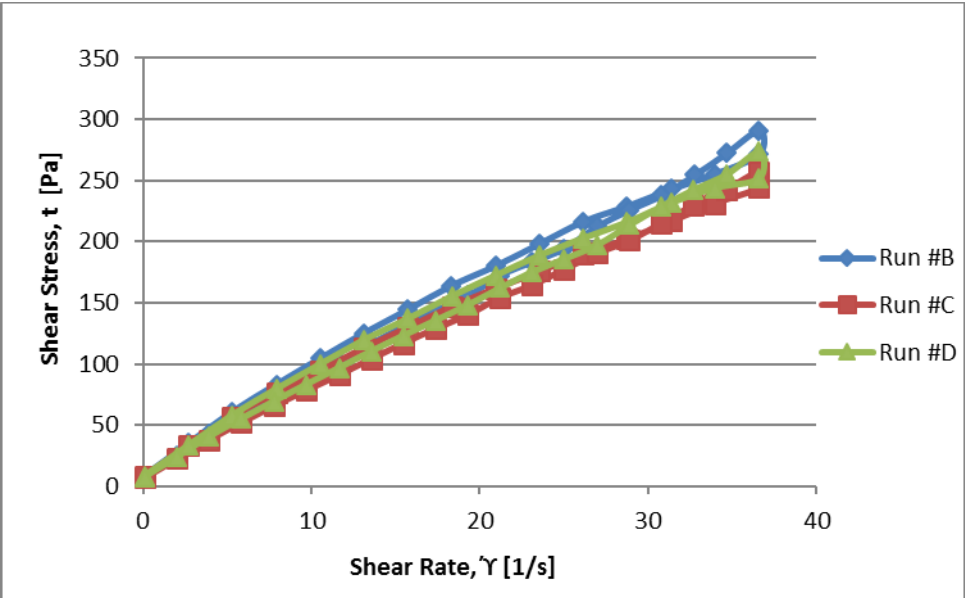


Figure A-1: Values for Mix A

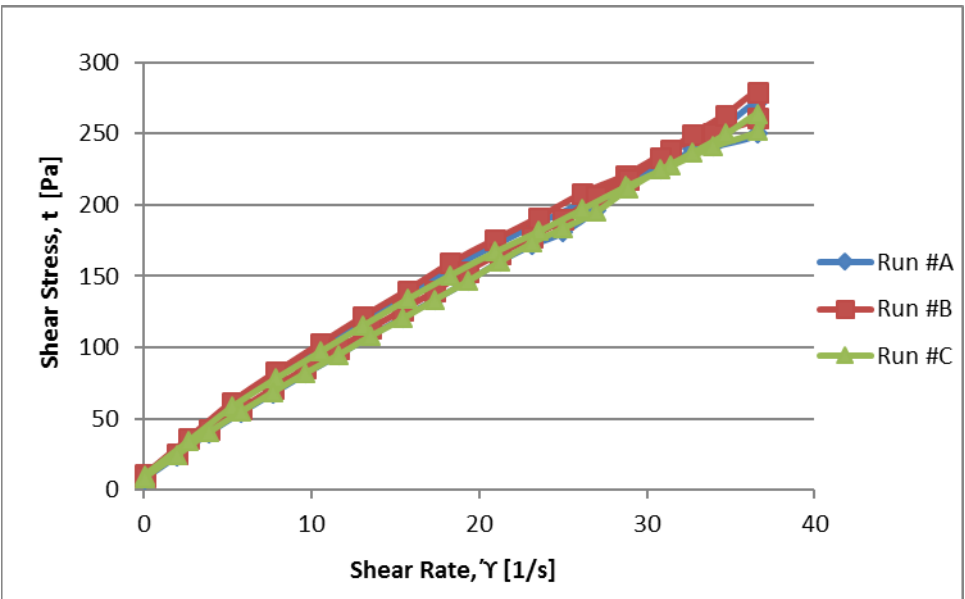


Figure A-2: Values for Mix B

Appendix B:

Original data measured from Coaxial Rheometer

This appendix provides all the original data obtained from each test that was recorded directly from the rheometer described in Section 5.1.1. Also included are graphs needed for interpretation of the results, which portray the repeatability of the measured data.

Notes:

Each mix was tested with three spindles used both using paste and then 1 mm beads (20% concentration by volume).

Each table will contain NIST codes showing the spindle and cup used, which are intended for NIST reference only.

Unit Notations:

SR = N: Rotational Speed [1/min]

SS = Γ : Measured Torque [$\mu\text{N}\cdot\text{m}$]

The conversion to fundamental units

*N: Rotational Speed \rightarrow [1/min] * $2\pi/60 =$ [rad/s]*

*Γ : Measured Torque \rightarrow [$\mu\text{N}\cdot\text{m}$] * $10^{-6} =$ [N·m]*

Table B-1: Measured data for Mix #A with 0 % beads (paste) using Double Spiral spindle.

Mix A - 7/21/15								
CR-46								
Run #E		Run #F		Run #G		Average		
SR (1/min)	SS (μNm)	SR (1/min)	SS (μNm)	SR (1/min)	SS (μNm)	SR (1/min)	SS (μNm)	Ratio
0.02	186.00	0.02	66.60	0.02	41.90	0.02	98.17	4859.74
0.03	347.00	0.03	278.00	0.03	165.00	0.03	263.33	8020.30
0.06	515.00	0.06	512.00	0.05	430.00	0.06	485.67	8798.31
0.09	670.00	0.09	664.00	0.09	635.00	0.09	656.33	7116.01
0.15	786.00	0.15	761.00	0.15	754.00	0.15	767.00	5046.05
0.25	865.00	0.25	836.00	0.25	838.00	0.25	846.33	3385.33
0.41	946.00	0.41	924.00	0.41	928.00	0.41	932.67	2280.36
0.67	1050.00	0.67	1030.00	0.67	1040.00	0.67	1040.00	1552.24
1.10	1200.00	1.10	1190.00	1.10	1200.00	1.10	1196.67	1087.88
1.80	1440.00	1.80	1430.00	1.80	1440.00	1.80	1436.67	798.15
2.94	1810.00	2.94	1810.00	2.94	1820.00	2.94	1813.33	616.78
4.82	2370.00	4.82	2380.00	4.82	2400.00	4.82	2383.33	494.47
7.90	3250.00	7.90	3270.00	7.90	3310.00	7.90	3276.67	414.77
12.90	4650.00	12.90	4680.00	12.90	4760.00	12.90	4696.67	364.08
21.20	6790.00	21.20	6850.00	21.20	6920.00	21.20	6853.33	323.27
21.20	6810.00	21.20	6870.00	21.20	6970.00	21.20	6883.33	324.69
14.70	5110.00	14.70	5160.00	14.70	5210.00	14.70	5160.00	351.02
10.20	3900.00	10.20	3930.00	10.20	3970.00	10.20	3933.33	385.62
7.12	3030.00	7.12	3050.00	7.12	3090.00	7.12	3056.67	429.31
4.95	2400.00	4.95	2410.00	4.95	2440.00	4.95	2416.67	488.22
3.44	1940.00	3.44	1950.00	3.44	1970.00	3.44	1953.33	567.83
2.39	1610.00	2.39	1620.00	2.39	1640.00	2.39	1623.33	679.22
1.66	1360.00	1.66	1370.00	1.66	1390.00	1.66	1373.33	827.31
1.16	1180.00	1.16	1190.00	1.16	1200.00	1.16	1190.00	1025.86
0.80	1050.00	0.80	1060.00	0.80	1070.00	0.80	1060.00	1320.05
0.56	952.00	0.56	957.00	0.56	965.00	0.56	958.00	1716.85
0.39	877.00	0.39	881.00	0.39	888.00	0.39	882.00	2273.20
0.27	819.00	0.27	823.00	0.27	829.00	0.27	823.67	3050.62
0.19	775.00	0.19	778.00	0.19	784.00	0.19	779.00	4165.78
0.13	740.00	0.13	743.00	0.13	748.00	0.13	743.67	5720.51
0.09	714.00	0.09	715.00	0.09	720.00	0.09	716.33	7915.29
0.06	692.00	0.06	694.00	0.06	697.00	0.06	694.33	11056.26
0.04	675.00	0.04	676.00	0.04	680.00	0.04	677.00	15527.52
0.03	661.00	0.03	662.00	0.03	666.00	0.03	663.00	21953.64
0.02	651.00	0.02	651.00	0.02	655.00	0.02	652.33	31212.12

	Run #E	Run #F	Run #G		Avg.	Std. Dev.
Intercept [μNm]	776.0	778.4	784.1		779.5	3.4
Slope [$\mu\text{Nm}\cdot\text{min}$]	294.3	297.1	301.1		297.5	2.8
R2	1.0	1.0	1.0		1.0	0.0

Table B-2: Measured data for Mix #A with 0 % beads (paste) using Double Spiral spindle.

Mix B - 7/28/15								
CR-58								
Run #D		Run #E		Run #F		Average		
SR (1/min)	SS (μNm)	SR (1/min)	SS (μNm)	SR (1/min)	SS (μNm)	SR (1/min)	SS (μNm)	Ratio
0.02	79.40	0.02	105.00	0.02	78.40	0.02	87.60	4322.37
0.03	231.00	0.03	404.00	0.03	256.00	0.03	297.00	9027.36
0.05	491.00	0.06	654.00	0.06	533.00	0.06	559.33	10138.97
0.09	763.00	0.09	801.00	0.09	760.00	0.09	774.67	8405.06
0.15	918.00	0.15	894.00	0.15	888.00	0.15	900.00	5921.05
0.25	1000.00	0.25	969.00	0.25	973.00	0.25	980.67	3922.67
0.41	1080.00	0.41	1050.00	0.41	1060.00	0.41	1063.33	2599.84
0.67	1190.00	0.67	1160.00	0.67	1170.00	0.67	1173.33	1751.24
1.10	1340.00	1.10	1310.00	1.10	1320.00	1.10	1323.33	1203.03
1.80	1560.00	1.80	1540.00	1.80	1550.00	1.80	1550.00	861.11
2.94	1910.00	2.94	1900.00	2.94	1910.00	2.94	1906.67	648.53
4.82	2440.00	4.82	2440.00	4.82	2450.00	4.82	2443.33	506.92
7.90	3270.00	7.90	3280.00	7.90	3320.00	7.90	3290.00	416.46
12.90	4610.00	12.90	4640.00	12.90	4700.00	12.90	4650.00	360.47
21.20	6620.00	21.20	6670.00	21.20	6760.00	21.20	6683.33	315.25
21.20	6650.00	21.20	6700.00	21.20	6800.00	21.20	6716.67	316.82
14.70	5030.00	14.70	5060.00	14.70	5120.00	14.70	5070.00	344.90
10.20	3880.00	10.20	3900.00	10.20	3960.00	10.20	3913.33	383.66
7.12	3060.00	7.12	3080.00	7.12	3120.00	7.12	3086.67	433.52
4.95	2460.00	4.95	2470.00	4.95	2500.00	4.95	2476.67	500.34
3.44	2020.00	3.44	2030.00	3.44	2050.00	3.44	2033.33	591.09
2.39	1710.00	2.39	1720.00	2.39	1730.00	2.39	1720.00	719.67
1.66	1480.00	1.66	1480.00	1.66	1490.00	1.66	1483.33	893.57
1.16	1310.00	1.16	1310.00	1.16	1320.00	1.16	1313.33	1132.18
0.80	1180.00	0.80	1180.00	0.80	1190.00	0.80	1183.33	1473.64
0.56	1080.00	0.56	1080.00	0.56	1090.00	0.56	1083.33	1941.46
0.39	1010.00	0.39	1000.00	0.39	1010.00	0.39	1006.67	2594.50
0.27	948.00	0.27	948.00	0.27	952.00	0.27	949.33	3516.05
0.19	904.00	0.19	902.00	0.19	906.00	0.19	904.00	4834.22
0.13	868.00	0.13	867.00	0.13	870.00	0.13	868.33	6679.49
0.09	840.00	0.09	840.00	0.09	842.00	0.09	840.67	9289.13
0.06	820.00	0.06	818.00	0.06	820.00	0.06	819.33	13025.97
0.04	803.00	0.04	802.00	0.04	803.00	0.04	802.67	18381.68
0.03	790.00	0.03	789.00	0.03	790.00	0.03	789.67	26061.61
0.02	782.00	0.02	781.00	0.02	781.00	0.02	781.33	37206.35

	Run #D	Run #E	Run #F	Avg.	Std. Dev.
Intercept [μNm]	909.1	907.5	911.1	909.2	1.5
Slope [$\mu\text{Nm.min}$]	280.1	282.5	287.1	283.2	2.9
R2	1.0	1.0	1.0	1.0	0.0

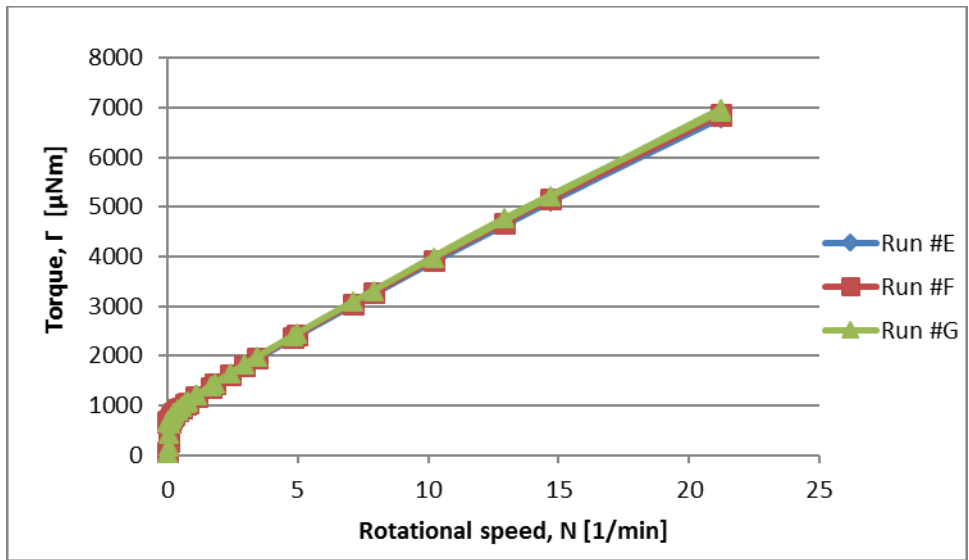


Figure B-1: Torque vs. Angular Speed using Double Spiral spindle on Mix# A, with 0% beads by volume. Portrays data from Table B-1.

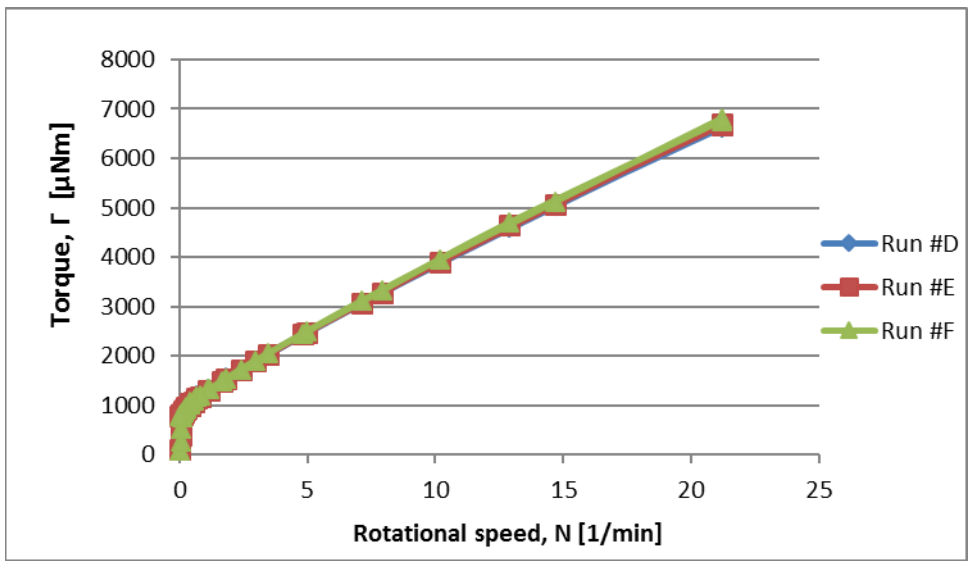


Figure B-2: Torque vs. Angular Speed using Double Spiral spindle on Mix# B, with 0% beads by volume. Portrays data from Table B-2.

Table B-3: Measured data for Mix #A with 0 % beads (paste) using 4-blades spindle.

Mix A - 7/21/15								
CR-46								
Run #H		Run #I		Run #J		Average		
SR (1/min)	SS (μNm)	SR (1/min)	SS (μNm)	SR (1/min)	SS (μNm)	SR (1/min)	SS (μNm)	Ratio
0.07	545.00	0.07	347.00	0.07	311.00	0.07	401.00	6042.19
0.11	843.00	0.11	757.00	0.11	748.00	0.11	782.67	7029.94
0.19	994.00	0.19	994.00	0.19	1010.00	0.19	999.33	5392.09
0.30	1080.00	0.30	1090.00	0.30	1120.00	0.30	1096.67	3607.46
0.50	1190.00	0.50	1200.00	0.50	1240.00	0.50	1210.00	2426.47
0.82	1360.00	0.82	1380.00	0.82	1410.00	0.82	1383.33	1695.26
1.34	1620.00	1.34	1640.00	1.34	1670.00	1.34	1643.33	1226.37
2.19	2020.00	2.19	2040.00	2.19	2080.00	2.19	2046.67	934.55
3.59	2620.00	3.59	2650.00	3.59	2690.00	3.59	2653.33	739.09
5.87	3560.00	5.87	3600.00	5.87	3650.00	5.87	3603.33	613.86
9.62	5020.00	9.62	5060.00	9.62	5140.00	9.62	5073.33	527.37
15.80	7290.00	15.80	7360.00	15.80	7460.00	15.80	7370.00	466.46
25.80	10800.00	25.80	11000.00	25.80	11100.00	25.80	10966.67	425.06
42.30	16400.00	42.30	16600.00	42.30	16800.00	42.30	16600.00	392.43
69.20	25100.00	69.20	25400.00	69.20	25700.00	69.20	25400.00	367.05
69.20	25000.00	69.20	25300.00	69.20	25600.00	69.20	25300.00	365.61
48.10	18200.00	48.10	18500.00	48.10	18700.00	48.10	18466.67	383.92
33.50	13400.00	33.50	13500.00	33.50	13700.00	33.50	13533.33	403.98
23.30	9880.00	23.30	10000.00	23.30	10100.00	23.30	9993.33	428.90
16.20	7400.00	16.20	7510.00	16.20	7590.00	16.20	7500.00	462.96
11.20	5610.00	11.20	5690.00	11.20	5760.00	11.20	5686.67	507.74
7.82	4320.00	7.82	4390.00	7.82	4440.00	7.82	4383.33	560.53
5.43	3380.00	5.43	3440.00	5.43	3480.00	5.43	3433.33	632.29
3.78	2700.00	3.78	2750.00	3.78	2790.00	3.78	2746.67	726.63
2.63	2210.00	2.63	2250.00	2.63	2290.00	2.63	2250.00	855.51
1.83	1850.00	1.83	1890.00	1.83	1920.00	1.83	1886.67	1030.97
1.27	1590.00	1.27	1620.00	1.27	1650.00	1.27	1620.00	1275.59
0.88	1390.00	0.88	1420.00	0.88	1450.00	0.88	1420.00	1609.98
0.61	1240.00	0.61	1270.00	0.61	1290.00	0.61	1266.67	2066.34
0.43	1130.00	0.43	1160.00	0.43	1180.00	0.43	1156.67	2715.18
0.30	1050.00	0.30	1080.00	0.30	1100.00	0.30	1076.67	3637.39
0.21	988.00	0.21	1010.00	0.21	1030.00	0.21	1009.33	4899.68
0.14	939.00	0.14	962.00	0.14	980.00	0.14	960.33	6715.62
0.10	901.00	0.10	924.00	0.10	942.00	0.10	922.33	9279.01
0.07	871.00	0.07	894.00	0.07	912.00	0.07	892.33	12926.12

	Run #H	Run #I	Run #J	Avg.	Std. Dev.
Intercept [μNm]	1246.4	1197.7	1225.4	1223.2	20.0
Slope[μNm.min]	361.1	352.9	357.1	357.0	3.4
R2	1.0	1.0	1.0	1.0	0.0

Table B-4: Measured data for Mix #B with 0 % beads (paste) using 4-blades spindle.

Mix B - 7/28/15								
CR-58								
Run #G		Run #H		Run #I		Average		
SR (1/min)	SS (μNm)	SR (1/min)	SS (μNm)	SR (1/min)	SS (μNm)	SR (1/min)	SS (μNm)	Ratio
0.07	424.00	0.06	376.00	0.06	610.00	0.06	470.00	7275.54
0.11	954.00	0.11	942.00	0.11	1090.00	0.11	995.33	8966.97
0.19	1210.00	0.19	1190.00	0.19	1220.00	0.19	1206.67	6510.79
0.31	1300.00	0.30	1280.00	0.30	1310.00	0.30	1296.67	4260.68
0.50	1410.00	0.50	1400.00	0.50	1430.00	0.50	1413.33	2832.33
0.82	1570.00	0.82	1570.00	0.82	1600.00	0.82	1580.00	1936.27
1.34	1820.00	1.34	1830.00	1.34	1860.00	1.34	1836.67	1370.65
2.19	2200.00	2.19	2220.00	2.19	2260.00	2.19	2226.67	1016.74
3.59	2810.00	3.59	2830.00	3.59	2880.00	3.59	2840.00	791.09
5.87	3750.00	5.87	3780.00	5.87	3840.00	5.87	3790.00	645.66
9.62	5190.00	9.62	5240.00	9.62	5310.00	9.62	5246.67	545.39
15.80	7450.00	15.80	7510.00	15.80	7620.00	15.80	7526.67	476.37
25.80	11000.00	25.80	11100.00	25.80	11200.00	25.80	11100.00	430.23
42.30	16500.00	42.30	16700.00	42.30	16900.00	42.30	16700.00	394.80
69.20	25300.00	69.20	25400.00	69.20	25900.00	69.20	25533.33	368.98
69.20	25200.00	69.20	25400.00	69.20	25800.00	69.20	25466.67	368.02
48.10	18400.00	48.10	18500.00	48.10	18800.00	48.10	18566.67	386.00
33.50	13500.00	33.50	13600.00	33.50	13900.00	33.50	13666.67	407.96
23.30	10100.00	23.30	10100.00	23.30	10300.00	23.30	10166.67	436.34
16.20	7570.00	16.20	7640.00	16.20	7770.00	16.20	7660.00	472.84
11.20	5790.00	11.20	5840.00	11.20	5940.00	11.20	5856.67	522.92
7.82	4500.00	7.82	4550.00	7.82	4630.00	7.82	4560.00	583.12
5.43	3570.00	5.43	3610.00	5.43	3680.00	5.43	3620.00	666.67
3.78	2900.00	3.78	2930.00	3.78	2990.00	3.78	2940.00	777.78
2.63	2410.00	2.63	2440.00	2.63	2480.00	2.63	2443.33	929.02
1.83	2040.00	1.83	2070.00	1.83	2110.00	1.83	2073.33	1132.97
1.27	1780.00	1.27	1800.00	1.27	1840.00	1.27	1806.67	1422.57
0.88	1580.00	0.88	1610.00	0.88	1640.00	0.88	1610.00	1825.40
0.61	1440.00	0.61	1460.00	0.61	1490.00	0.61	1463.33	2387.17
0.43	1330.00	0.43	1350.00	0.43	1370.00	0.43	1350.00	3169.01
0.30	1240.00	0.30	1260.00	0.30	1290.00	0.30	1263.33	4268.02
0.21	1180.00	0.21	1200.00	0.21	1220.00	0.21	1200.00	5825.24
0.14	1120.00	0.14	1140.00	0.14	1170.00	0.14	1143.33	7995.34
0.10	1080.00	0.10	1100.00	0.10	1130.00	0.10	1103.33	11099.93
0.07	1050.00	0.07	1070.00	0.07	1100.00	0.07	1073.33	15555.56

	Run #G	Run #H	Run #I		Avg.	Std. Dev.
Intercept [μNm]	1385.6	1405.5	1438.2		1409.7	21.7
Slope [$\mu\text{Nm.min}$]	352.7	354.9	360.7		356.1	3.4
R2	1.0	1.0	1.0		1.0	0.0

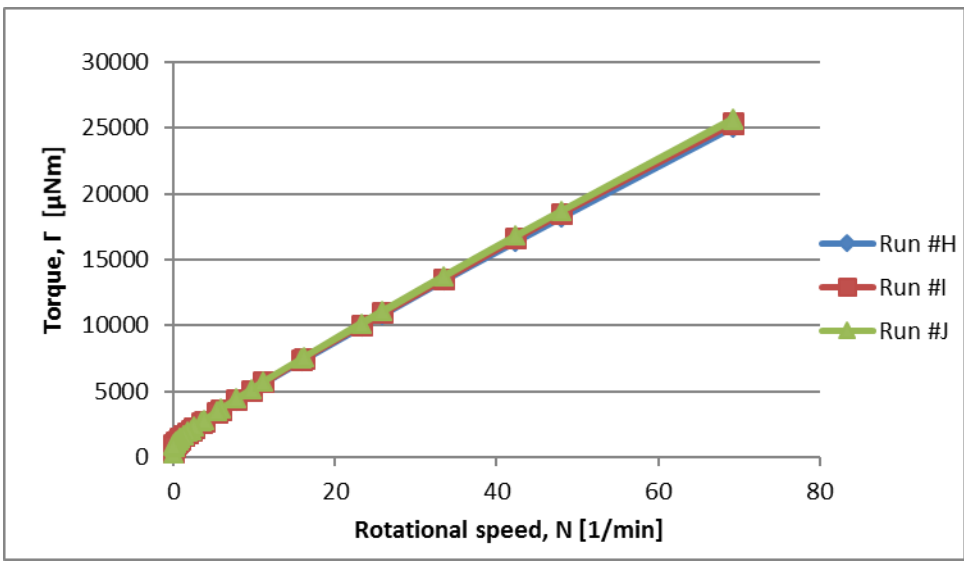


Figure B-3: Torque vs. Angular Speed using 4-Blades spindle on Mix# A, with 0 % beads by volume. Portrays data from Table B-3.

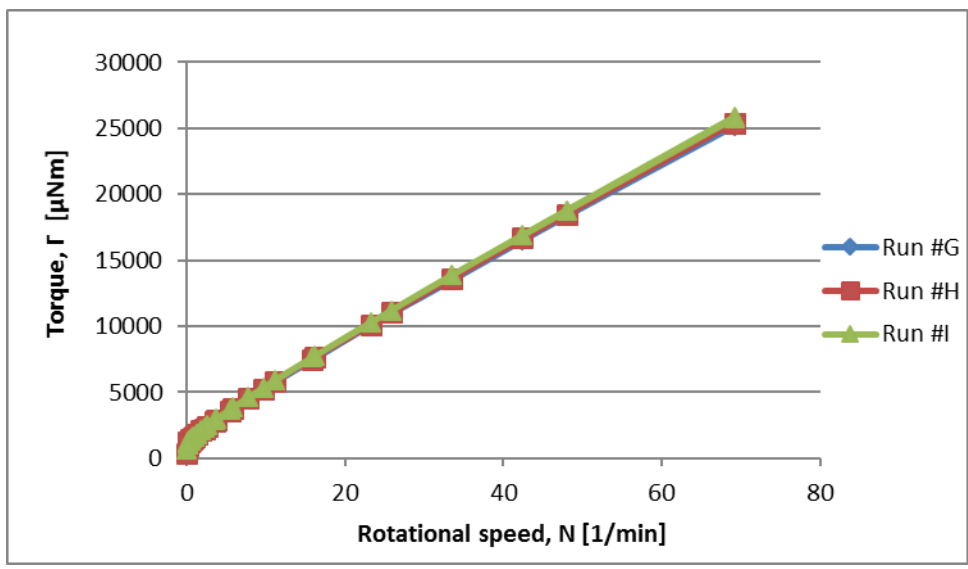


Figure B-4: Torque vs. Angular Speed using 4-Blades spindle on Mix# B, with 0 % beads by volume. Portrays data from Table B-4.

Table B-5: Measured data for Mix #A with 0 % beads (paste) using 6-blades spindle.

Mix A								
CR-46								
Run #K		Run #L		Run #M		Average		
SR (1/min)	SS (μNm)	SR (1/min)	SS (μNm)	SR (1/min)	SS (μNm)	SR (1/min)	SS (μNm)	Ratio
0.07	50.70	0.07	98.90	0.07	150.00	0.07	99.87	1463.61
0.11	154.00	0.11	236.00	0.11	253.00	0.11	214.33	1902.37
0.19	275.00	0.19	307.00	0.19	310.00	0.19	297.33	1601.44
0.30	336.00	0.30	343.00	0.30	343.00	0.30	340.67	1120.61
0.50	374.00	0.50	381.00	0.50	381.00	0.50	378.67	760.37
0.82	423.00	0.82	431.00	0.82	432.00	0.82	428.67	525.33
1.34	493.00	1.34	502.00	1.34	504.00	1.34	499.67	372.89
2.19	592.00	2.19	604.00	2.19	607.00	2.19	601.00	274.43
3.59	734.00	3.59	749.00	3.59	755.00	3.59	746.00	207.80
5.87	941.00	5.87	961.00	5.87	972.00	5.87	958.00	163.20
9.62	1250.00	9.62	1270.00	9.62	1290.00	9.62	1270.00	132.02
15.80	1710.00	15.80	1750.00	15.80	1770.00	15.80	1743.33	110.34
25.80	2420.00	25.80	2460.00	25.80	2500.00	25.80	2460.00	95.35
42.30	3530.00	42.30	3590.00	42.30	3630.00	42.30	3583.33	84.71
69.20	5260.00	69.20	5340.00	69.20	5400.00	69.20	5333.33	77.07
69.20	5250.00	69.20	5310.00	69.20	5390.00	69.20	5316.67	76.83
48.10	3890.00	48.10	3940.00	48.10	3990.00	48.10	3940.00	81.91
33.50	2920.00	33.50	2950.00	33.50	3000.00	33.50	2956.67	88.26
23.30	2220.00	23.30	2250.00	23.30	2280.00	23.30	2250.00	96.57
16.20	1710.00	16.20	1730.00	16.20	1760.00	16.20	1733.33	107.00
11.20	1350.00	11.20	1370.00	11.20	1390.00	11.20	1370.00	122.32
7.82	1080.00	7.82	1090.00	7.82	1110.00	7.82	1093.33	139.81
5.43	883.00	5.43	891.00	5.43	903.00	5.43	892.33	164.33
3.78	733.00	3.78	739.00	3.78	749.00	3.78	740.33	195.86
2.63	619.00	2.63	624.00	2.63	633.00	2.63	625.33	237.77
1.83	533.00	1.83	537.00	1.83	544.00	1.83	538.00	293.99
1.27	466.00	1.27	469.00	1.27	476.00	1.27	470.33	370.34
0.88	416.00	0.88	417.00	0.88	423.00	0.88	418.67	474.68
0.61	375.00	0.61	377.00	0.61	383.00	0.61	378.33	617.18
0.43	344.00	0.43	346.00	0.43	351.00	0.43	347.00	814.55
0.30	319.00	0.30	320.00	0.30	325.00	0.30	321.33	1085.59
0.21	300.00	0.21	300.00	0.21	305.00	0.21	301.67	1464.40
0.14	284.00	0.14	284.00	0.14	289.00	0.14	285.67	1997.67
0.10	271.00	0.10	271.00	0.10	276.00	0.10	272.67	2740.37
0.07	261.00	0.07	261.00	0.07	265.00	0.07	262.33	3790.94

	Run #K	Run #L	Run #M		Avg.	Std. Dev.
Intercept [μNm]	384.1	386.4	392.5		387.7	3.5
Slope [$\mu\text{Nm}.\text{min}$]	72.9	73.8	74.9		73.8	0.8
R2	1.0	1.0	1.0		1.0	0.0

Table B-6: Measured data for Mix #B with 0 % beads (paste) using 6-blades spindle.

Mix B								
CR-58								
Run #J		Run #K		Run #L		Average		
SR (1/min)	SS (μNm)	SR (1/min)	SS (μNm)	SR (1/min)	SS (μNm)	SR (1/min)	SS (μNm)	Ratio
0.07	71.30	0.07	67.50	0.07	205.00	0.07	114.60	1681.17
0.11	224.00	0.11	229.00	0.11	323.00	0.11	258.67	2309.52
0.19	357.00	0.19	368.00	0.19	369.00	0.19	364.67	1967.63
0.30	402.00	0.30	402.00	0.30	401.00	0.30	401.67	1321.27
0.50	440.00	0.50	439.00	0.50	439.00	0.50	439.33	882.20
0.82	492.00	0.82	492.00	0.82	493.00	0.82	492.33	603.35
1.34	564.00	1.34	565.00	1.34	567.00	1.34	565.33	421.89
2.19	665.00	2.19	670.00	2.19	672.00	2.19	669.00	305.48
3.59	810.00	3.59	819.00	3.59	823.00	3.59	817.33	227.67
5.87	1020.00	5.87	1040.00	5.87	1040.00	5.87	1033.33	176.04
9.62	1330.00	9.62	1350.00	9.62	1370.00	9.62	1350.00	140.33
15.80	1800.00	15.80	1830.00	15.80	1850.00	15.80	1826.67	115.61
25.80	2510.00	25.80	2550.00	25.80	2570.00	25.80	2543.33	98.58
42.30	3620.00	42.30	3670.00	42.30	3710.00	42.30	3666.67	86.68
69.20	5360.00	69.20	5430.00	69.20	5490.00	69.20	5426.67	78.42
69.20	5350.00	69.20	5410.00	69.20	5480.00	69.20	5413.33	78.23
48.10	3990.00	48.10	4030.00	48.10	4080.00	48.10	4033.33	83.85
33.50	3010.00	33.50	3040.00	33.50	3080.00	33.50	3043.33	90.85
23.30	2310.00	23.30	2330.00	23.30	2360.00	23.30	2333.33	100.14
16.20	1800.00	16.20	1820.00	16.20	1840.00	16.20	1820.00	112.35
11.20	1440.00	11.20	1450.00	11.20	1460.00	11.20	1450.00	129.46
7.82	1160.00	7.82	1170.00	7.82	1180.00	7.82	1170.00	149.62
5.43	960.00	5.43	967.00	5.43	976.00	5.43	967.67	178.21
3.78	807.00	3.78	811.00	3.78	819.00	3.78	812.33	214.90
2.63	690.00	2.63	693.00	2.63	699.00	2.63	694.00	263.88
1.83	600.00	1.83	603.00	1.83	608.00	1.83	603.67	329.87
1.27	532.00	1.27	533.00	1.27	538.00	1.27	534.33	420.73
0.88	478.00	0.88	479.00	0.88	483.00	0.88	480.00	544.22
0.61	436.00	0.61	437.00	0.61	439.00	0.61	437.33	713.43
0.43	403.00	0.43	403.00	0.43	406.00	0.43	404.00	948.36
0.30	376.00	0.30	376.00	0.30	379.00	0.30	377.00	1273.65
0.21	355.00	0.21	355.00	0.21	357.00	0.21	355.67	1726.54
0.14	338.00	0.14	338.00	0.14	341.00	0.14	339.00	2370.63
0.10	324.00	0.10	324.00	0.10	325.00	0.10	324.33	3259.63
0.07	313.00	0.07	312.00	0.07	314.00	0.07	313.00	4523.12

	Run #J	Run #K	Run #L		Avg.	Std. Dev.
Intercept [μNm]	448.5	449.2	452.0		449.9	1.5
Slope [$\mu\text{Nm}\cdot\text{min}$]	73.6	74.4	75.4		74.5	0.8
R2	1.0	1.0	1.0		1.0	0.0

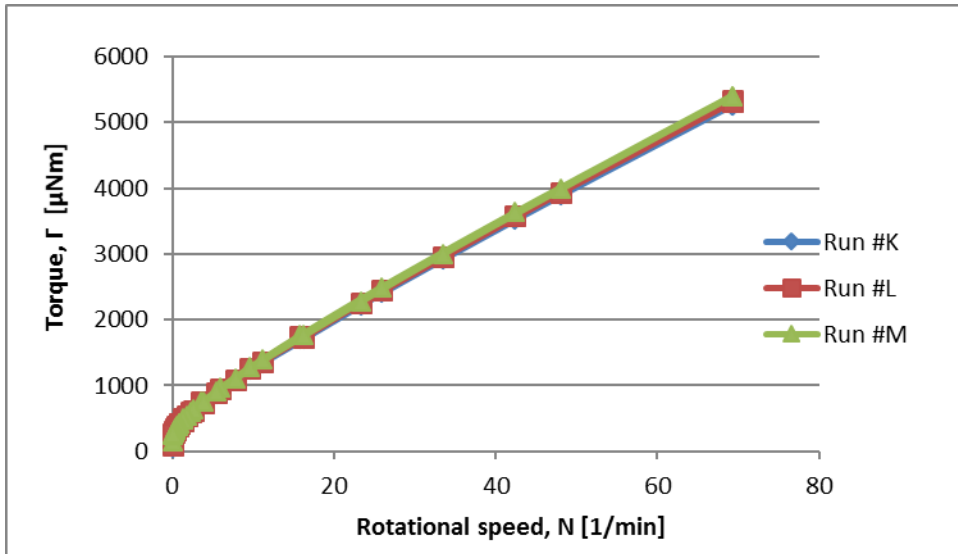


Figure B-5: Torque vs. Angular Speed using 6-Blades spindle on Mix# A, with 0 % beads by volume. Portrays data from Table B-5.

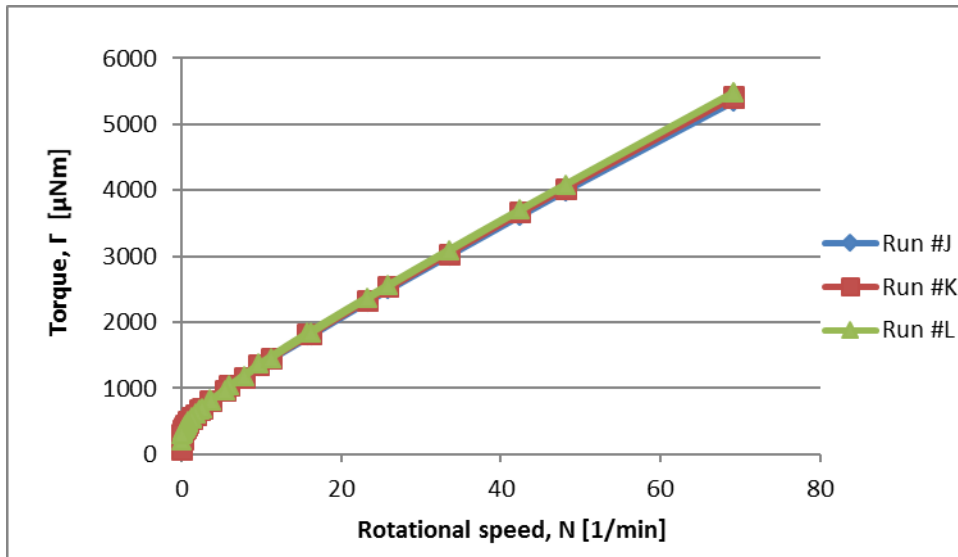


Figure B-6: Torque vs. Angular Speed using 6-Blades spindle on Mix# B, with 0 % beads by volume. Portrays data from Table B-6.

Table B-7: Measured data for Mix #A with 20 % beads (mortar) using Double Spiral spindle.

Mix A - 7/15/15								
CR-49								
Run #A		Run #B		Run #C		Average		
SR (1/min)	SS (μNm)	SR (1/min)	SS (μNm)	SR (1/min)	SS (μNm)	SR (1/min)	SS (μNm)	Ratio
0.02	194.00	0.02	312.00	0.02	242.00	0.02	249.33	13054.10
0.03	443.00	0.03	570.00	0.03	465.00	0.03	492.67	15112.47
0.05	726.00	0.06	780.00	0.06	688.00	0.06	731.33	13248.79
0.09	943.00	0.09	935.00	0.09	888.00	0.09	922.00	9992.77
0.15	1100.00	0.15	1050.00	0.15	1040.00	0.15	1063.33	6995.61
0.25	1220.00	0.25	1170.00	0.25	1170.00	0.25	1186.67	4746.67
0.41	1350.00	0.41	1310.00	0.41	1310.00	0.41	1323.33	3238.17
0.67	1540.00	0.67	1500.00	0.67	1500.00	0.67	1513.33	2258.71
1.10	1820.00	1.10	1790.00	1.10	1800.00	1.10	1803.33	1639.39
1.80	2240.00	1.80	2230.00	1.80	2230.00	1.80	2233.33	1240.74
2.94	2900.00	2.94	2910.00	2.94	2900.00	2.94	2903.33	987.53
4.82	3910.00	4.82	3950.00	4.82	3960.00	4.82	3940.00	817.43
7.90	5510.00	7.90	5580.00	7.89	5590.00	7.90	5560.00	704.09
12.90	8020.00	12.90	8020.00	12.90	8080.00	12.90	8040.00	623.26
21.20	11700.00	21.20	11700.00	21.20	11900.00	21.20	11766.67	555.03
21.20	11700.00	21.20	11700.00	21.20	11900.00	21.20	11766.67	555.03
14.70	8710.00	14.70	8720.00	14.70	8810.00	14.70	8746.67	595.01
10.20	6580.00	10.20	6590.00	10.20	6650.00	10.20	6606.67	647.71
7.11	5030.00	7.12	5060.00	7.11	5090.00	7.11	5060.00	711.34
4.95	3930.00	4.95	3920.00	4.95	3950.00	4.95	3933.33	794.61
3.44	3120.00	3.44	3120.00	3.44	3140.00	3.44	3126.67	908.91
2.39	2530.00	2.39	2540.00	2.39	2560.00	2.39	2543.33	1064.16
1.66	2100.00	1.66	2100.00	1.66	2120.00	1.66	2106.67	1269.08
1.15	1790.00	1.16	1780.00	1.16	1790.00	1.16	1786.67	1544.67
0.80	1560.00	0.80	1560.00	0.80	1570.00	0.80	1563.33	1946.87
0.56	1390.00	0.56	1380.00	0.56	1390.00	0.56	1386.67	2485.07
0.39	1260.00	0.39	1250.00	0.39	1260.00	0.39	1256.67	3238.83
0.27	1160.00	0.27	1150.00	0.27	1150.00	0.27	1153.33	4276.89
0.19	1080.00	0.19	1070.00	0.19	1080.00	0.19	1076.67	5757.58
0.13	1020.00	0.13	1010.00	0.13	1020.00	0.13	1016.67	7820.51
0.09	972.00	0.09	966.00	0.09	972.00	0.09	970.00	10730.09
0.06	930.00	0.06	934.00	0.06	932.00	0.06	932.00	14840.76
0.04	906.00	0.04	901.00	0.04	903.00	0.04	903.33	20687.02
0.03	887.00	0.03	882.00	0.03	880.00	0.03	883.00	29270.72
0.02	867.00	0.02	863.00	0.02	860.00	0.02	863.33	41373.80

	Run #A	Run #B	Run #C		Avg.	Std. Dev.
Intercept [μNm]	1079.6	1075.1	1074.8		1076.5	2.2
Slope [$\mu\text{Nm.min}$]	517.8	518.6	526.4		521.0	3.9
R2	1.0	1.0	1.0		1.0	0.0

Table B-8: Measured data for Mix #B with 20 % beads (mortar) using Double Spiral spindle.

Mix B - 7/29/15								
CR-63								
Run #A		Run #B		Run #C		Average		
SR (1/min)	SS (μ Nm)	SR (1/min)	SS (μ Nm)	SR (1/min)	SS (μ Nm)	SR (1/min)	SS (μ Nm)	Ratio
0.02	223.00	0.02	222.00	0.02	337.00	0.02	260.67	13299.32
0.03	462.00	0.03	505.00	0.03	584.00	0.03	517.00	15762.20
0.05	775.00	0.06	807.00	0.06	815.00	0.06	799.00	14483.38
0.09	1070.00	0.09	1030.00	0.09	1010.00	0.09	1036.67	11259.96
0.15	1220.00	0.15	1170.00	0.15	1150.00	0.15	1180.00	7763.16
0.25	1330.00	0.25	1290.00	0.25	1260.00	0.25	1293.33	5173.33
0.41	1460.00	0.41	1420.00	0.41	1400.00	0.41	1426.67	3488.18
0.67	1640.00	0.67	1600.00	0.67	1590.00	0.67	1610.00	2401.79
1.10	1890.00	1.10	1860.00	1.10	1850.00	1.10	1866.67	1696.97
1.80	2250.00	1.80	2260.00	1.80	2240.00	1.80	2250.00	1250.00
2.94	2830.00	2.94	2870.00	2.94	2860.00	2.94	2853.33	970.52
4.82	3740.00	4.82	3800.00	4.82	3810.00	4.82	3783.33	784.92
7.89	5190.00	7.89	5260.00	7.90	5280.00	7.89	5243.33	664.27
12.90	7430.00	12.90	7460.00	12.90	7550.00	12.90	7480.00	579.84
21.20	10700.00	21.20	10800.00	21.20	10900.00	21.20	10800.00	509.43
21.20	10800.00	21.20	10800.00	21.20	11000.00	21.20	10866.67	512.58
14.70	8040.00	14.70	8110.00	14.70	8210.00	14.70	8120.00	552.38
10.20	6170.00	10.20	6200.00	10.20	6260.00	10.20	6210.00	608.82
7.12	4790.00	7.12	4790.00	7.12	4850.00	7.12	4810.00	675.56
4.95	3790.00	4.95	3800.00	4.95	3810.00	4.95	3800.00	767.68
3.44	3060.00	3.44	3060.00	3.44	3080.00	3.44	3066.67	891.47
2.39	2540.00	2.39	2530.00	2.39	2550.00	2.39	2540.00	1062.76
1.66	2140.00	1.66	2140.00	1.66	2150.00	1.66	2143.33	1291.16
1.15	1860.00	1.16	1850.00	1.16	1850.00	1.16	1853.33	1602.31
0.80	1650.00	0.80	1650.00	0.80	1650.00	0.80	1650.00	2055.65
0.56	1490.00	0.56	1480.00	0.56	1480.00	0.56	1483.33	2655.13
0.39	1370.00	0.39	1360.00	0.39	1360.00	0.39	1363.33	3513.75
0.27	1280.00	0.27	1260.00	0.27	1260.00	0.27	1266.67	4691.36
0.19	1190.00	0.19	1190.00	0.19	1190.00	0.19	1190.00	6363.64
0.13	1140.00	0.13	1130.00	0.13	1140.00	0.13	1136.67	8743.59
0.09	1100.00	0.09	1090.00	0.09	1080.00	0.09	1090.00	12048.64
0.06	1060.00	0.06	1050.00	0.06	1050.00	0.06	1053.33	16755.04
0.04	1040.00	0.04	1030.00	0.04	1030.00	0.04	1033.33	23754.79
0.03	1020.00	0.03	1010.00	0.03	1000.00	0.03	1010.00	33333.33
0.02	1010.00	0.02	991.00	0.02	990.00	0.02	997.00	47779.55

	Run #A	Run #B	Run #C		Avg.	Std. Dev.
Intercept [μNm]	1206.8	1197.7	1191.8		1198.8	6.1
Slope [μNm.min]	467.0	469.2	477.7		471.3	4.6
R2	1.0	1.0	1.0		1.0	0.0

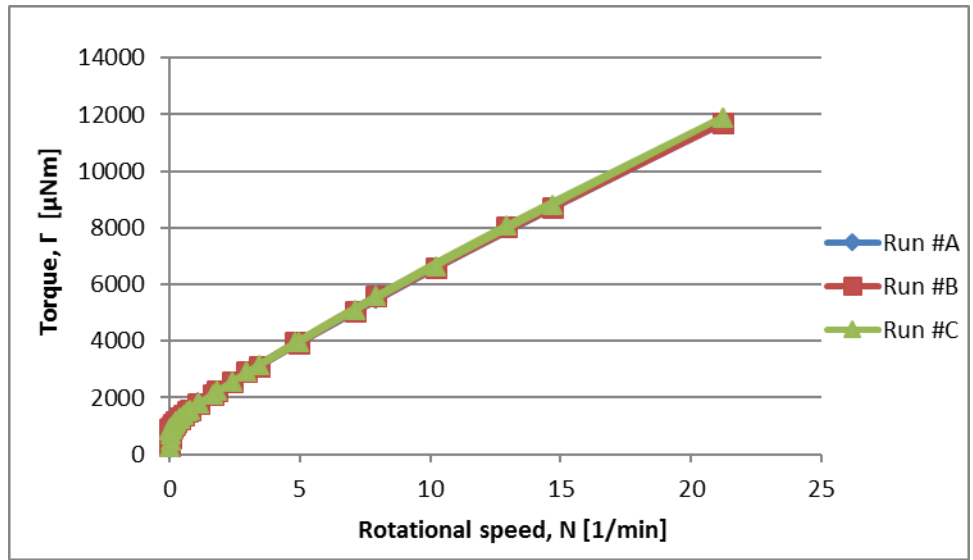


Figure B-7: Torque vs. Angular Speed using double spiral spindle on Mix# A, with 20 % beads by volume. Portrays data from Table B-7.

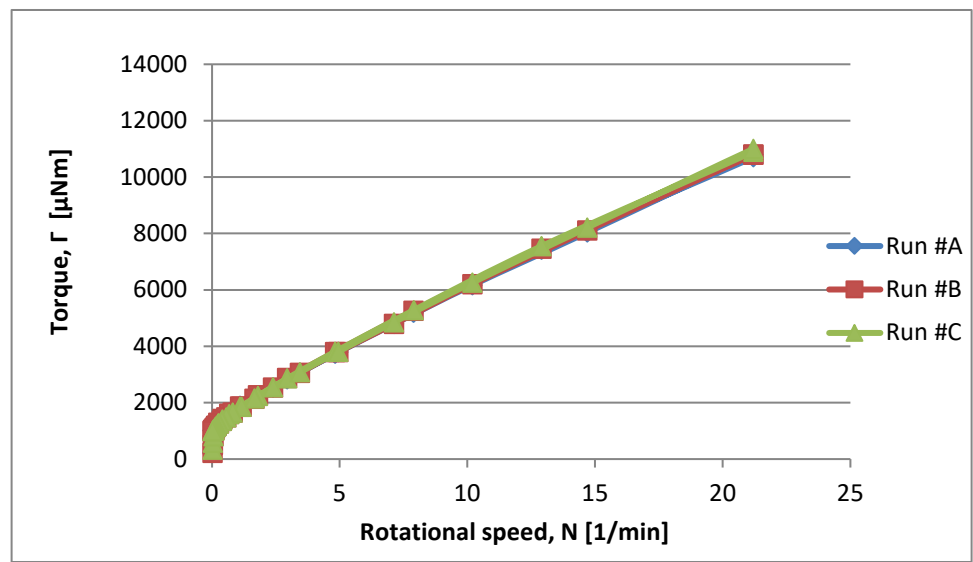


Figure B-8: Torque vs. Angular Speed using double spiral spindle on Mix# B, with 20 % beads by volume. Portrays data from Table B-8.

Table B-9: Measured data for Mix #A with 20 % beads (mortar) using 4-blades spindle.

Mix A - 7/15/15								
CR-49								
Run #F		Run #G		Run #H		Average		
SR (1/min)	SS (μNm)	SR (1/min)	SS (μNm)	SR (1/min)	SS (μNm)	SR (1/min)	SS (μNm)	Ratio
0.07	689.00	0.07	836.00	0.06	829.00	0.07	784.67	12053.25
0.11	1150.00	0.11	1300.00	0.11	1340.00	0.11	1263.33	11279.76
0.19	1400.00	0.19	1510.00	0.19	1570.00	0.19	1493.33	8028.67
0.30	1560.00	0.31	1680.00	0.30	1740.00	0.30	1660.00	5454.55
0.50	1770.00	0.50	1910.00	0.50	1980.00	0.50	1886.67	3785.95
0.82	2120.00	0.82	2230.00	0.82	2310.00	0.82	2220.00	2720.59
1.34	2600.00	1.34	2750.00	1.34	2830.00	1.34	2726.67	2034.83
2.19	3360.00	2.19	3560.00	2.19	3630.00	2.19	3516.67	1605.78
3.59	4530.00	3.59	4770.00	3.59	4870.00	3.59	4723.33	1315.69
5.87	6300.00	5.88	6580.00	5.88	6740.00	5.88	6540.00	1112.88
9.62	9080.00	9.62	9490.00	9.62	9710.00	9.62	9426.67	979.90
15.80	13500.00	15.80	14000.00	15.80	14300.00	15.80	13933.33	881.86
25.80	20500.00	25.80	21200.00	25.80	21600.00	25.80	21100.00	817.83
42.30	31400.00	42.30	32500.00	42.30	33200.00	42.30	32366.67	765.17
69.30	48800.00	69.20	50300.00	69.30	51300.00	69.27	50133.33	723.77
69.30	48800.00	69.20	50200.00	69.20	51200.00	69.23	50066.67	723.16
48.10	35400.00	48.10	36300.00	48.10	37000.00	48.10	36233.33	753.29
33.50	26000.00	33.50	26600.00	33.40	27000.00	33.47	26533.33	792.83
23.30	19000.00	23.30	19500.00	23.30	19900.00	23.30	19466.67	835.48
16.20	14100.00	16.20	14500.00	16.20	14700.00	16.20	14433.33	890.95
11.20	10600.00	11.20	10900.00	11.20	11100.00	11.20	10866.67	970.24
7.82	8090.00	7.81	8240.00	7.82	8390.00	7.82	8240.00	1054.16
5.43	6230.00	5.43	6360.00	5.43	6480.00	5.43	6356.67	1170.66
3.78	4870.00	3.78	4970.00	3.78	5080.00	3.78	4973.33	1315.70
2.63	3900.00	2.62	4000.00	2.63	4080.00	2.63	3993.33	1520.30
1.82	3210.00	1.83	3270.00	1.83	3350.00	1.83	3276.67	1793.80
1.27	2660.00	1.27	2740.00	1.27	2800.00	1.27	2733.33	2152.23
0.88	2290.00	0.88	2360.00	0.88	2420.00	0.88	2356.67	2669.94
0.61	2010.00	0.61	2090.00	0.61	2130.00	0.61	2076.67	3385.87
0.43	1800.00	0.43	1860.00	0.43	1910.00	0.43	1856.67	4354.96
0.30	1640.00	0.30	1700.00	0.30	1740.00	0.30	1693.33	5714.29
0.21	1510.00	0.21	1580.00	0.21	1620.00	0.21	1570.00	7646.10
0.14	1440.00	0.14	1480.00	0.14	1520.00	0.14	1480.00	10325.58
0.10	1360.00	0.10	1410.00	0.10	1450.00	0.10	1406.67	14194.42
0.07	1310.00	0.07	1360.00	0.07	1400.00	0.07	1356.67	19661.84

	Run #F	Run #G	Run #H		Avg.	Std. Dev.
Intercept [μNm]	1928.3	1972.3	2012.0		1970.9	34.2
Slope [$\mu\text{Nm.min}$]	694.2	713.6	727.3		711.7	13.6
R2	1.0	1.0	1.0		1.0	0.0

Table B-10: Measured data for Mix #B with 20 % beads (mortar) using 4-blades spindle.

Mix B - 7/29/15								
CR-63								
Run #E		Run #F		Run #G		Average		
SR (1/min)	SS (μ Nm)	SR (1/min)	SS (μ Nm)	SR (1/min)	SS (μ Nm)	SR (1/min)	SS (μ Nm)	Ratio
0.06	936.00	0.06	975.00	0.06	1060.00	0.06	990.33	15514.36
0.11	1390.00	0.11	1500.00	0.11	1570.00	0.11	1486.67	13234.42
0.19	1560.00	0.19	1720.00	0.19	1780.00	0.19	1686.67	9100.72
0.31	1720.00	0.30	1880.00	0.30	1940.00	0.30	1846.67	6067.91
0.50	1920.00	0.50	2100.00	0.50	2200.00	0.50	2073.33	4157.75
0.82	2230.00	0.82	2420.00	0.82	2510.00	0.82	2386.67	2921.26
1.34	2720.00	1.34	2920.00	1.34	3030.00	1.34	2890.00	2156.72
2.19	3450.00	2.19	3700.00	2.19	3830.00	2.19	3660.00	1671.23
3.59	4610.00	3.58	4900.00	3.59	5040.00	3.59	4850.00	1352.23
5.88	6350.00	5.87	6680.00	5.88	6850.00	5.88	6626.67	1127.62
9.62	9050.00	9.61	9490.00	9.62	9740.00	9.62	9426.67	980.24
15.80	13300.00	15.80	13800.00	15.80	14200.00	15.80	13766.67	871.31
25.80	19800.00	25.80	20600.00	25.80	21200.00	25.80	20533.33	795.87
42.30	30100.00	42.30	31500.00	42.30	32300.00	42.30	31300.00	739.95
69.20	46600.00	69.20	48700.00	69.20	49800.00	69.20	48366.67	698.94
69.20	46900.00	69.20	48700.00	69.30	49700.00	69.23	48433.33	699.57
48.10	34200.00	48.10	35400.00	48.10	36100.00	48.10	35233.33	732.50
33.50	25100.00	33.50	25900.00	33.50	26500.00	33.50	25833.33	771.14
23.30	18500.00	23.30	19100.00	23.30	19500.00	23.30	19033.33	816.88
16.20	13800.00	16.20	14300.00	16.20	14600.00	16.20	14233.33	878.60
11.20	10500.00	11.20	10800.00	11.20	11000.00	11.20	10766.67	961.31
7.82	7990.00	7.81	8250.00	7.81	8440.00	7.81	8226.67	1052.90
5.43	6220.00	5.43	6420.00	5.43	6600.00	5.43	6413.33	1181.09
3.77	4960.00	3.78	5130.00	3.78	5250.00	3.78	5113.33	1353.93
2.62	4030.00	2.63	4180.00	2.63	4260.00	2.63	4156.67	1582.49
1.82	3370.00	1.82	3480.00	1.83	3550.00	1.82	3466.67	1901.28
1.27	2850.00	1.27	2960.00	1.27	3030.00	1.27	2946.67	2320.21
0.88	2480.00	0.88	2590.00	0.88	2640.00	0.88	2570.00	2916.04
0.61	2210.00	0.61	2290.00	0.61	2340.00	0.61	2280.00	3717.39
0.43	1990.00	0.43	2070.00	0.43	2140.00	0.43	2066.67	4847.54
0.30	1840.00	0.30	1920.00	0.30	1980.00	0.30	1913.33	6463.96
0.21	1730.00	0.21	1800.00	0.21	1850.00	0.21	1793.33	8705.50
0.14	1650.00	0.14	1700.00	0.14	1750.00	0.14	1700.00	11915.89
0.10	1570.00	0.10	1640.00	0.10	1690.00	0.10	1633.33	16426.42
0.07	1530.00	0.07	1570.00	0.07	1620.00	0.07	1573.33	22768.93

	Run #E	Run #F	Run #G		Avg.	Std. Dev.
Intercept [μNm]	2131.8	2195.3	2256.9		2194.7	51.1
Slope [μNm.min]	664.3	688.6	702.0		685.0	15.6
R2	1.0	1.0	1.0		1.0	0.0

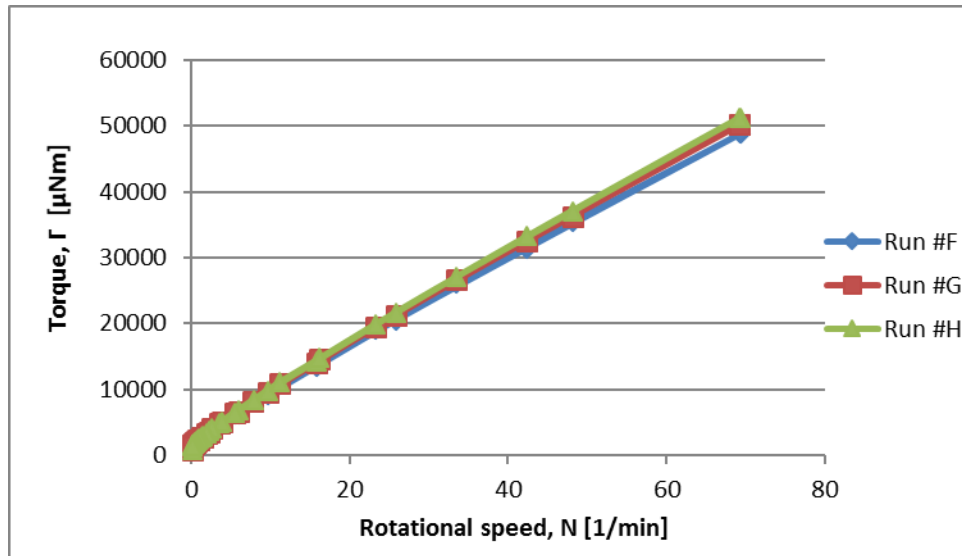


Figure B-9: Torque vs. Angular Speed using 4-blades spindle on Mix# A, with 20 % beads by volume. Portrays data from Table B-9.

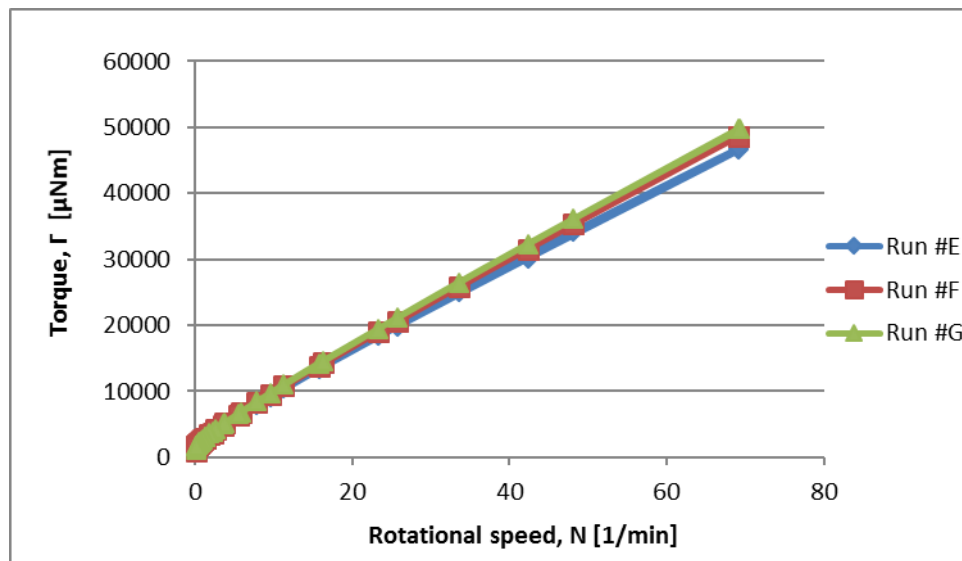


Figure B-10: Torque vs. Angular Speed using 4-blades spindle on Mix# B, with 20 % beads by volume. Portrays data from Table B-10.

Table B-11: Measured data for Mix #A with 20 % beads (mortar) using 6-blades spindle.

Mix A - 7/15/15								
CR-49								
Run #I		Run #J		Run #K		Average		
SR (1/min)	SS (μNm)	SR (1/min)	SS (μNm)	SR (1/min)	SS (μNm)	SR (1/min)	SS (μNm)	Ratio
0.07	239.00	0.07	286.00	0.07	247.00	0.07	257.33	3808.58
0.11	383.00	0.11	410.00	0.11	394.00	0.11	395.67	3511.83
0.19	468.00	0.19	470.00	0.19	477.00	0.19	471.67	2544.96
0.30	528.00	0.30	519.00	0.30	533.00	0.30	526.67	1732.46
0.50	593.00	0.50	587.00	0.50	600.00	0.50	593.33	1189.84
0.82	675.00	0.82	682.00	0.82	706.00	0.82	687.67	841.70
1.34	803.00	1.34	809.00	1.33	835.00	1.34	815.67	610.22
2.19	981.00	2.19	1000.00	2.19	1030.00	2.19	1003.67	458.30
3.59	1250.00	3.59	1280.00	3.59	1320.00	3.59	1283.33	357.47
5.87	1650.00	5.87	1710.00	5.87	1760.00	5.87	1706.67	290.74
9.62	2260.00	9.62	2320.00	9.62	2410.00	9.62	2330.00	242.20
15.80	3160.00	15.80	3290.00	15.80	3410.00	15.80	3286.67	208.02
25.80	4560.00	25.80	4760.00	25.80	4950.00	25.80	4756.67	184.37
42.30	6710.00	42.30	7020.00	42.30	7330.00	42.30	7020.00	165.96
69.20	10000.00	69.20	10500.00	69.20	10900.00	69.20	10466.67	151.25
69.20	10100.00	69.20	10500.00	69.20	10900.00	69.20	10500.00	151.73
48.10	7480.00	48.10	7760.00	48.10	8030.00	48.10	7756.67	161.26
33.50	5590.00	33.50	5790.00	33.50	5970.00	33.50	5783.33	172.64
23.30	4210.00	23.30	4340.00	23.30	4480.00	23.30	4343.33	186.41
16.20	3210.00	16.20	3320.00	16.20	3400.00	16.20	3310.00	204.32
11.20	2500.00	11.20	2560.00	11.20	2630.00	11.20	2563.33	228.87
7.82	1960.00	7.81	2020.00	7.82	2050.00	7.82	2010.00	257.14
5.43	1580.00	5.43	1610.00	5.43	1650.00	5.43	1613.33	297.11
3.78	1280.00	3.78	1310.00	3.78	1320.00	3.78	1303.33	344.80
2.62	1070.00	2.62	1080.00	2.62	1100.00	2.62	1083.33	413.49
1.82	894.00	1.82	911.00	1.83	918.00	1.82	907.67	497.81
1.27	773.00	1.27	775.00	1.27	797.00	1.27	781.67	615.49
0.88	677.00	0.88	682.00	0.88	689.00	0.88	682.67	773.41
0.61	609.00	0.61	605.00	0.61	614.00	0.61	609.33	993.48
0.43	545.00	0.43	552.00	0.43	563.00	0.43	553.33	1297.89
0.30	500.00	0.30	506.00	0.30	510.00	0.30	505.33	1705.29
0.21	466.00	0.21	474.00	0.21	467.00	0.21	469.00	2280.39
0.14	439.00	0.14	441.00	0.14	446.00	0.14	442.00	3090.91
0.10	423.00	0.10	424.00	0.10	424.00	0.10	423.67	4255.11
0.07	404.00	0.07	397.00	0.07	405.00	0.07	402.00	5817.66

	Run #I	Run #J	Run #K	Avg.	Std. Dev.
Intercept [μNm]	621.7	623.3	624.3	623.1	1.1
Slope [$\mu\text{Nm} \cdot \text{min}$]	142.2	148.0	153.7	148.0	4.7
R2	1.0	1.0	1.0	1.0	0.0

Table B-12: Measured data for Mix #B with 20 % beads (mortar) using 6-blades spindle. The numbers in red were not considered in the calculations due to an issue with the rheometer.

Mix B - 7/29/15								
CR-63								
Run #H		Run #I		Run #J		Average		
SR (1/min)	SS (μNm)	SR (1/min)	SS (μNm)	SR (1/min)	SS (μNm)	SR (1/min)	SS (μNm)	Ratio
0.07	248.00	0.07	276.00	0.07	271.00	0.07	265.00	3949.33
0.11	416.00	0.12	438.00	0.11	472.00	0.11	442.00	3888.56
0.19	525.00	0.19	559.00	0.19	567.00	0.19	550.33	2969.42
0.30	585.00	0.30	616.00	0.30	613.00	0.30	604.67	1995.60
0.50	657.00	0.51	329.00	0.50	683.00	0.50	556.33	1106.76
0.82	738.00	0.82	786.00	0.82	778.00	0.82	767.33	939.98
1.34	861.00	1.34	898.00	1.34	920.00	1.34	893.00	666.42
2.19	1040.00	2.19	1080.00	2.19	1120.00	2.19	1080.00	493.15
3.59	1310.00	3.46	1050.00	3.59	1410.00	3.55	1256.67	354.32
5.87	1690.00	5.73	674.00	5.87	1830.00	5.82	1398.00	240.07
9.62	2270.00	9.51	842.00	9.62	2460.00	9.58	1857.33	193.81
15.80	3170.00	15.60	997.00	15.80	3460.00	15.73	2542.33	161.59
25.80	4560.00	25.60	1050.00	25.80	5020.00	25.73	3543.33	137.69
42.30	6690.00	42.20	1090.00	42.30	7340.00	42.27	5040.00	119.24
69.20	9980.00	69.40	1720.00	69.20	10900.00	69.27	7533.33	108.76
69.20	9980.00	69.00	5110.00	69.20	10900.00	69.13	8663.33	125.31
48.10	7430.00	48.10	7940.00	48.10	8010.00	48.10	7793.33	162.02
33.50	5560.00	33.50	5900.00	33.50	5980.00	33.50	5813.33	173.53
23.30	4230.00	23.30	4440.00	23.30	4510.00	23.30	4393.33	188.56
16.20	3250.00	16.20	3400.00	16.20	3480.00	16.20	3376.67	208.44
11.20	2540.00	11.20	2650.00	11.20	2710.00	11.20	2633.33	235.12
7.81	2020.00	7.82	2100.00	7.81	2130.00	7.81	2083.33	266.64
5.43	1640.00	5.44	1700.00	5.43	1720.00	5.43	1686.67	310.43
3.78	1350.00	3.78	1380.00	3.78	1410.00	3.78	1380.00	365.08
2.63	1130.00	2.63	1150.00	2.63	1170.00	2.63	1150.00	437.26
1.83	971.00	1.83	986.00	1.83	998.00	1.83	985.00	538.25
1.27	837.00	1.27	862.00	1.27	871.00	1.27	856.67	674.54
0.88	745.00	0.88	758.00	0.88	765.00	0.88	756.00	856.82
0.61	672.00	0.61	679.00	0.61	686.00	0.61	679.00	1107.07
0.43	613.00	0.43	612.00	0.43	631.00	0.43	618.67	1451.13
0.30	572.00	0.30	571.00	0.30	585.00	0.30	576.00	1943.76
0.21	542.00	0.21	538.00	0.21	545.00	0.21	541.67	2629.45
0.14	508.00	0.14	507.00	0.14	514.00	0.14	509.67	3564.10
0.10	485.00	0.10	483.00	0.10	493.00	0.10	487.00	4899.40
0.07	470.00	0.07	467.00	0.07	480.00	0.07	472.33	6852.03

	Run #H	Run #I	Run #J	Avg.	Std. Dev.
Intercept [μNm]	693.9	650.8	701.9	682.2	22.4
Slope [$\mu\text{Nm.min}$]	139.5	156.9	152.2	149.5	7.3
R2	1.0	1.0	1.0	1.0	0.0

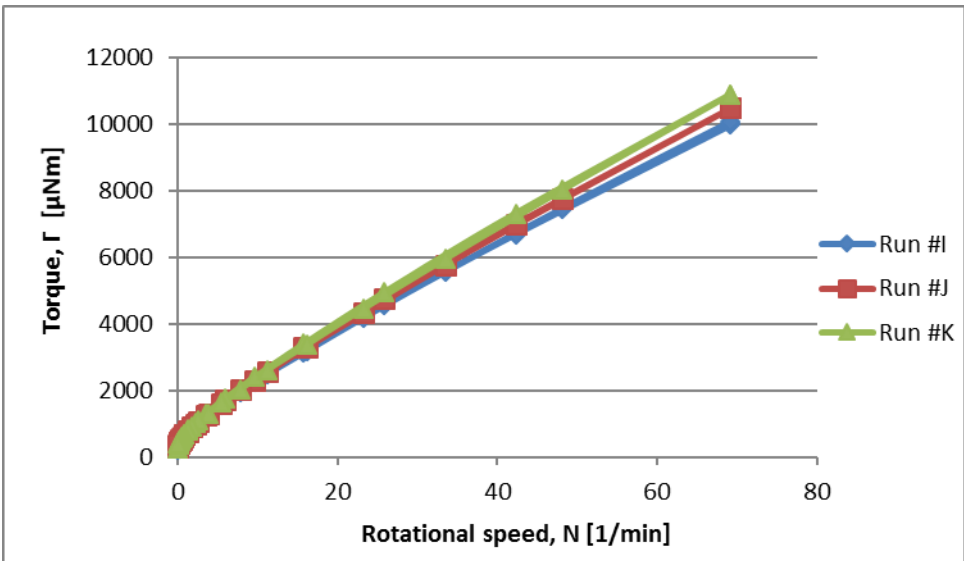


Figure B-11: Torque vs. Angular Speed using 6-blades spindle on Mix# A, with 20 % beads by volume. Portrays data from Table B-11.

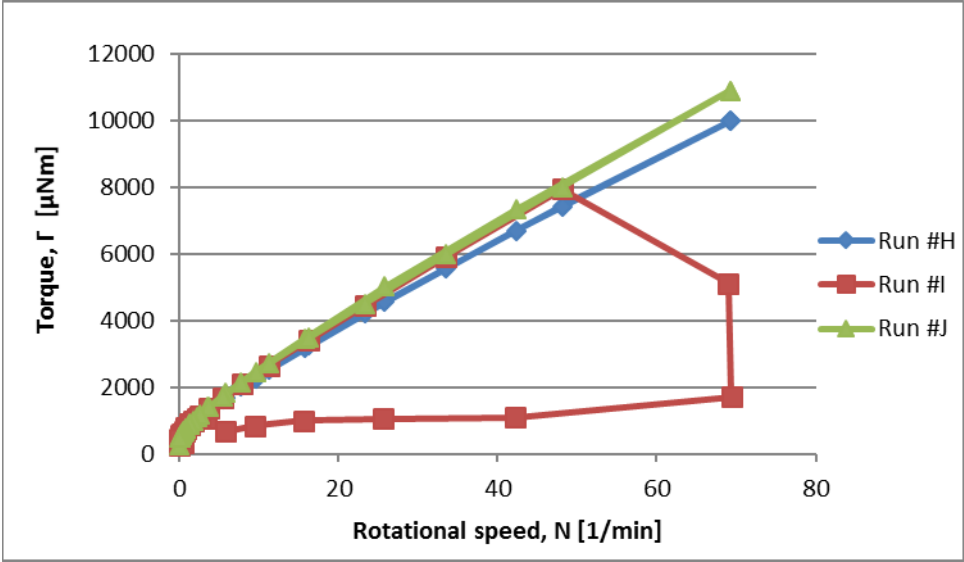


Figure B-12: Torque vs. Angular Speed using 6-blades spindle on Mix# B, with 20 % beads by volume. Portrays data from Table B-12.

Appendix C:

Original data measured from Concrete Rheometer

This appendix provides all the original data obtained from each test that was recorded directly from the rheometer described in Section 5.1.2. Also included are graphs needed for interpretation of the results, which portray the repeatability of the measured data.

Notes:

Each mix was tested with two spindles used both using paste and then 1 mm beads (20% concentration by volume) and 10-mm beads (40% concentration)

Each table will contain NIST codes showing the spindle and cup used, which are intended for NIST reference only.

Unit Notations:

SR = N: Rotational Speed [1/min]

SS = Γ : Measured Torque [$\mu\text{N}\cdot\text{m}$]

The conversion to fundamental units

*N: Rotational Speed \rightarrow [1/min] * $2\pi/60 =$ [rad/s]*

Γ : Measured Torque \rightarrow [$\mu\text{N}\cdot\text{m}$] $10^{-6} =$ [N·m]*

Table C-1: Measured data for Mix #A with 0 % beads (paste) using Spiral spindle.

Mix A - 7/15/15								
CR-47								
Run #B		Run #C		Run #D		Average		
SR (1/min)	SS (Nm)	SR (1/min)	SS (Nm)	SR (1/min)	SS (Nm)	SR (1/min)	SS (Nm)	Ratio
0.00	0.00	0.00	0.00	0.00	0.00	0.00	0.00	
0.15	0.00	0.15	0.00	0.16	0.00	0.15	0.00	0.02
0.25	0.02	0.25	0.02	0.25	0.02	0.25	0.02	0.08
0.40	0.03	0.40	0.02	0.40	0.03	0.40	0.02	0.06
0.63	0.03	0.63	0.03	0.63	0.03	0.63	0.03	0.05
1.00	0.03	1.00	0.03	1.00	0.03	1.00	0.03	0.03
1.58	0.04	1.59	0.04	1.58	0.04	1.58	0.04	0.03
2.51	0.05	2.51	0.05	2.51	0.05	2.51	0.05	0.02
3.98	0.06	3.98	0.06	3.98	0.06	3.98	0.06	0.01
6.32	0.07	6.31	0.07	6.31	0.07	6.31	0.07	0.01
10.01	0.09	10.01	0.09	10.01	0.09	10.01	0.09	0.01
15.87	0.13	15.85	0.13	15.86	0.13	15.86	0.13	0.01
25.14	0.17	25.13	0.17	25.13	0.18	25.13	0.17	0.01
39.85	0.25	39.83	0.25	39.84	0.25	39.84	0.25	0.01
63.13	0.36	63.17	0.36	63.15	0.36	63.15	0.36	0.01
100.07	0.54	100.04	0.54	100.06	0.54	100.06	0.54	0.01
100.10	0.54	100.07	0.54	100.14	0.54	100.10	0.54	0.01
72.02	0.40	72.03	0.40	72.06	0.41	72.04	0.40	0.01
51.85	0.31	51.83	0.31	51.79	0.31	51.82	0.31	0.01
37.30	0.24	37.28	0.24	37.29	0.24	37.29	0.24	0.01
26.85	0.18	26.85	0.18	26.83	0.18	26.84	0.18	0.01
19.32	0.14	19.12	0.14	19.32	0.15	19.26	0.14	0.01
13.90	0.11	13.90	0.11	13.90	0.12	13.90	0.11	0.01
10.01	0.09	10.01	0.09	10.00	0.09	10.01	0.09	0.01
7.20	0.08	7.20	0.08	7.20	0.08	7.20	0.08	0.01
5.18	0.06	5.19	0.06	5.18	0.06	5.18	0.06	0.01
3.73	0.05	3.73	0.05	3.73	0.05	3.73	0.05	0.01
2.69	0.05	2.68	0.05	2.68	0.05	2.68	0.05	0.02
1.93	0.04	1.93	0.04	1.93	0.04	1.93	0.04	0.02
1.39	0.04	1.39	0.04	1.39	0.04	1.39	0.04	0.03
1.00	0.03	1.00	0.03	1.00	0.03	1.00	0.03	0.03
0.72	0.03	0.72	0.03	0.72	0.03	0.72	0.03	0.04
0.52	0.03	0.54	0.03	0.51	0.03	0.52	0.03	0.05
0.37	0.03	0.37	0.03	0.37	0.03	0.37	0.03	0.07
0.27	0.03	0.27	0.03	0.27	0.03	0.27	0.03	0.09
0.19	0.02	0.19	0.02	0.19	0.02	0.19	0.02	0.13
0.14	0.02	0.14	0.02	0.14	0.02	0.14	0.02	0.16
0.10	0.02	0.10	0.02	0.10	0.02	0.10	0.02	0.22

Run #B		Run #C		Run #D		Avg.	Std. Dev.
Intercept [Nm]	0.0314		0.0314		0.0319	0.0316	0.000254
Slope[Nm.min]	0.0052		0.0052		0.0052	0.0052	0.000019
R2	1.0		1.0		1.0	0.997	0.000

Table C-2: Measured data for Mix #B with 0 % beads (paste) using Spiral spindle.

Mix B - 7/28/15								
CR-59								
Run #A		Run #B		Run #C		Average		
SR (1/min)	SS (Nm)	SR (1/min)	SS (Nm)	SR (1/min)	SS (Nm)	SR (1/min)	SS (Nm)	Ratio
-0.04	0.00	0.00	0.00	0.00	0.00	-0.01	0.00	
0.16	0.01	0.16	0.00	0.16	0.00	0.16	0.01	0.04
0.25	0.03	0.25	0.02	0.25	0.03	0.25	0.03	0.11
0.40	0.03	0.40	0.03	0.40	0.03	0.40	0.03	0.08
0.63	0.04	0.63	0.03	0.63	0.04	0.63	0.04	0.06
1.00	0.04	1.00	0.04	1.00	0.04	1.00	0.04	0.04
1.59	0.05	1.58	0.05	1.59	0.05	1.58	0.05	0.03
2.51	0.05	2.51	0.05	2.51	0.05	2.51	0.05	0.02
3.98	0.06	3.98	0.06	3.98	0.06	3.98	0.06	0.02
6.31	0.08	6.32	0.08	6.31	0.08	6.31	0.08	0.01
10.01	0.10	10.01	0.10	10.01	0.10	10.01	0.10	0.01
15.86	0.13	15.86	0.13	15.86	0.13	15.86	0.13	0.01
25.14	0.18	25.15	0.18	25.14	0.18	25.14	0.18	0.01
39.83	0.26	39.84	0.26	39.85	0.26	39.84	0.26	0.01
63.13	0.37	63.13	0.37	63.13	0.37	63.13	0.37	0.01
100.06	0.55	100.09	0.55	100.14	0.55	100.09	0.55	0.01
100.07	0.55	100.05	0.55	100.01	0.55	100.05	0.55	0.01
72.07	0.42	72.03	0.41	72.02	0.41	72.04	0.42	0.01
51.83	0.32	51.86	0.32	51.83	0.32	51.84	0.32	0.01
37.31	0.25	37.32	0.24	37.31	0.24	37.31	0.24	0.01
26.85	0.19	26.84	0.19	26.83	0.19	26.84	0.19	0.01
19.32	0.15	19.03	0.15	18.91	0.15	19.08	0.15	0.01
13.90	0.12	13.60	0.12	13.90	0.12	13.80	0.12	0.01
10.01	0.10	10.01	0.10	10.01	0.10	10.01	0.10	0.01
7.20	0.08	7.20	0.08	7.20	0.08	7.20	0.08	0.01
5.18	0.07	5.18	0.07	5.18	0.07	5.18	0.07	0.01
3.73	0.06	3.73	0.06	3.73	0.06	3.73	0.06	0.02
2.68	0.06	2.68	0.05	2.69	0.05	2.68	0.05	0.02
1.93	0.05	1.93	0.05	1.93	0.05	1.93	0.05	0.03
1.39	0.04	1.39	0.04	1.39	0.04	1.39	0.04	0.03
1.00	0.04	1.00	0.04	1.00	0.04	1.00	0.04	0.04
0.72	0.04	0.72	0.04	0.72	0.04	0.72	0.04	0.05
0.52	0.04	0.54	0.03	0.52	0.03	0.53	0.03	0.07
0.37	0.03	0.37	0.03	0.37	0.03	0.37	0.03	0.09
0.27	0.03	0.27	0.03	0.27	0.03	0.27	0.03	0.12
0.19	0.03	0.19	0.03	0.19	0.03	0.19	0.03	0.16
0.14	0.03	0.14	0.03	0.14	0.03	0.14	0.03	0.21
0.10	0.03	0.10	0.03	0.10	0.03	0.10	0.03	0.29

	Run #A	Run #B	Run #C		Avg.	Std. Dev.
Intercept [Nm]	0.0395	0.0377	0.0381		0.0384	0.000762
Slope[Nm.min]	0.0053	0.0053	0.0053		0.0053	0.000002
R2	1.0	1.0	1.0		0.997	0.000

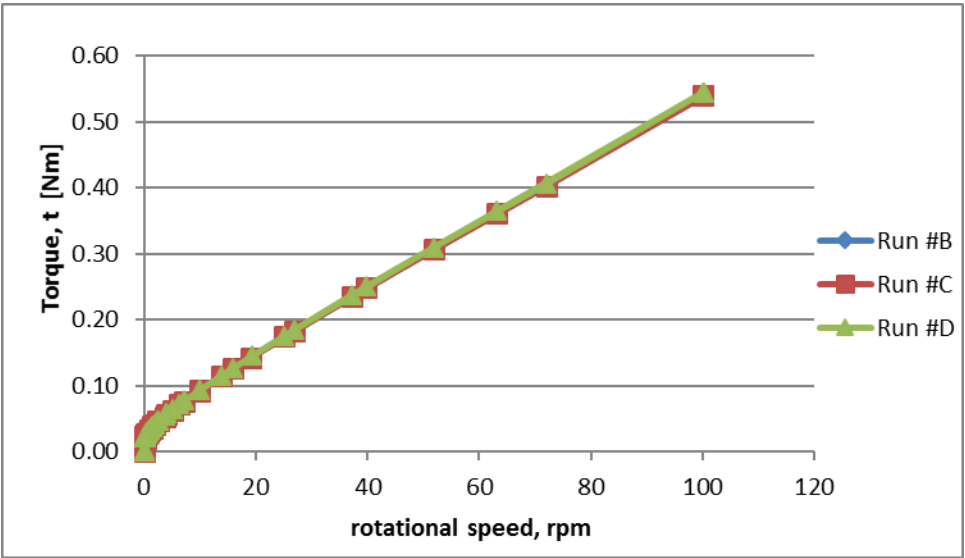


Figure C-1: Torque vs. Angular Speed using Spiral spindle on Mix# A, with 0 % beads by volume. Portrays data from Table C-1.

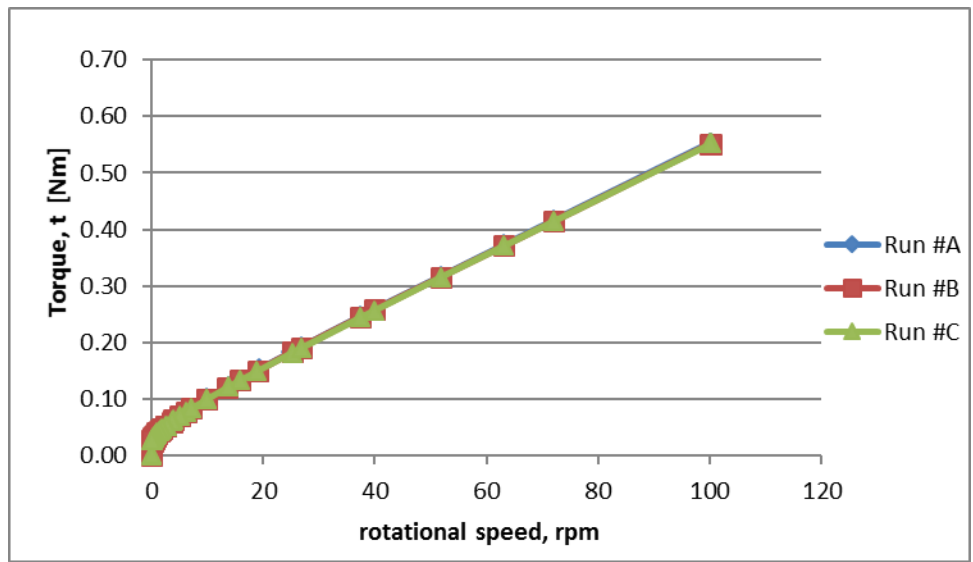


Figure C-2: Torque vs. Angular Speed using Spiral spindle on Mix# B, with 0 % beads by volume. Portrays data from Table C-2.

Table C-3: Measured data for Mix #A with 0 % beads (paste) using 4-Vane spindle.

Mix A - 7/15/15								
CR-47								
Run #E		Run #F		Run #G		Average		
SR (1/min)	SS (Nm)	SR (1/min)	SS (Nm)	SR (1/min)	SS (Nm)	SR (1/min)	SS (Nm)	Ratio
0.00	0.00	0.00	0.00	0.00	0.00	0.00	0.00	
0.16	0.01	0.16	0.01	0.16	0.01	0.16	0.01	0.04
0.25	0.03	0.25	0.03	0.25	0.03	0.25	0.03	0.13
0.40	0.04	0.40	0.04	0.40	0.04	0.40	0.04	0.09
0.63	0.04	0.63	0.04	0.63	0.04	0.63	0.04	0.07
1.00	0.05	1.00	0.05	1.00	0.05	1.00	0.05	0.05
1.59	0.06	1.58	0.05	1.58	0.06	1.58	0.05	0.03
2.51	0.06	2.51	0.06	2.51	0.07	2.51	0.06	0.03
3.98	0.08	3.98	0.08	3.98	0.08	3.98	0.08	0.02
6.31	0.10	6.31	0.10	6.31	0.10	6.31	0.10	0.02
10.01	0.13	10.00	0.13	10.01	0.13	10.01	0.13	0.01
15.86	0.18	15.85	0.18	15.85	0.18	15.85	0.18	0.01
25.14	0.25	25.14	0.25	25.15	0.25	25.14	0.25	0.01
39.84	0.36	39.84	0.36	39.84	0.36	39.84	0.36	0.01
63.19	0.53	63.13	0.53	63.16	0.53	63.16	0.53	0.01
100.09	0.80	100.09	0.80	100.09	0.80	100.09	0.80	0.01
100.07	0.80	100.05	0.80	100.02	0.80	100.05	0.80	0.01
72.02	0.59	72.06	0.60	72.01	0.59	72.03	0.59	0.01
51.88	0.45	51.81	0.45	51.81	0.45	51.83	0.45	0.01
37.31	0.34	37.31	0.34	37.30	0.34	37.31	0.34	0.01
26.84	0.26	26.83	0.27	26.84	0.26	26.84	0.26	0.01
17.82	0.19	18.93	0.20	18.82	0.20	18.52	0.20	0.01
13.90	0.16	13.91	0.16	13.90	0.16	13.90	0.16	0.01
10.01	0.13	10.01	0.13	10.01	0.13	10.01	0.13	0.01
7.20	0.11	7.20	0.11	7.20	0.11	7.20	0.11	0.01
5.18	0.09	5.18	0.09	5.18	0.09	5.18	0.09	0.02
3.73	0.08	3.73	0.08	3.73	0.08	3.73	0.08	0.02
2.68	0.06	2.69	0.07	2.68	0.07	2.68	0.06	0.02
1.93	0.06	1.93	0.06	1.93	0.06	1.93	0.06	0.03
1.39	0.05	1.39	0.05	1.39	0.05	1.39	0.05	0.04
1.00	0.04	1.00	0.05	1.00	0.05	1.00	0.05	0.05
0.72	0.04	0.72	0.04	0.72	0.04	0.72	0.04	0.06
0.52	0.04	0.52	0.04	0.52	0.04	0.52	0.04	0.07
0.37	0.04	0.37	0.04	0.37	0.04	0.37	0.04	0.10
0.27	0.03	0.27	0.03	0.27	0.03	0.27	0.03	0.13
0.19	0.03	0.19	0.03	0.19	0.03	0.19	0.03	0.17
0.14	0.03	0.14	0.03	0.14	0.03	0.14	0.03	0.21
0.10	0.03	0.10	0.03	0.10	0.03	0.10	0.03	0.29

	Run #E	Run #F	Run #G		Avg.	Std. Dev.
Intercept [Nm]	0.0413	0.0433	0.0416		0.0420	0.000875
Slope[Nm.min]	0.0077	0.0077	0.0077		0.0077	0.000008
R2	1.0	1.0	1.0		0.998	0.000

Table C-4: Measured data for Mix #B with 0 % beads (paste) using 4-Vane spindle.

Mix B - 7/28/15								
CR-59								
Run #E		Run #F		Run #G		Average		
SR (1/min)	SS (Nm)	SR (1/min)	SS (Nm)	SR (1/min)	SS (Nm)	SR (1/min)	SS (Nm)	Ratio
0.00	0.00	0.00	0.00	0.00	0.00	0.00	0.00	
0.16	0.01	0.16	0.01	0.16	0.01	0.16	0.01	0.05
0.25	0.04	0.25	0.04	0.25	0.04	0.25	0.04	0.16
0.40	0.05	0.40	0.05	0.40	0.05	0.40	0.05	0.12
0.63	0.05	0.63	0.05	0.63	0.05	0.63	0.05	0.08
1.00	0.05	1.00	0.05	1.00	0.05	1.00	0.05	0.05
1.58	0.06	1.58	0.06	1.58	0.06	1.58	0.06	0.04
2.51	0.07	2.51	0.07	2.51	0.07	2.51	0.07	0.03
3.98	0.09	3.98	0.09	3.98	0.09	3.98	0.09	0.02
6.32	0.11	6.31	0.11	6.31	0.11	6.31	0.11	0.02
10.01	0.14	10.00	0.14	10.01	0.14	10.01	0.14	0.01
15.86	0.19	15.85	0.19	15.85	0.19	15.85	0.19	0.01
25.14	0.26	25.12	0.26	25.13	0.26	25.13	0.26	0.01
39.84	0.37	39.85	0.37	39.85	0.37	39.84	0.37	0.01
63.12	0.54	63.13	0.55	63.14	0.55	63.13	0.55	0.01
100.06	0.82	100.10	0.82	100.17	0.82	100.11	0.82	0.01
100.15	0.82	100.04	0.82	100.09	0.82	100.09	0.82	0.01
72.05	0.61	71.98	0.61	72.02	0.61	72.02	0.61	0.01
51.81	0.46	51.85	0.46	51.84	0.46	51.83	0.46	0.01
37.31	0.35	37.32	0.36	37.29	0.35	37.30	0.35	0.01
26.84	0.27	26.85	0.28	26.85	0.28	26.85	0.28	0.01
19.32	0.22	19.03	0.21	19.34	0.21	19.23	0.22	0.01
13.91	0.17	13.91	0.17	13.91	0.17	13.91	0.17	0.01
10.01	0.14	10.01	0.14	10.00	0.14	10.01	0.14	0.01
7.20	0.12	7.20	0.12	7.20	0.12	7.20	0.12	0.02
5.18	0.10	5.18	0.10	5.18	0.10	5.18	0.10	0.02
3.73	0.08	3.73	0.09	3.73	0.08	3.73	0.08	0.02
2.69	0.07	2.68	0.07	2.68	0.07	2.68	0.07	0.03
1.93	0.07	1.93	0.07	1.93	0.06	1.93	0.07	0.03
1.39	0.06	1.39	0.06	1.39	0.06	1.39	0.06	0.04
1.00	0.05	1.00	0.05	1.00	0.05	1.00	0.05	0.05
0.72	0.05	0.72	0.05	0.72	0.05	0.72	0.05	0.07
0.54	0.05	0.52	0.05	0.52	0.05	0.53	0.05	0.09
0.37	0.04	0.37	0.04	0.37	0.04	0.37	0.04	0.12
0.27	0.04	0.27	0.04	0.27	0.04	0.27	0.04	0.15
0.19	0.04	0.19	0.04	0.19	0.04	0.19	0.04	0.21
0.14	0.04	0.14	0.04	0.14	0.04	0.14	0.04	0.27
0.10	0.04	0.10	0.04	0.10	0.04	0.10	0.04	0.37

	Run #E	Run #F	Run #G	Avg.	Std. Dev.
Intercept [Nm]	0.0493	0.0499	0.0496	0.0496	0.000241
Slope[Nm.min]	0.0078	0.0078	0.0078	0.0078	0.000008
R2	1.0	1.0	1.0	0.997	0.000

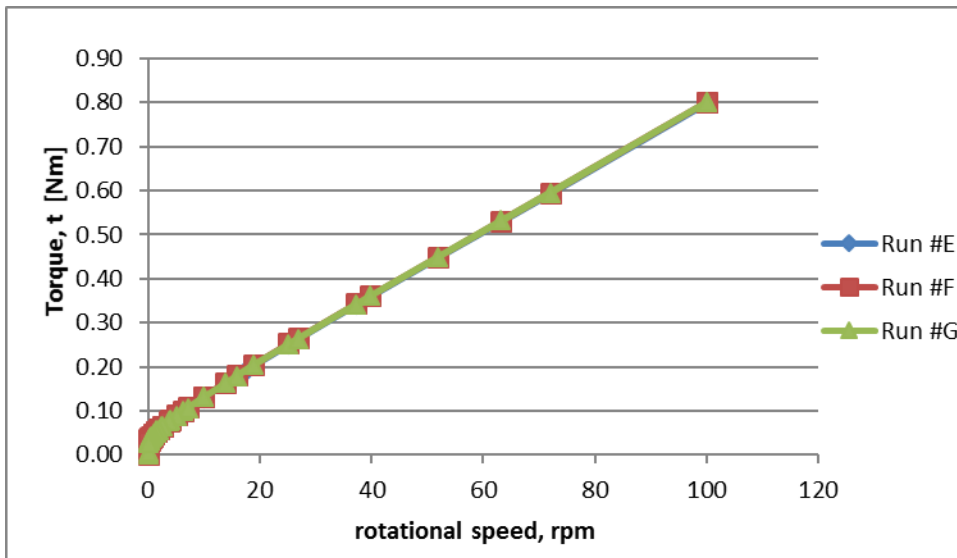


Figure C-3: Torque vs. Angular Speed using 4-blades spindle on Mix# A, with 0 % beads by volume. Portrays data from Table C-3.

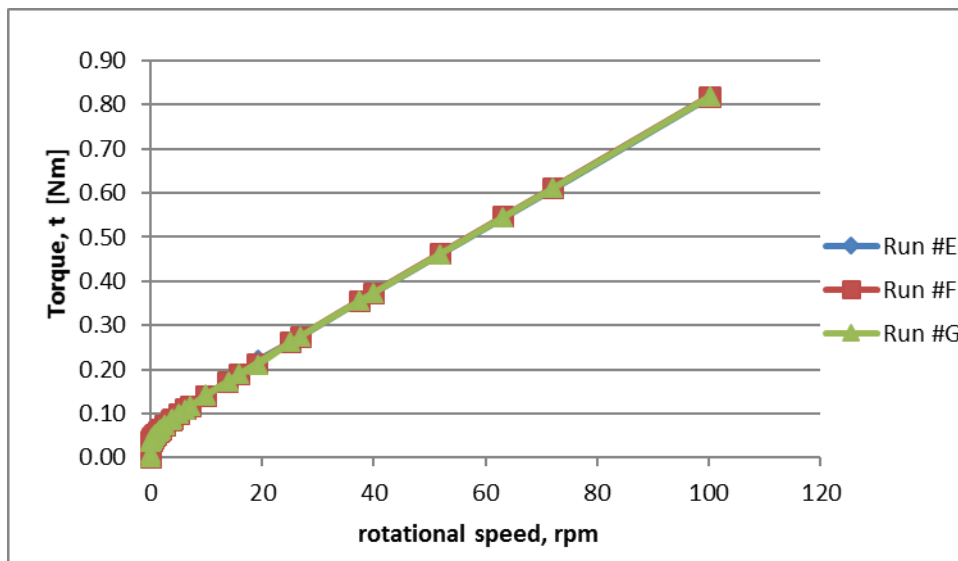


Figure C-4: Torque vs. Angular Speed using 4-blades spindle on Mix# B, with 0 % beads by volume. Portrays data from Table C-4.

Table C-5: Measured data for Mix #A with 20 % beads (mortar) using Spiral spindle.

Mix A - 7/15/15								
CR-50								
Run #D		Run #E		Run #F		Average		
SR (1/min)	SS (Nm)	SR (1/min)	SS (Nm)	SR (1/min)	SS (Nm)	SR (1/min)	SS (Nm)	Ratio
0.00	0.00	0.00	0.00	0.00	0.00	0.00	0.00	
0.16	0.01	0.15	0.01	0.16	0.01	0.16	0.01	0.04
0.25	0.03	0.25	0.03	0.25	0.03	0.25	0.03	0.13
0.40	0.04	0.40	0.04	0.40	0.04	0.40	0.04	0.10
0.63	0.04	0.63	0.04	0.63	0.04	0.63	0.04	0.07
1.00	0.05	1.00	0.05	1.00	0.05	1.00	0.05	0.05
1.59	0.06	1.58	0.06	1.58	0.06	1.58	0.06	0.04
2.51	0.07	2.51	0.07	2.51	0.07	2.51	0.07	0.03
3.98	0.09	3.98	0.09	3.98	0.09	3.98	0.09	0.02
6.31	0.12	6.31	0.12	6.31	0.12	6.31	0.12	0.02
10.00	0.16	10.01	0.16	10.01	0.16	10.00	0.16	0.02
15.86	0.22	15.86	0.21	15.86	0.21	15.86	0.21	0.01
25.12	0.30	25.14	0.30	25.14	0.30	25.14	0.30	0.01
39.83	0.43	39.83	0.43	39.84	0.43	39.83	0.43	0.01
63.17	0.63	63.17	0.63	63.13	0.63	63.16	0.63	0.01
100.09	0.93	100.01	0.93	100.09	0.93	100.06	0.93	0.01
100.04	0.93	100.10	0.93	100.05	0.93	100.06	0.93	0.01
72.03	0.70	72.01	0.70	72.02	0.70	72.02	0.70	0.01
51.83	0.53	51.81	0.53	51.83	0.53	51.83	0.53	0.01
37.31	0.41	37.31	0.41	37.30	0.41	37.31	0.41	0.01
26.85	0.31	26.83	0.32	26.84	0.32	26.84	0.32	0.01
19.32	0.25	19.31	0.25	19.32	0.25	19.32	0.25	0.01
13.90	0.19	13.90	0.19	13.90	0.19	13.90	0.19	0.01
10.01	0.16	10.01	0.16	10.01	0.15	10.01	0.16	0.02
7.20	0.12	7.20	0.13	7.20	0.13	7.20	0.13	0.02
5.18	0.10	5.18	0.10	5.18	0.10	5.18	0.10	0.02
3.73	0.09	3.73	0.09	3.73	0.09	3.73	0.09	0.02
2.68	0.07	2.68	0.07	2.69	0.07	2.68	0.07	0.03
1.93	0.07	1.93	0.07	1.93	0.06	1.93	0.06	0.03
1.39	0.06	1.39	0.06	1.39	0.06	1.39	0.06	0.04
1.00	0.05	1.00	0.05	1.00	0.05	1.00	0.05	0.05
0.72	0.05	0.72	0.05	0.72	0.05	0.72	0.05	0.06
0.52	0.05	0.52	0.04	0.52	0.04	0.52	0.04	0.09
0.37	0.04	0.37	0.04	0.37	0.04	0.37	0.04	0.11
0.27	0.04	0.27	0.04	0.27	0.04	0.27	0.04	0.14
0.19	0.04	0.19	0.04	0.19	0.04	0.19	0.04	0.19
0.14	0.03	0.14	0.03	0.14	0.03	0.14	0.03	0.24
0.10	0.03	0.10	0.03	0.10	0.03	0.10	0.03	0.32

	Run #D	Run #E	Run #F		Avg.	Std. Dev.
Intercept [Nm]	0.0496	0.0491	0.0482		0.0490	0.000576
Slope[Nm.min]	0.0090	0.0091	0.0091		0.0091	0.000027
R2	1.0	1.0	1.0		0.9961	0.000096

Table C-6: Measured data for Mix #B with 20 % beads (mortar) using Spiral spindle.

Mix B - 7/28/15								
CR-63								
Run #D		Run #E		Run #F		Average		
SR (1/min)	SS (Nm)	SR (1/min)	SS (Nm)	SR (1/min)	SS (Nm)	SR (1/min)	SS (Nm)	Ratio
0.00	0.00	0.00	0.00	0.00	0.00	0.00	0.00	
0.16	0.01	0.16	0.01	0.16	0.01	0.16	0.01	0.05
0.25	0.04	0.25	0.04	0.25	0.03	0.25	0.04	0.15
0.40	0.05	0.40	0.05	0.40	0.04	0.40	0.04	0.11
0.63	0.05	0.63	0.05	0.63	0.05	0.63	0.05	0.08
1.00	0.06	1.00	0.06	1.00	0.06	1.00	0.06	0.06
1.59	0.07	1.58	0.07	1.58	0.07	1.58	0.07	0.04
2.51	0.08	2.51	0.08	2.51	0.08	2.51	0.08	0.03
3.98	0.10	3.98	0.10	3.98	0.10	3.98	0.10	0.02
6.31	0.12	6.31	0.12	6.31	0.12	6.31	0.12	0.02
10.01	0.16	10.01	0.16	10.01	0.16	10.01	0.16	0.02
15.86	0.22	15.85	0.22	15.86	0.22	15.86	0.22	0.01
25.12	0.30	25.13	0.30	25.12	0.30	25.12	0.30	0.01
39.85	0.43	39.82	0.43	39.84	0.43	39.84	0.43	0.01
63.13	0.62	63.15	0.62	63.13	0.62	63.14	0.62	0.01
100.06	0.92	100.05	0.92	100.10	0.92	100.07	0.92	0.01
100.09	0.92	100.07	0.92	100.07	0.92	100.08	0.92	0.01
71.98	0.69	72.01	0.69	72.00	0.69	72.00	0.69	0.01
51.84	0.53	51.85	0.53	51.83	0.53	51.84	0.53	0.01
37.31	0.41	37.31	0.41	37.30	0.41	37.31	0.41	0.01
26.85	0.32	26.85	0.32	26.85	0.32	26.85	0.32	0.01
19.31	0.25	18.93	0.25	19.32	0.25	19.19	0.25	0.01
13.90	0.20	13.90	0.20	13.91	0.20	13.90	0.20	0.01
10.00	0.16	10.01	0.16	10.01	0.16	10.01	0.16	0.02
7.20	0.13	7.20	0.13	7.20	0.13	7.20	0.13	0.02
5.18	0.11	5.18	0.11	5.18	0.11	5.18	0.11	0.02
3.73	0.10	3.73	0.09	3.73	0.09	3.73	0.09	0.03
2.68	0.08	2.68	0.08	2.69	0.08	2.68	0.08	0.03
1.93	0.07	1.93	0.07	1.93	0.07	1.93	0.07	0.04
1.39	0.07	1.39	0.06	1.39	0.06	1.39	0.06	0.05
1.00	0.06	1.00	0.06	1.00	0.06	1.00	0.06	0.06
0.72	0.06	0.72	0.05	0.72	0.05	0.72	0.05	0.07
0.52	0.05	0.54	0.05	0.52	0.05	0.53	0.05	0.09
0.37	0.05	0.37	0.04	0.37	0.05	0.37	0.05	0.12
0.27	0.05	0.27	0.04	0.27	0.04	0.27	0.04	0.16
0.19	0.05	0.19	0.04	0.19	0.04	0.19	0.04	0.22
0.14	0.04	0.14	0.04	0.14	0.04	0.14	0.04	0.29
0.10	0.04	0.10	0.04	0.10	0.04	0.10	0.04	0.39

	Run #D	Run #E	Run #F	Avg.	Std. Dev.
Intercept [Nm]	0.0577	0.0554	0.0541	0.0557	0.001456
Slope[Nm.min]	0.0089	0.0089	0.0089	0.0089	0.000023
R2	1.0	1.0	1.0	0.9962	0.000105

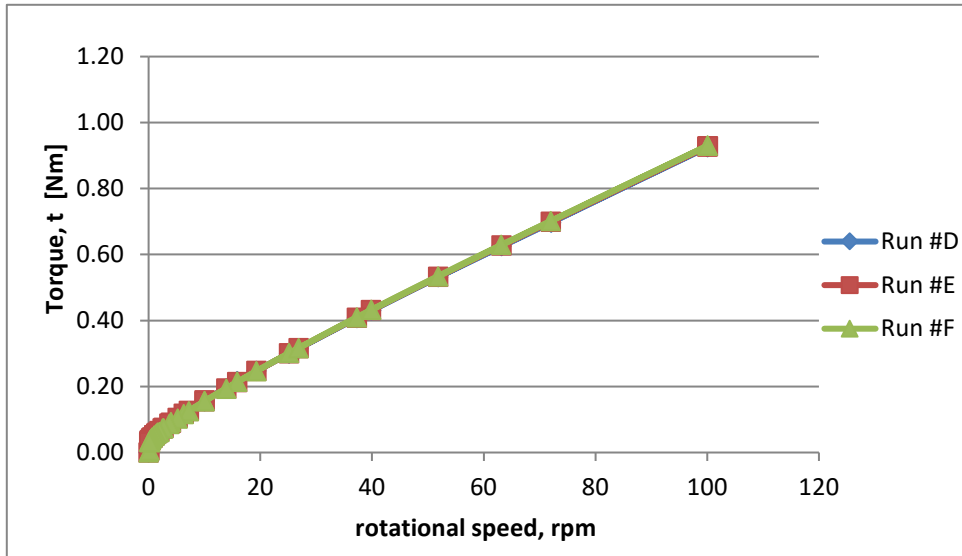


Figure C-5: Torque vs. Angular Speed using spiral spindle on Mix# A, with 20 % beads (mortar) by volume. Portrays data from Table C-5.

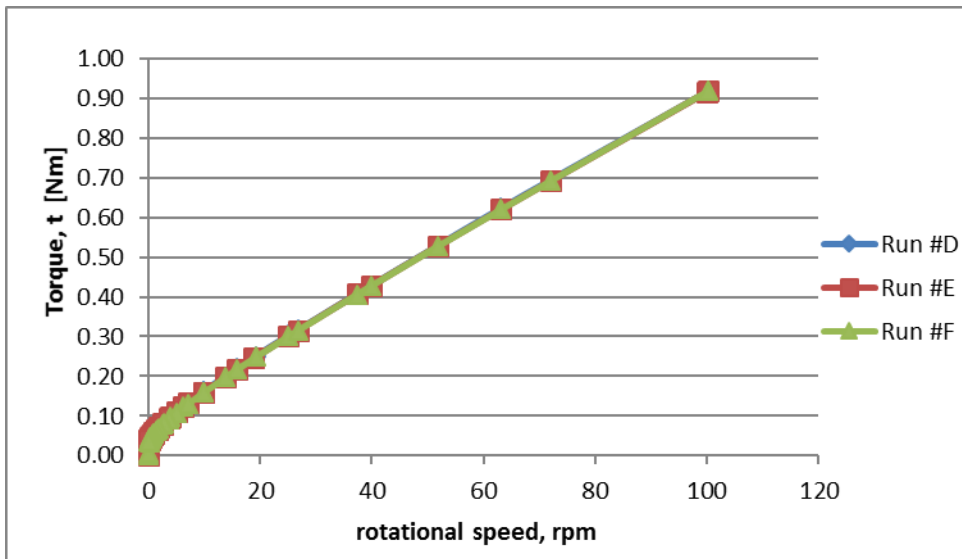


Figure C-6: Torque vs. Angular Speed using spiral spindle on Mix# B, with 20 % beads (mortar) by volume. Portrays data from Table C-6.

Table C-7: Measured data for Mix #A with 20 % beads (mortar) using 4-blade spindle.

Mix A - 7/15/15								
CR-50								
Run #A		Run #B		Run #C		Average		
SR (1/min)	SS (Nm)	SR (1/min)	SS (Nm)	SR (1/min)	SS (Nm)	SR (1/min)	SS (Nm)	Ratio
-0.04	0.01	0.00	0.00	0.00	0.00	-0.01	0.00	
0.16	0.04	0.16	0.01	0.16	0.01	0.16	0.02	0.13
0.25	0.05	0.25	0.05	0.25	0.05	0.25	0.05	0.18
0.40	0.05	0.40	0.05	0.40	0.05	0.40	0.05	0.13
0.63	0.06	0.63	0.06	0.63	0.06	0.63	0.06	0.10
1.00	0.07	1.00	0.07	1.00	0.07	1.00	0.07	0.07
1.58	0.08	1.59	0.08	1.59	0.08	1.58	0.08	0.05
2.51	0.10	2.51	0.10	2.51	0.10	2.51	0.10	0.04
3.99	0.13	3.98	0.13	3.98	0.13	3.98	0.13	0.03
6.31	0.16	6.31	0.16	6.31	0.16	6.31	0.16	0.03
10.01	0.22	10.01	0.22	10.01	0.22	10.01	0.22	0.02
15.86	0.31	15.86	0.31	15.86	0.31	15.86	0.31	0.02
25.15	0.44	25.14	0.44	25.14	0.44	25.14	0.44	0.02
39.81	0.63	39.84	0.63	39.84	0.63	39.83	0.63	0.02
63.10	0.92	63.17	0.93	63.17	0.93	63.15	0.92	0.01
100.11	1.37	100.11	1.38	100.11	1.38	100.11	1.38	0.01
100.04	1.37	100.14	1.38	100.14	1.38	100.10	1.38	0.01
72.02	1.03	72.01	1.04	72.01	1.04	72.02	1.04	0.01
51.84	0.78	51.81	0.79	51.81	0.79	51.82	0.79	0.02
37.30	0.60	37.31	0.60	37.31	0.60	37.31	0.60	0.02
26.85	0.46	26.85	0.46	26.85	0.46	26.85	0.46	0.02
18.91	0.35	18.97	0.36	18.97	0.36	18.95	0.35	0.02
13.91	0.28	13.90	0.28	13.90	0.28	13.90	0.28	0.02
10.00	0.23	10.00	0.22	10.00	0.22	10.00	0.22	0.02
7.20	0.18	7.20	0.18	7.20	0.18	7.20	0.18	0.02
5.18	0.15	5.18	0.15	5.18	0.15	5.18	0.15	0.03
3.73	0.12	3.73	0.12	3.73	0.12	3.73	0.12	0.03
2.68	0.10	2.68	0.11	2.68	0.11	2.68	0.10	0.04
1.93	0.09	1.93	0.09	1.93	0.09	1.93	0.09	0.05
1.39	0.08	1.39	0.08	1.39	0.08	1.39	0.08	0.06
1.00	0.07	1.00	0.07	1.00	0.07	1.00	0.07	0.07
0.72	0.06	0.72	0.06	0.72	0.06	0.72	0.06	0.09
0.52	0.06	0.51	0.06	0.51	0.06	0.51	0.06	0.11
0.37	0.05	0.37	0.06	0.37	0.06	0.37	0.05	0.15
0.27	0.05	0.27	0.05	0.27	0.05	0.27	0.05	0.19
0.19	0.04	0.19	0.05	0.19	0.05	0.19	0.05	0.24
0.14	0.04	0.14	0.04	0.14	0.04	0.14	0.04	0.32
0.10	0.04	0.10	0.04	0.10	0.04	0.10	0.04	0.44

	Run #A	Run #B	Run #C		Avg.	Std. Dev.
Intercept [Nm]	0.0643	0.0673	0.0673		0.0663	0.001416
Slope[Nm.min]	0.0135	0.0135	0.0135		0.0135	0.000037
R2	1.0	1.0	1.0		0.9965	0.000079

Table C-8: Measured data for Mix #B with 20 % beads (mortar) using 4-blade spindle.

Mix B - 7/28/15								
CR-63								
Run #A		Run #B		Run #C		Average		
SR (1/min)	SS (Nm)	SR (1/min)	SS (Nm)	SR (1/min)	SS (Nm)	SR (1/min)	SS (Nm)	Ratio
0.05	0.01	0.00	0.00	0.00	0.00	0.02	0.00	
0.16	0.05	0.16	0.01	0.16	0.01	0.16	0.03	0.16
0.25	0.06	0.25	0.05	0.25	0.06	0.25	0.06	0.22
0.40	0.06	0.40	0.06	0.40	0.06	0.40	0.06	0.15
0.63	0.07	0.63	0.07	0.63	0.07	0.63	0.07	0.11
1.00	0.08	1.00	0.08	1.00	0.08	1.00	0.08	0.08
1.58	0.09	1.58	0.09	1.58	0.09	1.58	0.09	0.06
2.51	0.11	2.51	0.11	2.51	0.11	2.51	0.11	0.04
3.99	0.13	3.98	0.13	3.99	0.13	3.98	0.13	0.03
6.31	0.17	6.32	0.17	6.32	0.17	6.31	0.17	0.03
10.01	0.23	10.01	0.23	10.01	0.23	10.01	0.23	0.02
15.86	0.31	15.86	0.31	15.86	0.31	15.86	0.31	0.02
25.14	0.44	25.14	0.44	25.12	0.44	25.13	0.44	0.02
39.82	0.63	39.83	0.63	39.85	0.63	39.83	0.63	0.02
63.15	0.92	63.13	0.92	63.16	0.92	63.15	0.92	0.01
100.07	1.36	100.05	1.36	100.05	1.37	100.06	1.36	0.01
100.06	1.36	100.10	1.36	100.10	1.37	100.09	1.36	0.01
72.03	1.02	72.02	1.02	72.03	1.03	72.03	1.03	0.01
51.84	0.78	51.81	0.78	51.85	0.78	51.83	0.78	0.02
37.30	0.59	37.31	0.60	37.30	0.60	37.30	0.60	0.02
26.84	0.46	26.84	0.46	26.85	0.46	26.84	0.46	0.02
18.92	0.35	18.93	0.35	18.94	0.36	18.93	0.35	0.02
13.91	0.28	13.91	0.29	13.91	0.29	13.91	0.28	0.02
10.00	0.23	10.00	0.23	10.01	0.23	10.00	0.23	0.02
7.20	0.19	7.20	0.19	7.20	0.19	7.20	0.19	0.03
5.19	0.15	5.18	0.15	5.18	0.16	5.18	0.16	0.03
3.73	0.13	3.73	0.13	3.73	0.13	3.73	0.13	0.04
2.68	0.11	2.68	0.11	2.68	0.11	2.68	0.11	0.04
1.93	0.10	1.93	0.10	1.93	0.10	1.93	0.10	0.05
1.39	0.09	1.39	0.09	1.39	0.09	1.39	0.09	0.06
1.00	0.08	1.00	0.08	1.00	0.08	1.00	0.08	0.08
0.72	0.07	0.72	0.07	0.72	0.07	0.72	0.07	0.10
0.60	0.07	0.52	0.07	0.52	0.07	0.54	0.07	0.12
0.37	0.06	0.37	0.06	0.37	0.06	0.37	0.06	0.17
0.27	0.06	0.27	0.06	0.27	0.06	0.27	0.06	0.22
0.19	0.05	0.19	0.06	0.19	0.06	0.19	0.06	0.29
0.14	0.05	0.14	0.05	0.14	0.05	0.14	0.05	0.39
0.10	0.05	0.10	0.05	0.10	0.05	0.10	0.05	0.52

	Run #A	Run #B	Run #C		Avg.	Std. Dev.
Intercept [Nm]	0.0730	0.0747	0.0762		0.0746	0.001269
Slope[Nm.min]	0.0132	0.0132	0.0133		0.0133	0.000022
R2	1.0	1.0	1.0		0.9968	0.000017

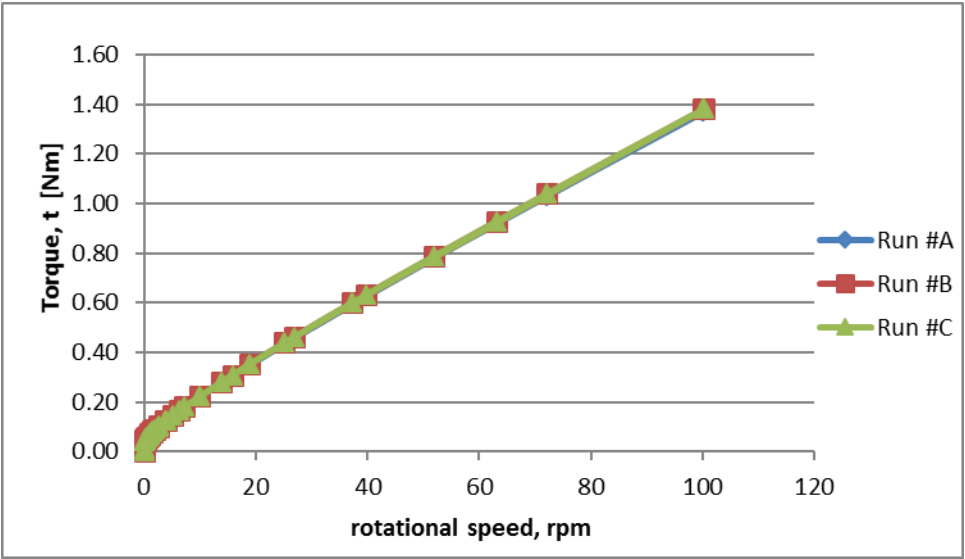


Figure C-7: Torque vs. Angular Speed using 4-blades spindle on Mix# A, with 20 % beads (mortar) by volume. Portrays data from Table C-7.

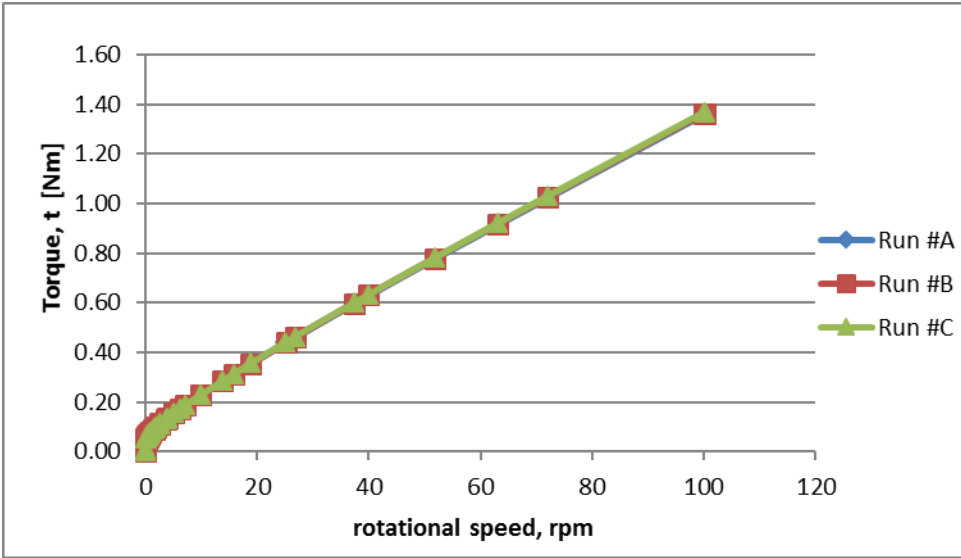


Figure C-8: Torque vs. Angular Speed using 4-blades spindle on Mix# B, with 20 % beads (mortar) by volume. Portrays data from Table C-8.

Table C-9: Measured data for Mix #A with mortar and 10-mm beads(Concrete) using Spiral spindle.

Mix A - 7/15/15								
CR-52								
Run #A		Run #D		Run #E		Average		
SR (1/min)	SS (Nm)	SR (1/min)	SS (Nm)	SR (1/min)	SS (Nm)	SR (1/min)	SS (Nm)	Ratio
-0.04	0.01	3.14	0.49	0.00	0.00	1.03	0.17	
0.15	0.08	0.16	0.16	0.16	0.06	0.16	0.10	0.63
0.25	0.09	0.25	0.19	0.25	0.17	0.25	0.15	0.60
0.40	0.13	0.40	0.21	0.40	0.22	0.40	0.19	0.47
0.63	0.16	0.63	0.25	0.63	0.24	0.63	0.22	0.35
1.00	0.21	1.00	0.28	1.00	0.28	1.00	0.26	0.26
1.58	0.25	1.59	0.34	1.58	0.34	1.58	0.31	0.20
2.51	0.36	2.51	0.46	2.51	0.41	2.51	0.41	0.16
3.99	0.46	3.98	0.58	3.99	0.56	3.98	0.53	0.13
6.32	0.63	6.31	0.75	6.31	0.74	6.31	0.71	0.11
10.01	0.90	10.01	1.03	10.01	0.98	10.01	0.97	0.10
15.86	1.27	15.86	1.40	15.86	1.39	15.86	1.35	0.09
25.13	1.77	25.14	2.04	25.14	1.82	25.13	1.88	0.07
39.82	2.52	39.83	2.83	39.85	2.54	39.83	2.63	0.07
63.13	3.64	63.19	3.99	63.15	3.55	63.16	3.73	0.06
100.10	4.94	100.11	5.65	100.11	4.91	100.11	5.17	0.05
100.04	4.86	100.04	4.90	100.05	4.95	100.04	4.90	0.05
72.04	3.71	72.08	3.73	72.01	3.62	72.04	3.69	0.05
51.81	2.89	51.83	2.92	51.82	2.76	51.82	2.86	0.06
37.32	2.27	37.29	2.32	37.31	2.22	37.31	2.27	0.06
26.85	1.77	26.83	1.87	26.85	1.69	26.84	1.78	0.07
19.32	1.40	19.32	1.42	19.31	1.37	19.32	1.40	0.07
13.90	1.13	13.90	1.16	13.90	1.10	13.90	1.13	0.08
10.01	0.91	10.01	0.96	10.01	0.91	10.01	0.93	0.09
7.20	0.78	7.20	0.79	7.20	0.78	7.20	0.78	0.11
5.18	0.62	5.18	0.64	5.18	0.66	5.18	0.64	0.12
3.73	0.51	3.73	0.56	3.73	0.53	3.73	0.53	0.14
2.69	0.48	2.68	0.50	2.68	0.47	2.68	0.48	0.18
1.93	0.38	1.93	0.38	1.93	0.39	1.93	0.38	0.20
1.39	0.33	1.39	0.33	1.39	0.36	1.39	0.34	0.24
1.00	0.33	1.00	0.30	1.00	0.31	1.00	0.31	0.31
0.72	0.28	0.72	0.26	0.72	0.31	0.72	0.29	0.40
0.52	0.26	0.54	0.24	0.52	0.28	0.53	0.26	0.50
0.37	0.21	0.37	0.23	0.37	0.23	0.37	0.22	0.60
0.27	0.21	0.27	0.23	0.27	0.21	0.27	0.21	0.81
0.19	0.20	0.19	0.20	0.19	0.23	0.19	0.21	1.08
0.14	0.19	0.14	0.21	0.14	0.21	0.14	0.20	1.48
0.10	0.18	0.10	0.19	0.10	0.22	0.10	0.20	1.97

	Run #A	Run #D	Run #E		Avg.	Std. Dev.
Intercept [Nm]	0.3136	0.3269	0.3182		0.3196	0.005517
Slope[Nm.min]	0.0476	0.0480	0.0471		0.0476	0.000359
R2	1.0	1.0	1.0		0.9914	0.002204

Table C-10: Measured data for Mix #B with mortar and 10-mm beads(Concrete) using Spiral spindle.

Mix B - 7/28/15								
CR-65								
Run #A		Run #B		Run #C		Average		
SR (1/min)	SS (Nm)	SR (1/min)	SS (Nm)	SR (1/min)	SS (Nm)	SR (1/min)	SS (Nm)	Ratio
-0.04	0.01	0.00	0.00	0.00	0.00	-0.01	0.00	
0.16	0.08	0.16	0.04	0.16	0.07	0.16	0.06	0.41
0.25	0.10	0.25	0.20	0.25	0.28	0.25	0.19	0.78
0.40	0.12	0.40	0.25	0.40	0.29	0.40	0.22	0.55
0.63	0.16	0.73	0.35	0.63	0.31	0.66	0.27	0.41
1.00	0.19	1.00	0.35	1.00	0.34	1.00	0.29	0.29
1.58	0.23	1.59	0.37	1.58	0.42	1.58	0.34	0.21
2.51	0.27	2.51	0.48	2.51	0.46	2.51	0.41	0.16
3.98	0.36	3.99	0.66	3.98	0.63	3.98	0.55	0.14
6.31	0.55	6.31	0.76	6.31	0.71	6.31	0.67	0.11
10.00	0.76	10.00	0.92	10.01	0.95	10.00	0.88	0.09
15.86	1.06	15.87	1.30	15.86	1.18	15.86	1.18	0.07
25.15	1.48	25.15	1.48	25.15	1.50	25.15	1.48	0.06
39.84	2.00	39.85	2.00	39.86	2.00	39.85	2.00	0.05
63.14	2.92	63.10	2.87	63.14	2.86	63.13	2.88	0.05
100.11	4.03	100.10	4.20	100.10	4.17	100.10	4.13	0.04
100.05	4.01	100.09	4.16	100.04	4.07	100.06	4.08	0.04
72.05	3.10	72.01	3.12	72.03	3.13	72.03	3.12	0.04
51.83	2.39	51.85	2.38	51.81	2.39	51.83	2.39	0.05
37.31	1.79	37.28	1.90	37.30	1.91	37.30	1.87	0.05
26.84	1.43	26.86	1.50	26.85	1.50	26.85	1.48	0.06
19.31	1.19	19.33	1.18	19.33	1.19	19.32	1.19	0.06
13.91	0.99	13.90	0.95	13.90	0.95	13.90	0.96	0.07
10.01	0.75	10.01	0.74	10.00	0.76	10.01	0.75	0.08
7.20	0.63	7.20	0.62	7.20	0.63	7.20	0.63	0.09
5.18	0.54	5.18	0.51	5.18	0.55	5.18	0.53	0.10
3.73	0.46	3.73	0.45	3.73	0.47	3.73	0.46	0.12
2.68	0.40	2.68	0.35	2.68	0.39	2.68	0.38	0.14
1.93	0.35	1.93	0.34	1.93	0.35	1.93	0.35	0.18
1.39	0.32	1.39	0.29	1.39	0.30	1.39	0.30	0.22
1.00	0.26	1.00	0.24	1.00	0.29	1.00	0.27	0.27
0.72	0.24	0.72	0.27	0.72	0.24	0.72	0.25	0.35
0.52	0.21	0.52	0.21	0.52	0.21	0.52	0.21	0.41
0.37	0.21	0.37	0.21	0.37	0.21	0.37	0.21	0.56
0.27	0.19	0.27	0.18	0.27	0.25	0.27	0.21	0.77
0.19	0.20	0.19	0.19	0.19	0.19	0.19	0.19	1.00
0.14	0.18	0.14	0.20	0.14	0.23	0.14	0.20	1.47
0.10	0.19	0.10	0.14	0.10	0.17	0.10	0.17	1.67

	Run #A	Run #B	Run #C		Avg.	Std. Dev.
Intercept [Nm]	0.2770	0.2623	0.2855		0.2749	0.009549
Slope[Nm.min]	0.0391	0.0403	0.0396		0.0396	0.000498
R2	1.0	1.0	1.0		0.9926	0.000623

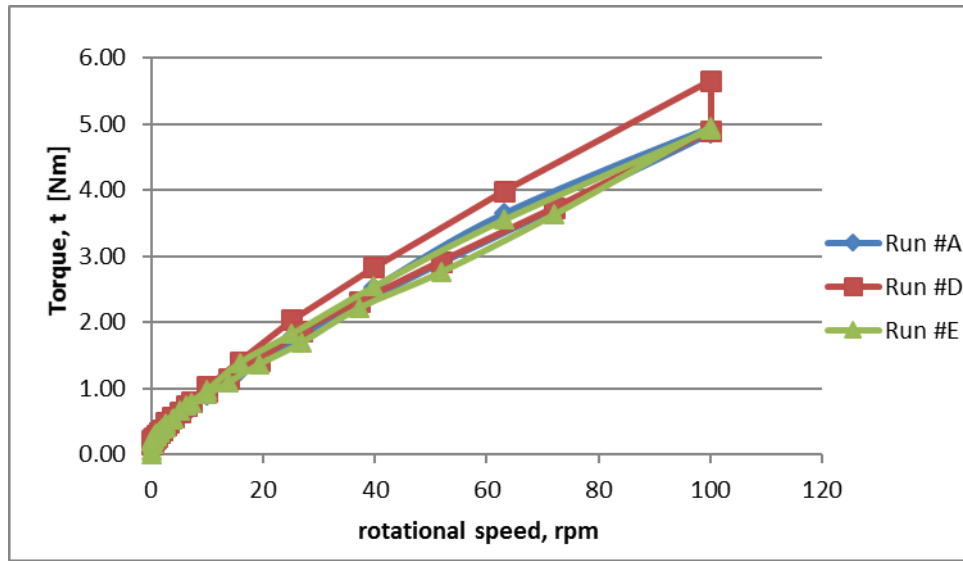


Figure C-9: Torque vs. Angular Speed using Spiral spindle on Mix# A, with mortar and 10 mm beads. Portrays data from Table C-9.

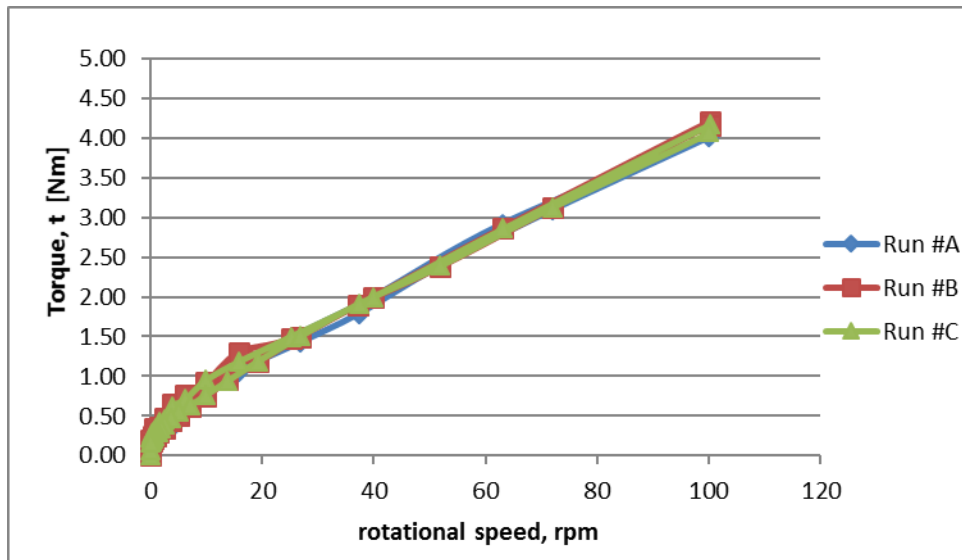


Figure C-10: Torque vs. Angular Speed using Spiral spindle on Mix# B, with mortar and 10 mm beads. Portrays data from Table C-10.

Table C-11: Measured data for Mix #A with mortar and 10-mm beads(Concrete) using Vane spindle.

Mix A - 7/15/15								
CR-52								
Run #F		Run #G		Run #H		Average		
SR (1/min)	SS (Nm)	SR (1/min)	SS (Nm)	SR (1/min)	SS (Nm)	SR (1/min)	SS (Nm)	Ratio
0.00	0.00	0.00	0.00	0.00	0.00	0.00	0.00	
0.16	0.17	0.16	0.23	0.16	0.11	0.16	0.17	1.09
0.25	0.61	0.25	0.40	0.25	0.34	0.25	0.45	1.80
0.40	0.50	0.40	0.35	0.40	0.39	0.40	0.41	1.04
0.63	0.48	0.63	0.39	0.63	0.44	0.63	0.44	0.69
1.00	0.60	1.00	0.48	1.00	0.43	1.00	0.50	0.50
1.59	0.67	1.59	0.53	1.58	0.62	1.59	0.61	0.38
2.51	0.82	2.51	0.73	0.00	0.03	1.68	0.53	0.31
3.98	1.09	3.98	0.91	3.99	0.84	3.98	0.95	0.24
6.31	1.31	6.31	1.28	6.32	1.15	6.31	1.25	0.20
10.01	1.67	10.01	1.58	10.01	1.50	10.01	1.58	0.16
15.85	2.25	15.86	1.99	15.86	2.12	15.86	2.12	0.13
25.13	3.07	25.14	2.78	25.14	2.77	25.13	2.87	0.11
39.84	3.62	39.82	3.88	39.83	3.56	39.83	3.69	0.09
63.10	5.00	63.17	4.88	63.18	4.51	63.15	4.80	0.08
100.05	6.50	100.01	5.43	100.09	5.61	100.05	5.85	0.06
100.04	5.70	100.05	5.16	100.09	5.26	100.06	5.38	0.05
72.02	4.27	72.06	3.91	72.04	3.99	72.04	4.06	0.06
51.82	3.22	51.83	2.97	51.84	3.04	51.83	3.08	0.06
37.31	2.58	37.30	2.41	37.30	2.39	37.30	2.46	0.07
26.86	1.99	26.84	1.91	26.84	1.93	26.85	1.94	0.07
19.32	1.81	19.31	1.58	19.32	1.57	19.32	1.65	0.09
13.92	1.48	13.90	1.29	13.91	1.26	13.91	1.35	0.10
10.00	1.23	10.00	1.05	10.01	1.12	10.00	1.13	0.11
7.20	0.97	7.20	0.84	7.20	0.93	7.20	0.91	0.13
5.18	0.81	5.19	0.70	5.18	0.77	5.18	0.76	0.15
3.73	0.72	3.73	0.64	3.73	0.63	3.73	0.66	0.18
2.68	0.60	2.68	0.54	2.68	0.56	2.68	0.57	0.21
1.93	0.50	1.93	0.47	1.93	0.44	1.93	0.47	0.24
1.39	0.48	1.39	0.38	1.39	0.44	1.39	0.43	0.31
1.00	0.37	1.00	0.40	1.00	0.44	1.00	0.40	0.40
0.72	0.32	0.72	0.32	0.72	0.32	0.72	0.32	0.44
0.52	0.36	0.57	0.30	0.52	0.28	0.53	0.32	0.59
0.37	0.32	0.37	0.30	0.38	0.28	0.37	0.30	0.81
0.27	0.28	0.27	0.23	0.27	0.26	0.27	0.26	0.97
0.19	0.25	0.19	0.23	0.19	0.22	0.19	0.24	1.23
0.14	0.27	0.14	0.22	0.14	0.32	0.14	0.27	1.97
0.10	0.23	0.10	0.21	0.10	0.25	0.10	0.23	2.32

	Run #F	Run #G	Run #H	Avg.	Std. Dev.
Intercept [Nm]	0.4264	0.3792	0.3960	0.4005	0.019510
Slope[Nm.min]	0.0544	0.0498	0.0504	0.0515	0.002031
R2	1.0	1.0	1.0	0.9889	0.001081

Table C-12: Measured data for Mix #B with mortar and 10-mm beads(Concrete) using Vane spindle.

Mix B - 7/28/15								
CR-65								
Run #D		Run #E		Run #F		Average		
SR (1/min)	SS (Nm)	SR (1/min)	SS (Nm)	SR (1/min)	SS (Nm)	SR (1/min)	SS (Nm)	Ratio
0.00	0.00	0.00	0.00	0.00	0.00	0.00	0.00	
0.16	0.24	0.16	0.08	0.16	0.17	0.16	0.16	1.03
0.25	0.45	0.25	0.35	0.25	0.77	0.25	0.52	2.08
0.40	0.56	0.40	0.34	0.40	0.57	0.40	0.49	1.22
0.63	0.46	0.63	0.42	0.63	0.46	0.63	0.45	0.71
1.00	0.61	1.00	0.43	1.00	0.59	1.00	0.54	0.54
1.58	0.65	1.59	0.50	1.59	0.70	1.58	0.62	0.39
2.51	0.78	2.51	0.66	2.51	0.85	2.51	0.76	0.30
3.98	0.88	3.98	0.78	3.98	0.98	3.98	0.88	0.22
6.31	1.19	6.31	1.03	6.31	1.21	6.31	1.14	0.18
10.01	1.44	10.01	1.39	10.00	1.48	10.01	1.44	0.14
15.86	1.89	15.86	1.84	15.86	1.93	15.86	1.89	0.12
25.15	2.68	25.14	2.43	25.13	2.56	25.14	2.56	0.10
39.84	3.33	39.81	3.28	39.84	3.27	39.83	3.29	0.08
63.18	4.53	63.14	4.38	63.17	4.25	63.17	4.39	0.07
100.07	5.11	100.05	6.14	100.07	5.79	100.06	5.68	0.06
100.05	4.66	100.10	4.72	100.09	5.21	100.08	4.86	0.05
72.00	3.50	72.02	3.56	72.04	3.79	72.02	3.61	0.05
51.84	2.69	51.83	2.78	51.84	2.95	51.84	2.81	0.05
37.32	2.16	37.31	2.22	37.30	2.31	37.31	2.23	0.06
26.84	1.71	26.86	1.71	26.85	1.92	26.85	1.78	0.07
19.32	1.40	19.32	1.37	19.33	1.59	19.32	1.46	0.08
13.90	1.20	13.90	1.39	13.91	1.25	13.90	1.28	0.09
10.01	1.02	10.01	1.07	10.01	1.07	10.01	1.05	0.11
7.20	0.91	7.21	0.87	7.20	0.93	7.20	0.90	0.13
5.19	0.74	5.18	0.79	5.18	0.74	5.18	0.76	0.15
3.73	0.63	3.73	0.70	3.73	0.62	3.73	0.65	0.17
2.68	0.60	2.68	0.57	2.68	0.57	2.68	0.58	0.22
1.93	0.51	1.93	0.51	1.93	0.50	1.93	0.50	0.26
1.39	0.46	1.39	0.42	1.39	0.45	1.39	0.44	0.32
1.00	0.38	1.00	0.41	1.00	0.40	1.00	0.40	0.40
0.72	0.36	0.72	0.38	0.72	0.36	0.72	0.37	0.51
0.52	0.39	0.52	0.33	0.52	0.32	0.52	0.35	0.67
0.37	0.33	0.37	0.29	0.37	0.30	0.37	0.31	0.82
0.27	0.26	0.27	0.27	0.27	0.29	0.27	0.28	1.03
0.19	0.31	0.19	0.25	0.19	0.28	0.19	0.28	1.45
0.14	0.25	0.14	0.24	0.14	0.24	0.14	0.24	1.75
0.10	0.26	0.10	0.25	0.10	0.26	0.10	0.25	2.56

	Run #D	Run #E	Run #F	Avg.	Std. Dev.
Intercept [Nm]	0.4152	0.4175	0.4046	0.4124	0.005626
Slope[Nm.min]	0.0437	0.0446	0.0489	0.0457	0.002298
R2	1.0	1.0	1.0	0.9882	0.002247

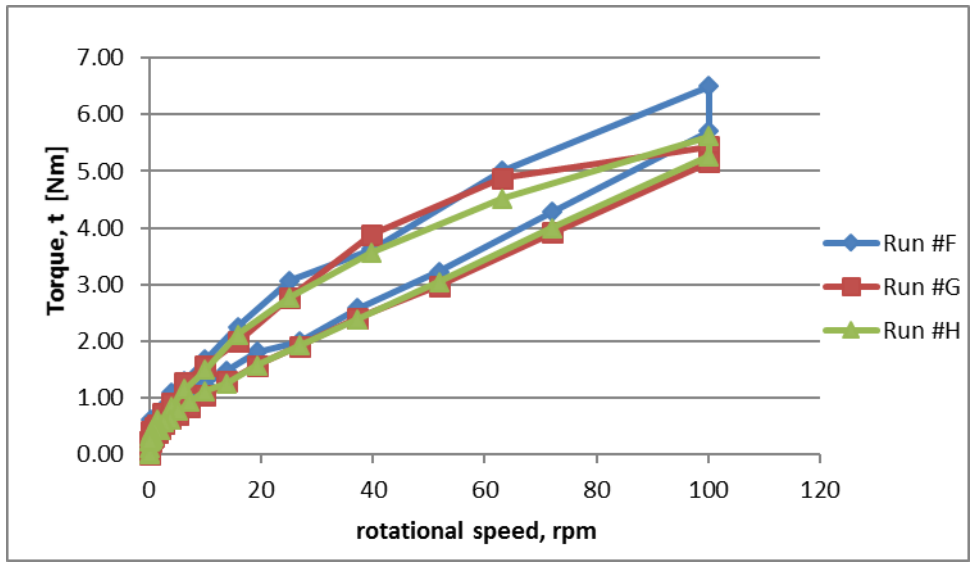


Figure C-11: Torque vs. Angular Speed using Vane spindle on Mix# A, with mortar and 10 mm beads. Portrays data from Table C-11.

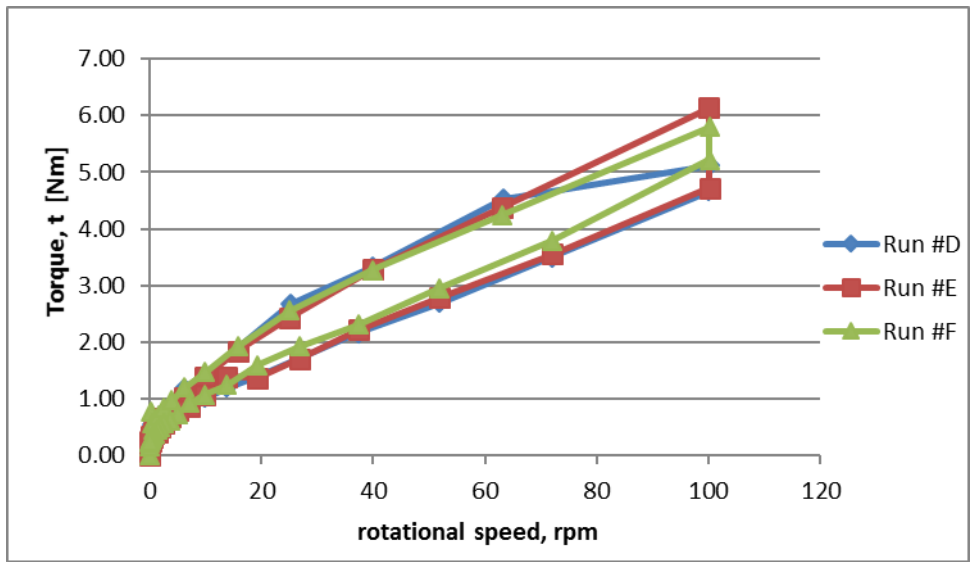


Figure C-12: Torque vs. Angular Speed using Vane spindle on Mix# B, with mortar and 10 mm beads. Portrays data from Table C-12.